Reliability of transmission networks

Impact of EHV underground cables & interaction of offshore-onshore networks

Tuinema, Bart

DOI
10.4233/uuid:98c73893-a400-4fb2-9266-a9b5e19ccc69

Publication date
2017

Document Version
Final published version

Citation (APA)
Tuinema, B. (2017). *Reliability of transmission networks: Impact of EHV underground cables & interaction of offshore-onshore networks*. [Dissertation (TU Delft), Delft University of Technology].
https://doi.org/10.4233/uuid:98c73893-a400-4fb2-9266-a9b5e19ccc69

Important note
To cite this publication, please use the final published version (if applicable).
Please check the document version above.

Reliability of Transmission Networks

Impact of EHV Underground Cables & Interaction of Offshore-Onshore Networks

Bart W. Tuinema

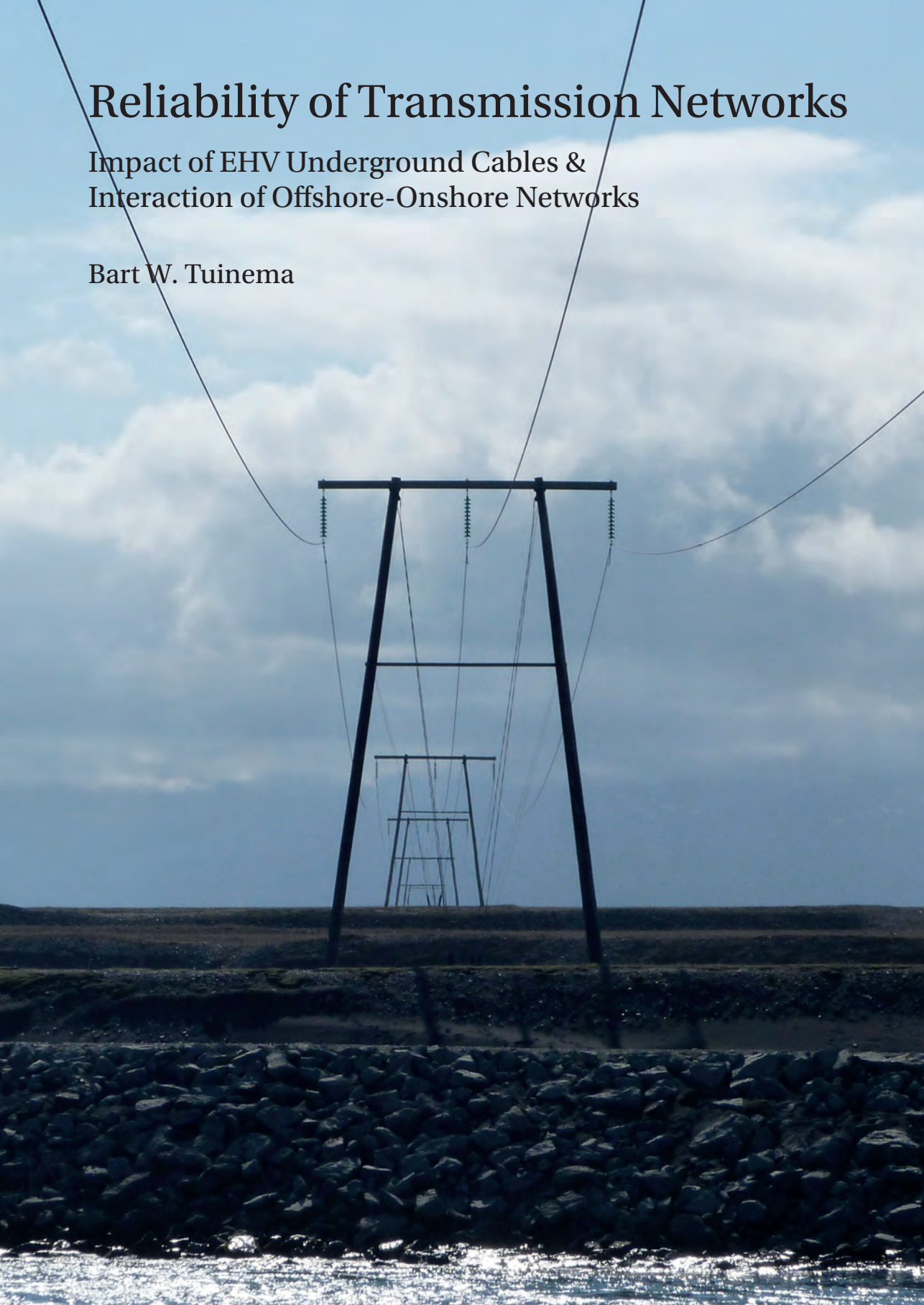

RELIABILITY OF TRANSMISSION NETWORKS

IMPACT OF EHV UNDERGROUND CABLES & INTERACTION OF OFFSHORE-ONSHORE NETWORKS

RELIABILITY OF TRANSMISSION NETWORKS

IMPACT OF EHV UNDERGROUND CABLES & INTERACTION OF OFFSHORE-ONSHORE NETWORKS

Proefschrift

ter verkrijging van de graad van doctor
aan de Technische Universiteit Delft,
op gezag van de Rector Magnificus prof. ir. K. C. A. M. Luyben,
voorzitter van het College voor Promoties,
in het openbaar te verdedigen op donderdag 23 november 2017 om 10:00 uur

door

Bart Wiebren TUINEMA

elektrotechnisch ingenieur
geboren te Den Haag, Nederland.

Dit proefschrift is goedgekeurd door de

promotors: prof. ir. M.A.M.M. van der Meijden en prof. ir. L. van der Sluis en
copromotor: dr. ir. J.L. Rueda Torres

Samenstelling promotiecommissie:

Rector Magnificus,	voorzitter
prof. ir. M.A.M.M. van der Meijden,	EWI, TU Delft
prof. ir. L. van der Sluis,	EWI, TU Delft
dr. ir. J.L. Rueda Torres,	EWI, TU Delft

Onafhankelijke leden:

prof. dr. M. Zeman,	EWI, TU Delft
prof. dr. ing. habil. K. Rudion,	University Stuttgart
prof. dr. ing. habil. L. Hofmann,	Leibniz University of Hannover
dr. G.R. Kuik,	TenneT TSO B.V.

Reservelid:

prof. dr. P. Palensky,	EWI, TU Delft

This research was financially supported by TenneT TSO B.V.

Published by:	Bart Tuinema
E-mail:	B.W.Tuinema@tudelft.nl
Printed by:	Ridderprint B.V. (www.ridderprint.nl)
Electronic version:	http://repository.tudelft.nl/

ISBN 978-94-6299-778-3

Keywords: reliability analysis, EHV underground cables, offshore networks

Front & Back: Transmission lines near Jökulsárlón, Iceland, 2015.

To my parents

SUMMARY

For the future, several developments of the power system are expected. The transition towards a more sustainable energy supply puts new requirements on the design and operation of power systems, and the transmission network in particular. Offshore, a transmission grid will be implemented to collect large-scale wind energy and to interconnect national power systems. Onshore, the transmission network needs to be reinforced to transmit the large-scale renewable energy to the main load centers. As all these developments will impact the reliability of transmission networks, it is important to study and quantify these impacts in reliability analysis.

Traditional overhead lines are facing more and more opposition from local society, such that underground extra-high voltage (EHV) cable connections become a promising alternative for future grid extension. As EHV underground cables are a relatively new technology, not much is known yet about their behavior in large transmission networks. Underground cable connections (consisting of cables, joints and terminations) are in general less reliable than traditional overhead lines, mainly because of their much longer repair time. This can negatively influence the reliability of the transmission network as well. In this thesis, the reliability of EHV underground cables and overhead lines are compared, from the level of individual connections to transmission network level. It is studied which factors are of influence and what measures can be taken to improve the reliability.

For offshore grids, network redundancy is a topic of discussion. Implementing offshore redundancy can be costly, but no network redundancy might lead to large capacity outages when connecting large offshore wind farms. In this thesis, the reliability of various offshore configurations is compared and it is discussed what level of redundancy is the most optimal. The consequences of offshore network outages for the operation of the onshore power system are considered as well. Recommendations for the implementation of offshore redundancy are given.

The studies in this thesis show the importance of an integrated reliability analysis, where network design and system operation are combined, to find the most optimal solution. Decisions on network design will have consequences for system operation and vice versa. The studies in this thesis show how the reliability of underground cables and offshore networks can be assessed, which factors are of influence and what measures can be taken to improve power system reliability in the future.

SAMENVATTING

Voor de nabije toekomst worden verscheidene veranderingen van het elektriciteitsnet verwacht. De transitie naar een duurzame energievoorziening leidt tot nieuwe eisen voor het ontwerp en de bedrijfsvoering van energievoorzieningssystemen, het elektriciteitsnet in het bijzonder. Op zee zal een netwerk ontwikkeld worden om grootschalige windenergie te winnen en nationale elektriciteitsnetten te verbinden. Op land zal het elektriciteitsnet versterkt moeten worden om de grootschalige windenergie naar de belangrijkste belastingsgebieden te vervoeren. Omdat al deze ontwikkelingen de betrouwbaarheid van elektriciteitsnetten zullen beïnvloeden, is het van belang om dit in een betrouwbaarheidsanalyse te bestuderen en te quantificeren.

Vanuit de samenleving is er een groeiende weerstand tegen traditionele bovengrondse hoogspanningslijnen, waardoor ondergrondse extrahoogspanningskabels (EHS-kabels) een veelbelovend alternatief vormen voor toekomstige netuitbreiding. Omdat EHS-kabels een relatief nieuwe technologie zijn, is er nog weining bekend over hun gedrag in grote transportnetten. Ondergrondse kabelverbindingen (bestaande uit kabels, moffen en eindsluitingen) zijn over het algemeen minder betrouwbaar dan traditionele bovengrondse verbindingen, voornamelijk vanwege de veel langere reparatietijd. Dit kan de betrouwbaarheid van het elektriciteitsnet negatief beïnvloeden. In dit proefschrift wordt de betrouwbaarheid van EHS-kabels en bovengrondse lijnen vergeleken, vanaf het niveau van individuele verbindingen tot een transportnetniveau. Bestudeerd wordt welke factoren van invloed zijn en welke maatregelen genomen kunnen worden om de betrouwbaarheid te verbeteren.

Voor netwerken op zee is redundantie een onderwerp van discussie. De implementatie van redundantie in netten op zee kan kostbaar zijn, maar geen redundantie op zee kan leiden tot uitval van een groot vermogen wanneer grootschalige windparken op zee verbonden worden. In dit proefschrift wordt de betrouwbaarheid van verscheidene configuraties van netwerken op zee vergeleken en wordt besproken welk niveau van redundantie optimaal is. Het gevolg van netstoringen op zee voor de bedrijfsvoering van het elektriciteitsnet op land worden ook beschouwd. Aanbevelingen worden gegeven voor de implementatie van redundantie in netten op zee.

De studies in dit proefschrift laten het belang zien van een geïntegreerde betrouwbaarheidsanalyse, waarin netontwikkeling en bedrijfsvoering gecombineerd worden, om zo de meest optimale oplossing te vinden. Beslissingen over netontwikkeling zullen gevolgen hebben voor de bedrijfsvoering en vice versa. De studies in dit proefschrift laten zien hoe de betrouwbaarheid van ondergrondse EHS-kabels en netten op zee bepaald kan worden, welke factoren van invloed zijn en welke maatregelen genomen kunnen worden om de betrouwbaarheid van het elektriciteitsnet in de toekomst te verbeteren.

CONTENTS

1

INTRODUCTION

1.1. MOTIVATION

In the modern society, it is hard to imagine how to live without electricity. Electricity has proven to be one of the best carriers of energy for various smaller and larger applications and is therefore widely used. When the supply of electricity is interrupted, the results can be catastrophic. For instance, the production processes within factories are interrupted, the transport system is affected and even the security within neighborhoods can be in danger. It is therefore of importance that the power system is as reliable as possible.

Although the reliability of power systems has been a topic of interest for long, the related concepts are not always defined clearly and can thereby cause confusion. Basically, system reliability can be defined as the ability of a system to fulfill its function (for a certain time and under certain conditions) [1]. As the main function of a power system is to supply the load, a power system can be regarded as reliable as long as it is able to supply the load. This is reflected in concepts like the Security of Supply. Although this definition holds for traditional power systems, it can be argued that the function of a power system is more than just supplying the load. Connecting generation (renewable and conventional) and enabling the trade in electricity could be seen as additional functions of the power system. These functions should be included in the concept of power system reliability as well, as will be discussed later in this thesis.

Several recent developments have made reliability of power systems even more important. The most important one probably is the transition towards a more renewable energy supply. In its targets for 2020, the European Union aims at 20% of renewable energy generation [2]. New energy sources like wind, solar and biomass will become major contributors of renewable electricity generation [3]. Large-scale centralized generation like offshore wind will be combined with small-scale local generation like solar photovoltaic [4]. For western Europe, wind energy is probably the most promising renewable source for the near future. For example, Ecofys mentions a potential of 230GW offshore wind capacity by 2045, of which 180GW deployed in the North Sea [5]. And EWEA mentions an installed capacity between 250 and 390GW in its wind scenarios for 2030 [6].

1

The transition towards a renewable energy supply puts new requirements on the way in which power systems are designed and operated. For example, the variability and intermittent character of Renewable Energy Sources (RES) can have an impact on the security of electricity supply as the stochastic behavior of renewable generation does not always match with the electricity demand. Also, variable production by renewables results in a variable use of the electrical infrastructure. In combination with the ongoing economic optimization of the infrastructure, new techniques like probabilistic reliability analysis of transmission networks will effectively being applied.

In the past, deterministic approaches (e.g. deterministic contingency analysis and worst-case analysis) and deterministic criteria (like $n-1$ redundancy) were widely used in the design and operation of transmission networks. Although deterministic rules are easy to understand and mostly effectively secure the electricity supply, their meaning has been discussed for long, like e.g. in [7]. For example, what will be the risk if we deviate from $n-1$ redundancy? And what is the difference in reliability between underground cable connections and traditional overhead lines? In these cases, deterministic methods often do not lead to discriminatory results and, thereby, do not provide sufficient insight. In probabilistic reliability analysis, probabilities are taken into account, providing more insight into the reliability of the power system and the risks involved.

Regarding offshore networks, various research institutes have created a variety of possible configurations [8]. This variety of possible configurations is illustrative for the quest for the most optimal offshore topology. Nevertheless, a very important topic of discussion and open research question is the level of redundancy within offshore networks. Full $n-1$ redundancy, as common practice in onshore transmission networks, might not be an economical solution as the additional costs of the infrastructure are larger than the extra income because of less lost wind energy. No redundancy might lead to large amounts of lost wind energy, while large wind capacity outages can have a substantial impact on the security of supply in the onshore power system.

Onshore, reinforcements of the transmission network are needed to transport the offshore wind energy to the load centers. In densely populated areas, traditional overhead lines are facing more opposition from local society. Therefore, underground Extra-High-Voltage (EHV) AC cables are becoming more popular for the extension of existing transmission grids. The main drivers for this are the visual impact of high-voltage towers on the landscape and health concerns related to electromagnetic fields. Although there is more experience with oil-filled cables, plastics like XLPE (cross-linked polyethylene) are preferred as insulator to avoid environmental damage caused by leakage. Currently in the Netherlands, XLPE EHV underground cables are applied in the Randstad380 project [9]. The configuration of Randstad380: a double circuit of 2x2635MVA, with 6 individual underground cables per circuit (2 per circuit phase), a total cable connection length of 20km divided over several locations, and the fact that this is part of the backbone of the 380kV transmission network, make this project rather unique. As these cable connections facilitate high volumes of power transfer, a thorough understanding of the possible implications on the reliability of the transmission network is urgent.

Whereas there is much experience with underground cables at HV and lower voltage levels, XLPE EHV underground cables are a relatively new technology and not much is known yet about their behavior in large, heavily-loaded transmission networks. For the

Randstad380 project, various aspects like resonant behavior [10], transient performance [11], and the reliability are under study [12]. As far as reliability is concerned, the focus of existing research is on the components of cable circuits. A comprehensive approach to assess the reliability of underground cable connections and to analyze the impact on the reliability of large transmission networks is still missing.

The liberalization of the energy market is another development with an impact on the way how reliability studies are performed. Many traditional reliability studies of power systems assume that there is one Transmission System Operator (TSO) that can take any necessary action to secure the electricity supply to the consumers. The liberalization of the energy market has however led to different actors on the electricity market: consumers, producers, service providers and network operators. These actors have different views on system reliability. Generally, consumers desire a reliable electricity supply, while producers wish to be able to produce electricity and sell this electricity to their customers. The main tasks of the network operators are to connect customers (consumers and producers) and to enable the trade in electrical energy [13]. Whenever customers (load or generation) are interrupted, or whenever the market is hindered, e.g. by transmission restrictions, the power system is not able to fulfill its functions and can be regarded as unreliable. Reliability analysis of power systems should address this by not only focusing on the security of supply for the consumers, but also on the other (financial) risks for TSOs and generating companies (e.g. offshore wind farm owners).

While probabilistic reliability analysis can provide more insight, the presentation and interpretation of the results still remain a challenge. With the many existing calculation methods, a variety of reliability indicators can be calculated. It is often left as a decision of the system operator to decide what values of these reliability indicators are acceptable and desirable. In reality, this decision is complicated: Why would a security of supply of 0.9999 be acceptable and a security of supply of 0.9998 not? In this sense, deterministic criteria have proven to be unambiguous, effective, and easy to translate into decisions and actions. This is the reason why, especially in system operation, deterministic criteria like $n-1$ redundancy are still widely used, and are also prescribed in grid codes like [13]. It therefore remains a challenge to present the results of probabilistic reliability analysis in a clear way and to study the relation between deterministic and probabilistic reliability analysis.

1.2. PROBLEM DEFINITION

In this research, probabilistic reliability analysis is applied to study two major developments of the transmission network in detail: EHV underground cables and offshore networks. For both, the reliability is analyzed considering all factors that are of influence and the impact on the reliability of the onshore power system as a whole. During the research, attention is paid to the presentation of the results in clear reliability indicators while the relation between probabilistic and deterministic methods is compared as well.

The research questions of this thesis can then be described as follows:

- EHV underground cables with respect to transmission networks
  - How can the reliability of EHV underground cable connections be assessed

and compared to the reliability of overhead line connections?
  - What is the impact of EHV underground cable connections on the reliability of large transmission networks?
  - Which measures can be taken to improve the reliability of transmission networks with EHV underground cable connections?
- Offshore networks and onshore power systems
  - How can the reliability of offshore networks be properly assessed to accurately capture the uncertainty introduced by the reliability of the offshore network components?
  - What is the impact of offshore networks on the reliability of onshore power systems in comparison to other risks (like wind/load forecast errors and generator failures)?
  - Should n-1 redundancy be applied in offshore networks or is it possible to arrange offshore redundancy differently?
- Probabilistic reliability analysis of power systems
  - How can the results of probabilistic reliability analysis best be presented?
  - How can the other risks (like financial risks for producers and TSOs) be reflected by reliability indicators?
  - How are the results of probabilistic reliability analysis related to the results of deterministic approaches?

1.3. RESEARCH OBJECTIVE

Based on the research questions, the main research objective can now be described as:

To apply probabilistic reliability analysis to study EHV underground cables and offshore networks, providing insight into the reliability impact of these developments on the onshore transmission network.

This objective can be split into two research objectives:

1. To develop a probabilistic approach to assess the reliability of EHV underground cable connections and the impact on the reliability of large transmission networks.
2. To provide insight into the reliability of offshore networks and the impact on the reliability of onshore power systems in comparison to other reliability risks.

1.4. RESEARCH APPROACH

In this section, the approach followed in this research work is described. In this research, the Dutch transmission network will be used as a test system to develop new methods and obtain insight. As the Dutch transmission network includes the Randstad380 cable connections as well as large-scale offshore wind energy, this network is a suitable

Table 1.1: Research approach.

Research Approach	
Literature study Data collection (load/generation scenario, network model, failure statistics)	
Failure statistic underground cables Reliability of a cable connection Cables in a small EHV network Cables in large transmission networks Solutions to improve the reliability	Characteristics of offshore wind Failure statistics offshore components Reliability of an offshore connection Reliability of near-shore networks Impact on onshore power systems
General conclusions and recommendations	

test system to study the impact of EHV underground cables and offshore networks. The developed models and obtained insight are generally applicable to other transmission networks as well. The simulations and calculations in this research are performed in MATLAB [14].

The general approach followed in this research is shown in table 1.1. The study starts with a literature review and the collection of the required data for the research. After this, the research concentrates on two developments: EHV underground cables and offshore networks. As failure statistics are the main input for probabilistic reliability analysis, first the failure statistics of underground cables are studied. Then, an approach based on reliability networks is developed to assess the reliability of a cable connection. The possibilities to increase the reliability are investigated as well. The impact on the reliability of transmission networks is first studied for a part of the Dutch EHV transmission network. Then, the occurrence of failures in large transmission networks and the risk of further cabling of the network are studied with the focus on the complete Dutch EHV transmission network. Finally, the possible measures to mitigate the risk caused by underground cabling are discussed and ranked according to their efficacy.

For offshore networks, the characteristics of offshore wind are studied first. Then, failure statistics for offshore networks are collected and compared. The reliability of an offshore connection is assessed, after which the reliability of near-shore networks is studied. The impact on the onshore power system is assessed by comparing offshore network redundancy with onshore generation reserve. The results of all these studies are evaluated, and general conclusions about the reliability of offshore networks in respect to onshore power systems are drawn. When considering these two developments of the transmission network, the results of the probabilistic analyses are evaluated based on selected reliability indicators

1.5. OUTLINE OF THIS THESIS

This thesis is organized as follows. First, chapter 2 describes the theoretical background that is needed for the reliability analysis in this research. In chapter 3, the reliability of EHV underground cables and their impact on the reliability of the transmission network is analyzed. Chapter 4 provides an investigation of the reliability of offshore networks and the interplay with onshore transmission networks. General conclusions are drawn in chapter 5, while recommendations and future work are given in chapter 6.

2

PROBABILISTIC RELIABILITY ANALYSIS OF POWER SYSTEMS

2.1. INTRODUCTION

In this thesis, the reliability of transmission networks is analyzed by using a probabilistic approach. To understand the studies described in this thesis, a basic knowledge of probabilistic power system reliability analysis is needed. In this chapter, an overview of the methods used in this research is given. Various methods have been developed for reliability analysis of power systems. Some of these originate from general reliability analysis or mathematics, while other methods have been specially developed for reliability analysis of power systems. Several books are devoted to this topic, for example [15–17]. A more detailed description of the theory presented in this chapter is given in [18].

This chapter is organized as follows. First, the concept of power system reliability is discussed in section 2.2. Then, in section 2.3 the reliability modeling of components is explained. Section 2.4 describes the approaches to study the reliability of small systems, while reliability analysis of large systems is discussed in section 2.5. Finally, some concluding remarks regarding the described methods are given in section 2.6.

2.2. POWER SYSTEM RELIABILITY

2.2.1. RELIABILITY AND RISK

To study the reliability of power systems, first the concept 'reliability' should be defined well. In literature, system reliability is generally defined as [1, 15]:

"*System reliability is the ability of a system to fulfill its function*" (*definition* 1)

For this definition, it must first be clear what a system is. Generally, a system is a group of components, separated from the system environment by a system boundary, and working together to fulfill a system function [1]. A component then, is a part of the

system that is not split up in smaller parts in further analysis [19]. Furthermore, to use this definition of system reliability, it must be clear what the function of the system is. The most basic function of a power system probably is to supply the load. If the load is interrupted, then the power system is not able to fulfill its function and is therefore unreliable. According to this definition, it does not matter *how* the load is supplied (by a conventional generator or by wind energy, by AC overhead lines or by DC underground cables), as long as the load *is* supplied.

Reliability is also related to risk, defined as the product of probability and effect [16]:

"*Risk = Probability x Effect*" (*definition* 2)

Because probability is dimensionless, the risk has the same dimension as the effect: if the effect is expressed in lost money, the risk is expressed in (expected) lost money as well. In reality, the effects of certain events can be diverse. For instance, TenneT TSO uses the Risk Matrix as a tool to determine the risk of future network developments. In the Risk Matrix, seven business values are defined: safety, security of supply, financial, reputation, customers, environment and compliance [20]. For new developments, the risk for each business value is estimated and indicated in the Risk Matrix as shown in figure 2.1. This provides insight into the risks of a new development. The risk matrix assumes a small modification of the definition of risk: the effects are combined with the frequency of an event instead of the probability of an event. Whereas a probability indicates the likelihood that something occurs, a frequency is an indication of how often something occurs. As a consequence, the risk takes over the dimension of the frequency and effect: if the frequency is given in /year and the effect is given as lost money, then the risk has the unit of (expected) lost money/year.

The previously mentioned definition of system reliability, definition 1, is mainly reflected in the Risk Matrix by security of supply. Security of supply is a reliability indicator that reflects the reliability for the consumer, and is often measured as the product of interrupted customers (number or MW) and the duration (hours). In practice, various reliability indicators exist that describe this security of supply (like e.g. the Expected Energy Not Supplied, EENS). Security of supply does not reflect the network reliability for the

		Severity of effect						
		Minor	Very small	Small	Moderate	Considerable	Serious	Extreme
Frequency	Very often							
	Often							
	Regular							
	Probable							
	Possible							
	Unlikely							
	Hardly possible							

Figure 2.1: Risk Matrix used by TenneT TSO. [20]

producers, but this can be seen as a financial risk for the TSO and is therefore included in the business value financial. Some business values in the risk matrix are directly related to the definition of system reliability. For example, the disconnection of consumers causes a financial risk, while large blackouts will also be a risk for the business values reputation, customers and compliance. Safety and environment are less directly related to the basic definition of system reliability.

The actual point-of-view of system reliability depends on the particular study. For example, an offshore wind farm owner might be concerned about the financial risk related to the offshore grid, while he is less interested in the security of supply for the final consumers. A TSO might be mainly concerned with the security of supply, but is as well interested in the other risks as given in the Risk Matrix.

2.2.2. TSO ACTIVITIES

In the planning and operation of power systems, actions are taken in different processes and time horizons [21]. The purpose of these actions is to secure a high reliability level of the power system. The three main processes (i.e. grid development, asset management and system operation) are performed on different time horizons (i.e. long-term, mid-term and short-term), and focus on an actual time scale (decades, years, months, etc.). An overview of some typical TSO activities is given in figure 2.2.

To maintain a high level of reliability, all TSO activities must be performed in the most optimal way. There is always a certain overlap between the different processes. For example, small modifications of the network can be required because of grid development or because of asset management. Also, planned maintenance might be canceled during system operation because of a contingency. In the past, the three processes consisted of more or less separate activities, which can be described as a sequential approach.

In the future, the overlap and interaction between the three main processes is expected to increase, leading to an interacted approach [21]. An illustrative example is the development of offshore grids. Earlier studies, like e.g. [22, 23], showed that offshore network redundancy is mostly not economical. To maintain a high level of relia-

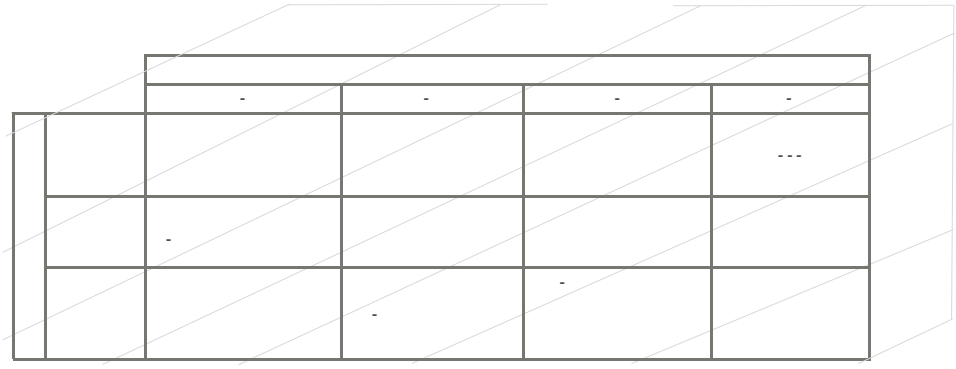

Figure 2.2: Actions performed by the Transmission System Operator [21].

bility of supply, redundancy should be created differently. For example, onshore spinning generation reserve could serve as redundancy for the offshore network. If redundancy is not created in the offshore network (a long-term grid development activity), this has consequences for activities in other time horizons. For example, operational policies would have to be adapted and generation redispatch or load curtailment would be needed more often in short-term system operation. The connection between grid development and operational activities is typically not considered in long-term grid development studies. The relation between long-term grid development and short-term system operation will therefore be studied later in the thesis for the application of EHV underground cables and offshore networks for wind energy.

2.2.3. FRAMEWORK FOR OPERATIONAL RISK ASSESSMENT

In system operation, it is common practice to use a framework of operational risk categories like the one presented in [24]. This framework generally consists of four operating states: normal, alert, emergency and restorative. The preventive/corrective control actions that are performed during system operation are related to the states of this risk framework and to the level of redundancy within the network, as shown in table 2.1.

The table shows that in normal operation, the network is n-1 redundant, such that a single failure will not lead to a failure of the system. In the alert state, there are no serious problems yet, but one more contingency can lead to serious system issues. Because there are just enough components in operation, the alert state corresponds to the n-0 state. The emergency state can also be called the ≥n+1 state [25], because one or more components too much have failed. During an emergency, there are serious overloads and/or overvoltages in the network. If the level of redundancy in the network is higher than in normal operation (≤n-2), the system is in a robust normal operation. The risk categories are also often indicated by colors (red, yellow, green and blue), which gives an easier interpretation during system operation.

The risk framework is especially useful because the system states are directly related to operational control actions. Some typical control actions are shown in table 2.1 as well. For example, in the emergency state, there are serious overloads and/or overvoltages in the network. The TSO has to take immediate action. Corrective generation redispatch and load curtailment are effective actions to relieve the network and to restore n-0 operation. When the network is in the alert state (n-0), there are no serious problems yet, but the TSO can perform preventive actions to avoid possible emergency situations. Preventive redispatch is one of the actions taken in the alert state. The objective of preventive redispatch is to restore n-1 redundancy. During normal operation, the network is

Table 2.1: Risk categories, n-α states and TSO activities.

Risk category	Color	Redundancy state	Operational control actions
Emergency	Red	≥n+1	Corrective redispatch/ Load curtailment
Alert	Orange	n-0	Preventive redispatch
Normal	Green	n-1	Maintenance rescheduling
Robust normal	Blue	≤n-2	

n-1 redundant and no corrective actions are required. Still, the TSO can perform actions like maintenance rescheduling to prevent the network from going to the alert state.

In fact, there are two kinds of remedial actions:

1. Modifying the network: This can be done by switching actions, using Phase Shifting Transformers (PSTs), or by canceling maintenance activities.

2. Changing the load/generation: This can be done by preventive/corrective redispatch, wind curtailment, or load curtailment.

In practice, the different remedial actions cause different (financial) risks, as modifying the network does not require the interruption of customers. Switching actions and the use of PSTs are preferred. Then, generation redispatch can be applied or maintenance can be canceled. Load curtailment is the last resort as this leads to high (societal) costs.

In system operation and planning practice, the reliability of the network is still often regarded from a deterministic point-of-view. This means for example that the network is in the n+1 state, or not. And corrective control actions are performed, or not. And this is the same for the n-0 state and preventive control actions. Reality is however less clear. For example, in some cases it might be worth to take the risk of being in the n-0 state for a short time. Generally, it could be helpful if more would be known about the probability that the network is in each of these states, such that the necessity of taking risk mitigating actions becomes quantitative. What is the frequency and extent of corrective/preventive redispatch control actions? And if the network is 10h/y not n-1 redundant, what is then the probability of the emergency state (n+1)? These questions cannot be answered by deterministic criteria alone, but could be answered by combining the results of probabilistic reliability analysis with these deterministic criteria and the risk framework.

2.3. RELIABILITY ANALYSIS OF COMPONENTS

2.3.1. UNREPAIRABLE COMPONENTS

In reliability analysis of components, a distinction can be made between repairable components and unrepairable components. To describe the failure behavior of components without repairs, several basic reliability functions are defined [1, 26]:

- $F(t)$: **Unreliability function** or **failure distribution** [-]
  The probability of finding a healthy component in a failed state after time t.

- $R(t)$: **Reliability function** [-]
  The probability of finding a healthy component in a healthy state after time t.

- $f(t)$: **Failure density distribution** [/y]
  The rate at which a component fails at time t.

- $h(t)$: **Hazard rate** [/y]
  The rate at which a component fails at time t, given that it is healthy until time t.

Table 2.2 shows the relation between the different reliability functions.

When studying the failure behavior of components in practice, it is found that the hazard rate often follows the so-called bathtub curve as shown in figure 2.3. The bathtub

Table 2.2: Relation between reliability functions [26].

Function of:	$f(t)$	$F(t)$	$R(t)$	$h(t)$
$f(t) =$	$f(t)$	$\frac{dF(t)}{dt}$	$-\frac{dR(t)}{dt}$	$h(t)e^{-\int_0^t h(t)dt}$
$F(t) =$	$\int_0^t f(t)dt$	$F(t)$	$1-R(t)$	$1-e^{-\int_0^t h(t)dt}$
$R(t) =$	$\int_t^\infty f(t)dt$	$1-F(t)$	$R(t)$	$e^{-\int_0^t h(t)dt}$
$h(t) =$	$\frac{f(t)}{\int_t^\infty f(t)dt}$	$\frac{\frac{dF(t)}{dt}}{1-F(t)}$	$-\frac{d(lnR(t))}{dt}$	$h(t)$

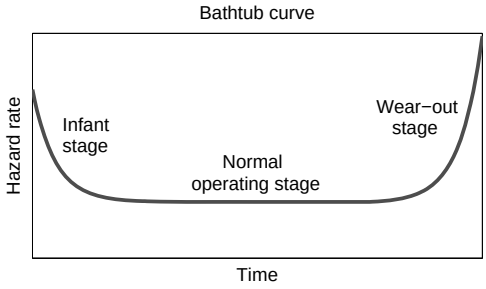

Figure 2.3: Bathtub curve of component failures.

curve shows that a component first experiences an infant stage with a decreasing hazard rate. In this infant stage, the hazard rate is larger because some components are still vulnerable to early failures like production failures. Then, a normal operating stage follows in which the hazard rate stays constant. Finally, the component reaches the wear-out stage, in which the hazard rate increases significantly. In this stage, the component reaches its end-of-life and failures like wear-out failures are very likely to occur.

A constant hazard rate is often assumed in reliability analysis and is then called the failure rate (λ). If a constant failure rate is assumed, the reliability functions become [1]:

$$h(t) = \lambda \tag{2.1}$$

$$F(t) = 1 - e^{-\lambda t} \tag{2.2}$$

$$R(t) = 1 - F(t) = e^{-\lambda t} \tag{2.3}$$

$$f(t) = \frac{dF(t)}{dt} = \lambda e^{-\lambda t} \tag{2.4}$$

Where:
$F(t)$ = failure distribution (or unreliability function) [-]
$R(t)$ = reliability function [-]
$f(t)$ = failure density distribution [/y]
$h(t)$ = hazard rate [/y]
λ = failure rate [/y]
t = time [y]

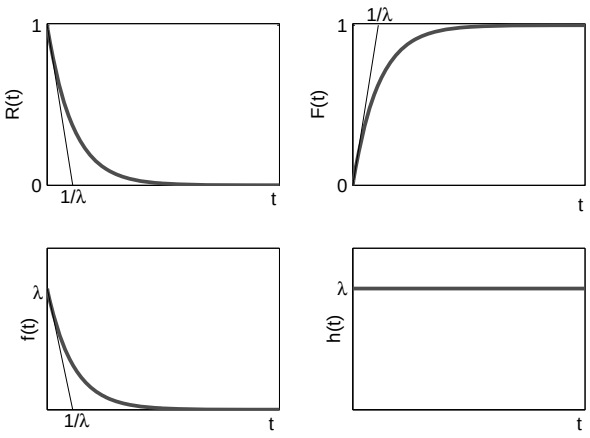

Figure 2.4: Reliability functions according to the exponential distribution.

In figure 2.4, the graphs of these reliability functions are shown. The probability distribution of the reliability function is known as the (negative) exponential distribution. As generally a constant failure rate is assumed, this exponential distribution is often used in reliability analysis. The exponential distribution has some characteristics that make further reliability analysis easier. For example, the expected lifetime according to the exponential function is $\frac{1}{\lambda}$.

2.3.2. REPAIRABLE COMPONENTS

In power systems, most components are repairable. If a component fails, it is repaired and brought back into operation. Consequently, a component then follows a component life cycle which consists of periods in which the components is working and periods in which the component is out of service, as illustrated in figure 2.5. In the figure, several parameters are indicated which describe the failure behavior of components [16]:

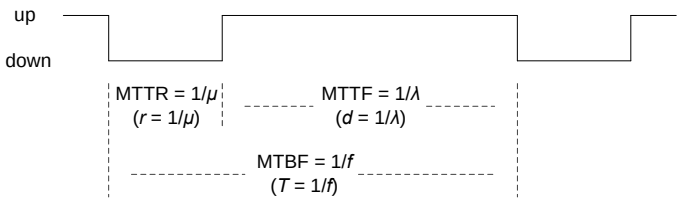

Figure 2.5: Life cycle of a component.

- **MTTF** (or ***d***): **Mean Time To Failure** [y]
  The average time it takes for a healthy component before it fails.

- **MTTR** (or ***r***): **Mean Time To Repair** or **Repair Time** [y]
  The average time it takes to repair a failed component.

- **MTBF** (or ***T***): **Mean Time Between Failures** [y]
  The average time between two failures of the component.

From these parameters, some other parameters can be derived (when assuming the negative exponential distribution) [16, 27]:

- $\boldsymbol{\lambda} = 1/\text{MTTF}$ (or $\lambda = 1/d$): **Failure rate** [/y]
  The rate at which a healthy component fails.

- $\boldsymbol{\mu} = 1/\text{MTTR}$ (or $\mu = 1/r$: **Repair rate** [/y]
  The rate at which a failed component is repaired.

- $\boldsymbol{f} = 1/\text{MTBF}$ (or $f = 1/T$: **Failure frequency** [/y]
  The average frequency at which a component fails.

- **A**$= d/T$: **Availability** [-]
  The probability that a component is found in a healthy state at an arbitrary time
  (or: The average fraction of time that a component is in a healthy state.)

- **U**$= r/T$: **Unavailability** [-]
  The probability that a component is found under repair at an arbitrary time
  (or: The average fraction of time that a component is under repair after a failure.)

Although these parameters can be given in any time unit, it is recommended to use the same unit for all parameters to keep consistency. This to avoid mistakes when using these parameters in further reliability calculations. In practice, the repair time is often given in hours. It can be changed to the unit years easily by dividing the repair time in [h] by 8760 [h/y].

2.3.3. TWO-STATE MARKOV MODEL

Another model often used in reliability analysis of components is the Markov model [1, 26]. A Markov model is a stochastic model based on the states in which a system can reside and the possible transitions between these states. The two stochastic variables state (S) and time (t) play an important role. These two variables can either be discrete or continuous, leading to four different kinds of Markov models. The case in which the states are discrete and the time continuous is the most common for reliability analysis and is also called Markov process. If the transition rates in a Markov model are independent of the time, the Markov model is called homogeneous and the state transitions can be described by failure and repair rates (λ & μ).

Figure 2.6 shows the Markov model of a single (unrepairable) component. As can be seen, it consists of an UP and a DOWN state, called S_0 and S_1. The probabilities of these states can be indicated as P_{S_0} and P_{S_1}. The figure also shows the state transition from

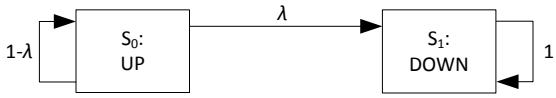

Figure 2.6: Two-state Markov model of an unrepairable component.

state S_0 to S_1, which is the failure process of the component (described by the failure rate). State transitions from and to the same state are normally omitted from the model.

The state transitions can also be described by the transition matrix:

$$T = \begin{bmatrix} 1-\lambda & \lambda \\ 0 & 1 \end{bmatrix} \tag{2.5}$$

Where:
T = transition matrix
λ = failure rate [/y]

For a repairable component, the repair process is included in the two-state Markov model as well. As shown in figure 2.7, this is the state transition from state S_1 to state S_0. The state transitions are now indicated with the failure rate (λ) and repair rate (μ), respectively. The transition matrix now becomes:

$$T = \begin{bmatrix} 1-\lambda & \lambda \\ \mu & 1-\mu \end{bmatrix} \tag{2.6}$$

Where:
T = transition matrix
λ = failure rate [/y]
μ = repair rate [/y]

Although Markov models can describe the time-behavior of systems (e.g. a new component is more likely to be in the UP-state, while it is more likely to be in the DOWN-state as time increases), Markov models are often assumed to be in equilibrium in reliability analysis. In equilibrium, the state probabilities do not change with time anymore and have become time-independent. For the transition matrix, this means [16]:

$$\mathbf{p}T = \mathbf{p} \tag{2.7}$$

$$\mathbf{p}(T - I) = \mathbf{0} \tag{2.8}$$

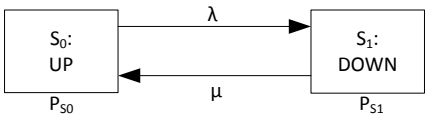

Figure 2.7: Two-state Markov model of a repairable component.

Where:
p = state probability vector [-]
I = identity matrix

From the state transitions in a Markov model, the (state) transition frequencies describe how often these state transitions occur. The (state) transition frequencies can be calculated as:

$$f_{S_i \to S_j} = P_{S_i} h_{ij} \tag{2.9}$$

Where:
S_i = state i
$f_{S_i \to S_j}$ = transition frequency from state S_i to state S_j [/y]
P_{S_i} = probability of state S_i [-]
h_{ij} = transition rate from state S_i to state S_j [/y]

Equilibrium also means that the sum of the (state) transition frequencies entering a state must be equal to the sum of the state transition frequencies leaving a state:

$$\sum f_{in} = \sum f_{out} \tag{2.10}$$

Where:
f_{in} = transition frequency entering a state [/y]
f_{out} = transition frequency leaving a state [/y]

Furthermore, as the system must be in one of the Markov states:

$$\sum P_{S_i} = 1 \tag{2.11}$$

These equilibrium conditions can be used to calculate the state probabilities in equilibrium. Equilibrium normally occurs when $t \to \infty$.

2.4. RELIABILITY ANALYSIS OF SMALL SYSTEMS

2.4.1. RELIABILITY NETWORKS

In the previous section, it was discussed how the reliability of repairable components can be described by their availability (A) and unavailability (U). When individual components are interconnected, small networks are created. These networks can be modeled by reliability networks. One must be aware here of the fact that the network configuration in reliability analysis does not necessarily have to be similar to the network configuration in reality. For example, when all components of a parallel network are needed for correct operation, the network is a series connection in reliability analysis.

Figure 2.8 shows a series connection of components. The connection is available if all of the individual components are available, such that the availability of the connection becomes the product of the availabilities of the components [1, 16]:

$$A_{total} = \prod_{i=1}^{N} A_i \tag{2.12}$$

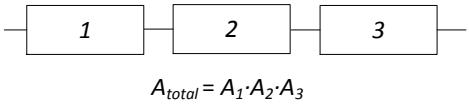

Figure 2.8: Series Connection.

Where:
A_{total} = availability of the connection [-]
N = number of components in the connection [-]
A_i = availability of component i [-]

Figure 2.9 shows a parallel connection of components. The availability of the connection now depends on the number of components that is minimally required to have a working connection. If at least one component is required, it is called a 1-out-of-N connection. The connection is then unavailable if all of the individual components are unavailable, such that the unavailability of the connection becomes the product of the unavailabilities of the components [1, 16]:

$$U_{total} = \prod_{1}^{N} U_i \tag{2.13}$$

Where:
U_{total} = unavailability of the connection [-]
N = number of components in the connection [-]
U_i = unavailability of component i [-]

If all components of a parallel network need to be available for a working connection, the connection is unavailable if any of the components is unavailable. This is effectively the same as a series connection of the components. And if at least M components of a parallel connection of N components are needed for a working connection, this is called an **m-out-of-N** connection [1]. If all components have the same availability A_0, the avail-

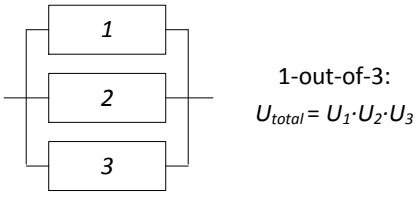

Figure 2.9: Parallel Connection (1-out-of-N).

ability of the total connection can then be calculated by:

$$A_{total} = \sum_{i=m}^{N} \binom{N}{i} (A_0)^i (1 - A_0)^{(N-i)} \tag{2.14}$$

Where:
A_{total} = availability of the connection [-]
N = number of components in the connection [-]
m = number of components needed for a working connection [-]
A_0 = availability of the individual components [-]

In practice however, these m-out-of-N networks are somewhat more complicated. The equations above assume that the connection is either available or unavailable (as $A = 1 - U$) and the connections is either reliable or unreliable (as $R(t) = 1 - F(t)$). In reality, if there are two connections in parallel and one of these fails, still half the transmission capacity is available. Therefore, in practical studies, often the probabilities of having a certain transmission capacity are calculated.

Dependent (common-cause) failures can be included in series-parallel networks as well. Mostly, these common-cause failures are modeled as a separate component which is placed in series with the components that can fail dependently [1]. This is illustrated in figure 2.10.

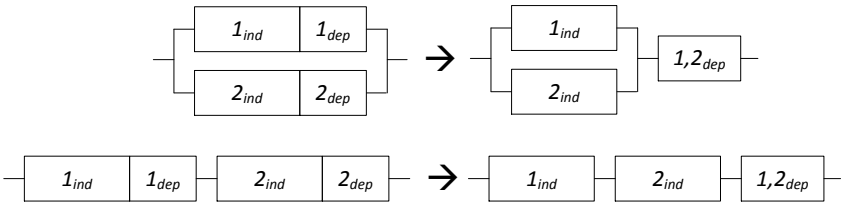

Figure 2.10: Modeling of dependent (common-cause) failures.

2.4.2. MARKOV MODELS

In section 2.3.3, it was described how the reliability of individual components can be modeled by a two-state Markov model. Markov models can be expanded to include more states. In this way, a Markov model can represent more system states of the same component. Moreover, the reliability of a (small) system of individual components can effectively be modeled by a Markov model.

A Markov model can be created in the following steps:

1. Start with a system state in which all components are working.
2. From this 'all-ok' state, investigate which component failures can occur.
3. For every possible component failure, draw a new system state. The transition rate to this new system state is the failure rate of the specific component.
4. For every new system state, investigate what failures (or repairs) might occur next:
   - If a failure (or repair) leads to a new system state, draw this system state. The transition rate to this new system state is the failure rate (or repair rate) of the specific component.
   - If a failure (or repair) leads to an already existing system state, the transition rate to this existing system state is the failure rate (or repair rate) of the specific component.
5. Repeat step 4 until there are no other new states or state transitions.
6. Double check whether all possible system states and state transitions are included in the Markov model.
7. If necessary and possible, apply reduction techniques to reduce the size of the Markov model.
8. Indicate in the Markov model the different categories of the system states: (e.g. system is working or defect, system works at full/half/zero capacity).

To calculate the state probabilities in equilibrium, the matrix equation 2.8 must be solved. Or, for every state of the Markov model equation 2.10 must apply. Under the condition of equation 2.11. Figure 2.11 shows a Markov model for two transformers and one spare.

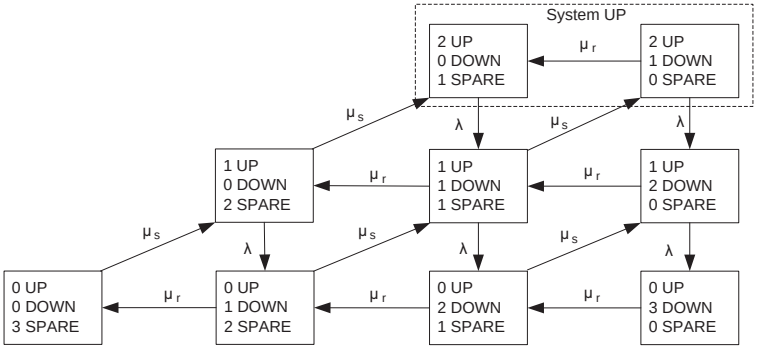

Figure 2.11: More advanced state model.

2.4.3. FAULT TREE AND EVENT TREE ANALYSIS

System outages can be the result of various causes. For some systems, it can be complicated to study the impact of these various causes on the reliability of the system by reliability models like reliability networks and Markov models. In other cases, it might be desired to obtain knowledge about the direct relation between cause and effect. In these cases, an investigation of the component failures that finally lead to a system failure can be made by creating a fault tree or event tree [1, 19].

Fault tree analysis is an analytical technique which describes by boolean operators how individual component failures can lead to a failure of the complete system. A fault tree consists of events and boolean operators, as shown in figure 2.12.

In figure 2.13, two example fault trees are shown, one using an AND-gate and the other using an OR-gate. On top of the fault trees is the top event, which is a failure of the system in this case. On the bottom are the basic events, which are the component failures of component A and B in this case. If the probabilities of the basic events are described by $P[A]$ and $P[B]$, the probability of the top event for the AND-gate can be

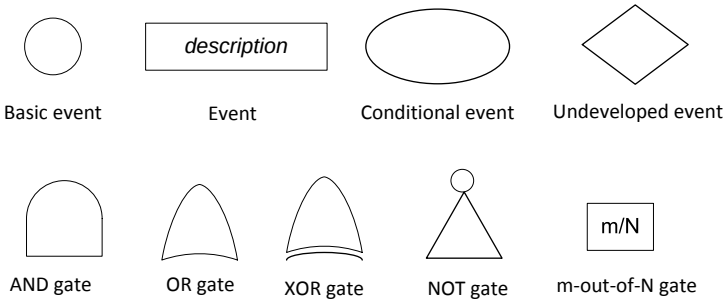

Figure 2.12: Fault tree symbols.

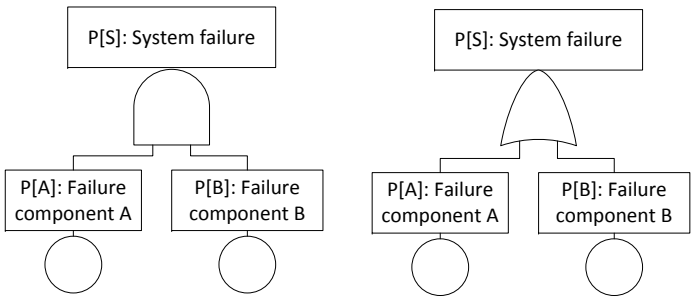

Figure 2.13: OR-gate and AND-gate.

calculated by [28]:

$$P[S] = P[A \cap B] = P[AB] = P[A|B]P[B] \tag{2.15}$$

Where:
S, A, B = event S, A, B
$P[S]$ = probability of event S [-]
$\cap$ = intersection operator
$P[A \cap B]$ = probability that event A and event B occur [-]
$P[A|B]$ = probability of event A, given that event B occurs [-]

If events A and B are independent, $P[A|B] = P[A]$ and:

$$P[S] = P[A \cap B] = P[AB] = P[A]P[B] \tag{2.16}$$

The probability of the top event for the OR-gate can be calculated by [28]:

$$P[S] = P[A \cup B] = P[A] + P[B] - P[AB] \tag{2.17}$$

Where:
$\cup$ = union operator
$P[A \cup B]$ probability that event A or event B occurs [-]

If events A and B are independent:

$$P[S] = P[A \cup B] = P[A] + P[B] - P[A]P[B] \tag{2.18}$$

In most reliability studies, the probabilities of the basic events are very small. If $P[A] \approx 0$ and $P[B] \approx 0$, then $P[A]P[B] \ll P[A] + P[B]$, such that:

$$P[S] \approx P[A] + P[B] \tag{2.19}$$

Event tree analysis is a variation to fault tree analysis. The main difference is that fault tree analysis studies the combination of component failures that lead to a system failure, while event tree analysis studies the sequence of events that lead to a system failure [19, 29, 30]. It is therefore especially useful to study the response of a system to component failures, like the response of the protection system.

Figure 2.14 shows an example of an event tree. It can be seen that an event tree is drawn from left to right, in contrast to the fault tree, which is drawn from top to bottom. On the left of the event tree is the initiating event, which can be a component failure like a short-circuit. The initiating event will induce a secondary event, which can be the operation of the protection system. In this example, if the protection system works properly, there will not be a system failure. However, if the protection system fails, this will result into the final event: a failure of the system.

The probabilities of the final states of the event tree can be calculated from the probabilities of the initial event and the events that follow. Here, it must be realized that the probabilities of these secondary (and further) events are conditional probabilities. In the example of figure 2.14, the probability must be known that the protection system fails if the initial event occurs. The probability of a system failure can then be calculated by:

$$P[\text{system failure}] = P[\text{protection system fails}|\text{initiating event}] \cdot P[\text{initiating event}] \tag{2.20}$$

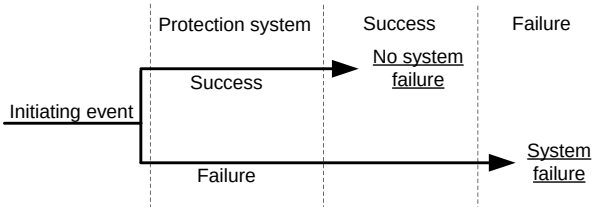

Figure 2.14: Example event tree.

Sometimes, the failure frequency of the initiating event is used instead of its probability. This is possible and results into the failure frequency of the final event as the other (conditional) probabilities are dimensionless:

$$f[\text{system failure}] = P[\text{protection system fails}|\text{initiating event}] \cdot f[\text{initiating event}] \quad (2.21)$$

In most systems, there are many initiating events possible. Then, event trees are made for every possible initiating event. The results of these event trees are then combined to calculate the total probability of a system failure, for example by adding up the probabilities of a system failure. Similar to the fault tree, it is then assumed that the probabilities of the initiating events are small and that the initiating events are independent.

2.5. RELIABILITY ANALYSIS OF LARGE SYSTEMS

2.5.1. GENERATION ADEQUACY ANALYSIS

In generation adequacy analysis, the reliability of the generation system is studied. Generation adequacy analysis is based on the stress-strength model used to study the reliability of components. In generation adequacy analysis, the total load in the power system is the system stress, while the strength of the generation system (i.e. all generators together) is the system strength. If the load level is higher than the capacity of the available generators, the generation system fails to serve the load. This is illustrated in figure 2.15. The area where the capacity of the generation system is smaller than the total system load is the area where the generation system fails. The transmission network is normally not considered and is modeled as a copper plate.

Both the system load and the generation capacity must be described by probability distributions. The distribution of the load is mostly based on historical load levels, which can be combined with expected future load developments. In its simplest form, it can be a normal distribution (with mean and variance), but most domestic load shows a combination of two normal distributions (day/night load levels). Also, a histogram of historical load values (e.g. hourly load values for one year) is possible.

The generation system must be represented by a probability distribution as well. This can be done by constructing a Capacity Outage Probability Table (COPT) [15] of the generation system. A COPT is a table that gives an overview of the possible generation capacity outages and the corresponding probabilities. The basic input information are the

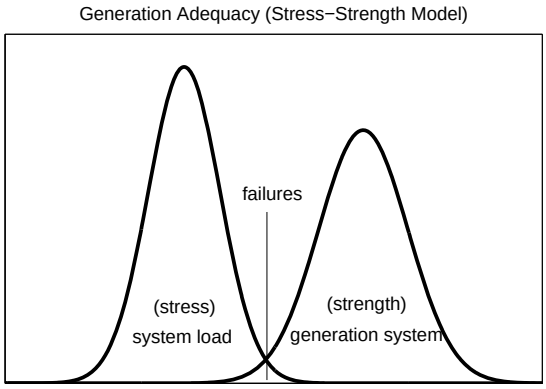

Figure 2.15: Generation adequacy.

capacities of the generators and their (forced) unavailabilities. For the calculation of the COPT of large generation systems, a structured algorithm is described in [15]. According to this algorithm, a COPT can be created in a few steps:

1. Start with the first generator and create a COPT for this generator. If we assume that the capacity of the first generator is C_{g1} and the (forced) unavailability U_{g1}, the COPT of this generator becomes as follows:

Table 2.3: COPT of a single generator.

C_{out} [MW]	P [-]	$1-\sum_1^{n-1} P$[-]
0	A_{g1}	1
C_{g1}	U_{g1}	U_{g1}

2. Now a second generator is considered, with capacity C_{g2} and (forced) unavailability U_{g2}. Two new (temporary) COPTs can be created, based on the initial COPT of the first generator. The first new COPT reflects the case where the second generator is available, while the second new COPT reflect the case where the second generator is unavailable. The first new COPT is created by multiplying the probabilities in the second column of the initial COPT by A_{g2}, while the second new COPT is created by multiplying the probabilities in the second column of the initial COPT by U_{g2}. The third column can be left empty. The two new COPTs now become as follows:

Table 2.4: 2 new COPTs for the second generator.

C_{out} [MW]	P [-]	$1-\sum_1^{n-1} P$[-]
0	$A_{g1}A_{g2}$	
C_{g1}	$U_{g1}A_{g2}$	

C_{out} [MW]	P [-]	$1-\sum_1^{n-1} P$[-]
C_{g2}	$A_{g1}U_{g2}$	
$C_{g1}+C_{g2}$	$U_{g1}U_{g2}$	

3. The two new COPTs are now merged into one COPT for the two generators, such that the capacity outages are increasing. If capacity outages happen to be the same, the probabilities of these capacity outage can be added. The third column starts with 1 and for every following cell within this column, the probability in the cell on the left is subtracted. Assuming that $C_{g2} < C_{g1}$, the combined COPT becomes as shown below:

Table 2.5: Combined COPT for the two generators.

C_{out} [MW]	P [-]	$1 - \sum_1^{n-1} P$[-]
0	$A_{g1}A_{g2}$	1
C_{g2}	$A_{g1}U_{g2}$	$1 - A_{g1}A_{g2}$
C_{g1}	$U_{g1}A_{g2}$	$1 - A_{g1}A_{g2} - A_{g1}U_{g2}$
$C_{g1} + C_{g2}$	$U_{g1}U_{g2}$	$1 - A_{g1}A_{g2} - A_{g1}U_{g2} - U_{g1}A_{g2}$

4. Steps 2 and 3 are now repeated for every next generator, until all generators are included in the COPT. Care must be taken when combining the two temporary COPTs. The third column can be left empty until the final COPT is created.

With the COPT, probabilistic indicators known as the Loss-of-Load and Loss-of-Energy Indices can be calculated to show the reliability of the generation system [15]. Some of these indicators are:

- **LOLP**: **Loss Of Load Probability** [-]
  The probability that the demanded power cannot be supplied (partially or completely) by the generation system. The LOLP is often determined based on a per-hour study for a studied time period (usually a year).

$$LOLP = P[C < L] = \frac{\sum_{i=1}^{n} P_i[C_i < L_i]}{n} \tag{2.22}$$

  Where:
  $P[C < L]$ = probability that the generation capacity is smaller than the load [-]
  $P_i[C_i < L_i]$ = probability that the gen. capacity is smaller than the load for hour i [-]
  C = total available generation capacity [MW]
  C_i = total available generation capacity for hour i [MW]
  L = total load level [MW]
  L_i = total load level for hour i [MW]
  n = total time of the studied period (8760h for a whole year) [h]

- **LOLE**: **Loss Of Load Expectation** [h/y]
  Expected amount of time per period that the demanded power cannot be supplied (partially or completely) by the generation system.

$$LOLE = \sum_{i=1}^{n} P_i[C_i < L_i] = n \cdot LOLP \tag{2.23}$$

Where:
$P_i[C_i < L_i]$ = probability that the gen. capacity is smaller than the load for hour i [-]
C_i = total available generation capacity for hour i [MW]
L_i = total load level for hour i [MW]
n = total time of the studied period (8760h for a whole year) [h]
$LOLP$ = loss of load probability [-]

- **LOEE**: **Loss Of Energy Expectation** [MWh/y]
  Total amount of energy that is expected not to be supplied during a given time period (usually on a yearly basis) because of failures of the generation system.

$$LOEE = \sum_{i=1}^{n} \sum_{j \in S_g} P_j L_{i,j} \tag{2.24}$$

Where:
P_j = probability of generation capacity outage j [-]
$L_{i,j}$ = not delivered load because of capacity outage j for hour i [MW]
n = total time of the studied period (8760h/y for a whole year) [h]
S_g = set of possible generation capacity outages

In reality, not all generators are always available. For example, it might be necessary to consider the maintenance and start-up times of generators. Some generators will be unavailable because of planned maintenance, other generators (like coal power plants) might not be available within a short time. A COPT can then be made of the generators that can become available within the desired time interval. This COPT can also vary throughout the year. Using these COPTs, a more accurate calculation of the generation system reliability can be performed for the conditions of a specific study.

2.5.2. STATE ENUMERATION

For large systems, special reliability analysis approaches were developed. One of these approaches is state enumeration. Before describing state enumeration into detail, it is helpful to discuss deterministic contingency analysis before. In deterministic contingency analysis, components are taken out of the power system in a simulation. It is analyzed whether component failures lead to serious issues in the power system, like component overloading and over- and under-voltages.

The procedure which is followed is illustrated in figure 2.16. Normally, the results of the simulations are used to determine whether the system meets certain deterministic criteria. For example, the n-1 redundancy criterion states that a failure of a single component must not result into a failure of the power system. Deterministic contingency analysis is performed up to a certain level. Usually, single contingencies and certain critical (dependent) double contingencies are considered. There are too many higher-order contingencies to analyze, while the probabilities of these failure states are usually assumed very small.

State enumeration follows a rather similar approach as deterministic contingency analysis. In state enumeration, system states are defined according to their order of failure as well, as illustrated in figure 2.16. The lower-order states, with less component

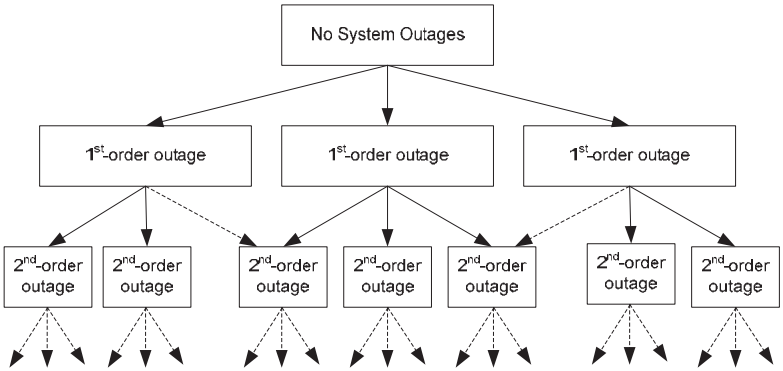

Figure 2.16: State enumeration.

failures and a higher probability, are considered first. Then the higher-order states, with more failures and lower probability, are considered. It is assumed that the lowest-order states, with the highest probability, are representative for the system reliability. State enumeration is mainly used in systems with low failure probabilities and when no additional information like probability distributions or switching sequence is required.

The main difference with deterministic contingency analysis is that in state enumeration, the probabilities and the effects of the states combined to calculate probabilistic reliability indicators. Security-of-supply probably is the most important indicator. It is of interest to determine how often, how long and how much load is disconnected. Some probabilistic reliability indicators directly related to this are [15, 17, 31]:

- **PLC**: **Probability of Load Curtailment** [-]
  The probability that the demanded load cannot be supplied (partially or completely). The PLC is often determined based on a set of considered contingencies (single contingencies as well as higher-order contingencies) and a studied time period (usually on a yearly basis).

$$PLC = \sum_{i \in S_c} (P[load\ curt.|i] \cdot P_i) = \sum_{i \in S_c} \left(\frac{t_i}{T} \cdot P_i \right) \tag{2.25}$$

  Where:

i	contingency i
S_c	= set of considered contingencies
$P[load\ curt.|i]$	= probability that contingency i causes load curtailment [-]
P_i	= probability of contingency i [-]
t_i	= total time that there is load curtailment during the studied period, given that contingency i is present [h]
T	= total time of the studied period [h]

- **EENS**: **Expected Energy Not Supplied** [MWh]
  Total amount of energy that is expected not to be supplied during a given time

period (usually on a yearly basis) due to supply interruptions.

$$EENS = \sum_{i \in S_c} (E_i \cdot P_i) \tag{2.26}$$

Where:
S_c = set of considered contingencies
E_i = total curtailed energy in the study period if contingency i is present [MWh]
P_i = probability of contingency i [-]

- **SAIDI**: **System Average Interruption Duration Index** [min]
  Average outage duration of each customer during a given time period (usually on a yearly basis).

$$SAIDI = \frac{\sum_i^n (r_i \cdot N_i)}{N_t} \tag{2.27}$$

Where:
n = number of interruptions [-]
r_i = duration of interruption i [min]
N_i = number of customers not served by interruption i [-]
N_t = total number of customers [-]

- **SAIFI**: **System Average Interruption Frequency Index** [-]
  Average number of interruptions per customer during a given time period (usually on a yearly basis).

$$SAIFI = \frac{\sum_i^n (N_i)}{N_t} \tag{2.28}$$

Where:
n = number of interruptions [-]
N_i = number of customers not served by interruption i [-]
N_t = total number of customers [-]

- **CAIDI**: **Customer Average Interruption Duration Index** [min]
  Average interruption duration per interrupted customer during a given time period (usually on a yearly basis).

$$CAIDI = \frac{\sum_i^n (r_i \cdot N_i)}{\sum_i^n N_i} = \frac{SAIDI}{SAIFI} \tag{2.29}$$

Where:
n = number of interruptions [-]
r_i = duration of interruption i [min]
N_i = number of customers not served by interruption i [-]

As already discussed before, the interruption of consumers is not the only risk of a TSO. The disconnection of producers and generator redispatch can be as risk as well. Also, a combination of probabilistic reliability analysis and the risk framework would be useful to obtain insight about how often the transmission network is in a particular risk state. Therefore, additional probabilistic reliability indicators can be defined [31]:

- **Probability of Overload** [-]
  The probability that one or more connections in the network are overloaded during a given time period (usually on a yearly basis).

$$P_{overload} = \sum_{i \in S_c} (P[overload|i] \cdot P_i) = \sum_{i \in S_c} \left(\frac{t_{ovl,i}}{T} \cdot P_i \right) \tag{2.30}$$

  Where:
  S_c = set of considered contingencies
  $P[overload|i]$ = probability that contingency i causes an overloaded connection [-]
  P_i = probability of contingency i [-]
  $t_{ovl,i}$ = total time that there is an overload during the studied period, given that contingency i is present [h]
  T = total time of the studied period [h]

- **Probability of Generation Redispatch** [-]
  The probability that generation redispatch is applied during a given time period (usually on a yearly basis).

$$P_{redispatch} = \sum_{i \in S_c} \left(P[redispatch|i] \cdot P_i \right) = \sum_{i \in S_c} \left(\frac{t_{rd,i}}{T} \cdot P_i \right) \tag{2.31}$$

  Where:
  S_c = set of considered contingencies
  $P[redispatch|i]$ = probability that contingency i causes generation redispatch [-]
  P_i = probability of contingency i [-]
  $t_{rd,i}$ = total time that redispatch is applied during the studied period, given that contingency i is present [h]
  T = total time of the studied period [h]

- **Expected Redispatch Costs** [currency]
  Expected costs of generation redispatch during a given time period (usually on a yearly basis).

$$C_{redispatch} = \sum_{i \in S_c} \left(C_{rd,i} \cdot P_i \right) \tag{2.32}$$

  Where:
  S_c = set of considered contingencies
  $C_{rd,i}$ = total redispatch costs during the study period, given that contingency i is present [currency]
  P_i = probability of contingency i [-]

- **Probability of the Alert State** [-]
  The probability that the power system is in the alert state during a given time period (usually on a yearly basis).

$$P_{alert} = \sum_{i \in S_c} (P[alert|i] \cdot P_i) = \sum_{i \in S_c} \left(\frac{t_{al,i}}{T} \cdot P_i \right) \tag{2.33}$$

Where:

S_c	= set of considered contingencies
$P[alert\|i]$	= probability that contingency i leads to the alert state [-]
P_i	= probability of contingency i [-]
$t_{al,i}$	= total time that the network is in the alert state during the studied period, given that contingency i is present [h]
T	= total time of the studied period [h]

Figure 2.17 shows a typical state enumeration algorithm. The algorithm studies every contingency that has to be considered. Contingencies can be described in contingency lists, e.g. a list of independent single contingencies and a list of dependent double contingencies. Failure states up to a certain order are analyzed, such that for example independent single contingencies, dependent double contingencies, and combinations of two of these are considered.

For every studied contingency, a certain snapshot of the system generation and load is considered. This can, for example, be a specific hour of a year scenario, but could also be sampled from set of generation/load snapshots. Then, a load flow is performed. This can be a dc load flow, if only active power is to be considered, or an ac load flow, if reactive power and voltage behavior is to be studied as well. If any problems in the network are found, like component overloading or over-/undervoltages, remedial actions must be applied to relieve the network. Typical remedial actions are local generation redispatch, international generation redispatch and load curtailment. Remedial actions are performed until the load flow does not show any problems in the network. The state enumeration proceeds until all generation/load snapshots and all to be studied contingencies are considered. The results of the remedial actions are then collected and reliability indicators are calculated.

State enumeration shares some characteristics with Markov models. System states and state transitions are described in both methods. In both methods, the probabilities of the system states can be calculated by the product of the component (un)availabilities. Also, the equation for the state transition frequencies can be applied to state enumeration as well. This is particularly useful when calculating state probabilities and state transition frequencies in a state enumeration.

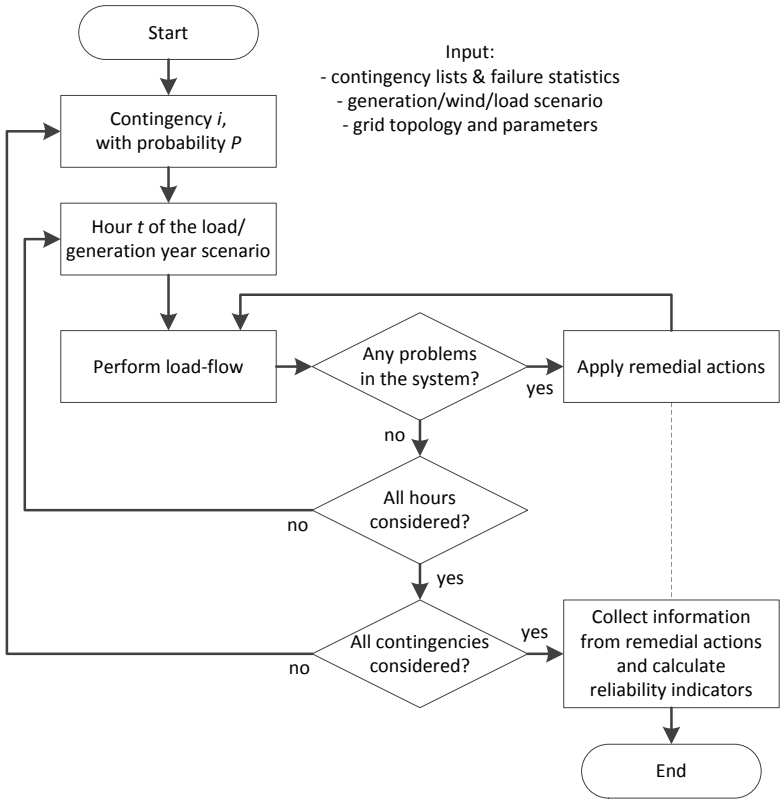

Figure 2.17: Typical algorithm of state enumeration.

2.5.3. MONTE-CARLO SIMULATION

Monte Carlo simulation is another approach to analyze the reliability of large power systems. Monte Carlo simulation is a computer simulation in which the system behavior is simulated and from which results like probabilistic reliability indicators are extracted. Because it is a simulation of the system, it is possible to include real system behavior like load/generation time series, switching actions and protection systems into the study. Monte Carlo simulation is applied to a wide variety of studies, not only power system reliability analysis.

One characteristic of Monte Carlo simulation is that it is less sensitive to the complexity and dimension of the studied problem [32]. In fact, the accuracy of the results is directly related to the required number of simulations. The benefit is that studying a more complex system does not require more simulations. But the disadvantage is that the number of simulations mostly has to be very large in order to obtain a reasonable ac-

curacy of the results. This disadvantage is such big that Monte Carlo simulation is often considered as a last resort.

Monte Carlo simulation basically consists of three parts:

1. Sampling of component failures
2. System simulation (load flow, remedial actions)
3. Processing of results

In Monte Carlo simulation, a distinction can be made between sequential and non-sequential Monte Carlo simulation. In a non-sequential Monte Carlo simulation, time is not considered. For every simulation instant, the load and generation are sampled from a load/generation probability distribution and the component failures are sampled using their unavailabilities. In a sequential Monte Carlo simulation, the time is considered. This means that the load and generation follow a time scenario, for example a year scenario of hourly values. For the component failures, the time to failure and time to repair are then sampled, mostly from the exponential distribution.

Sampling from the component (un)availabilities in a non-sequential Monte Carlo simulation is straightforward. If u is a sample from the unit uniform distribution, then a component n is assumed to be failed if the random sample is smaller than the unavailability of the component $u < U_n$. In this way, the statuses of all components are determined. Sampling from the exponential distribution in a sequential Monte Carlo simulation is somewhat different. If we consider the failure distribution (equation 2.2):

$$F(t) = 1 - e^{-\lambda t} \tag{2.34}$$

And the inverse function:

$$F^{-1}(t) = \frac{-\ln(1 - F(t))}{\lambda} \tag{2.35}$$

Then, if u is a sample from the unit uniform distribution, a sample from the exponential distribution is:

$$\frac{-\ln(1-u)}{\lambda} \tag{2.36}$$

If λ is the failure rate in [/y], a sampled time-to-failure in [h] is:

$$-8760 \cdot \frac{\ln(u)}{\lambda} \tag{2.37}$$

And if r is the average repair rate in [h] or μ is the repair rate in [/y], a sampled time-to-repair is:

$$-8760 \cdot \frac{\ln(u)}{\mu} = -r \cdot \ln(u) \tag{2.38}$$

The sampling of times-to-failure and times-to-repair results into a time series which shows when components fail and are repaired, as illustrated in figure 2.19. This is used together with the load/generation scenario in the Monte Carlo simulation.

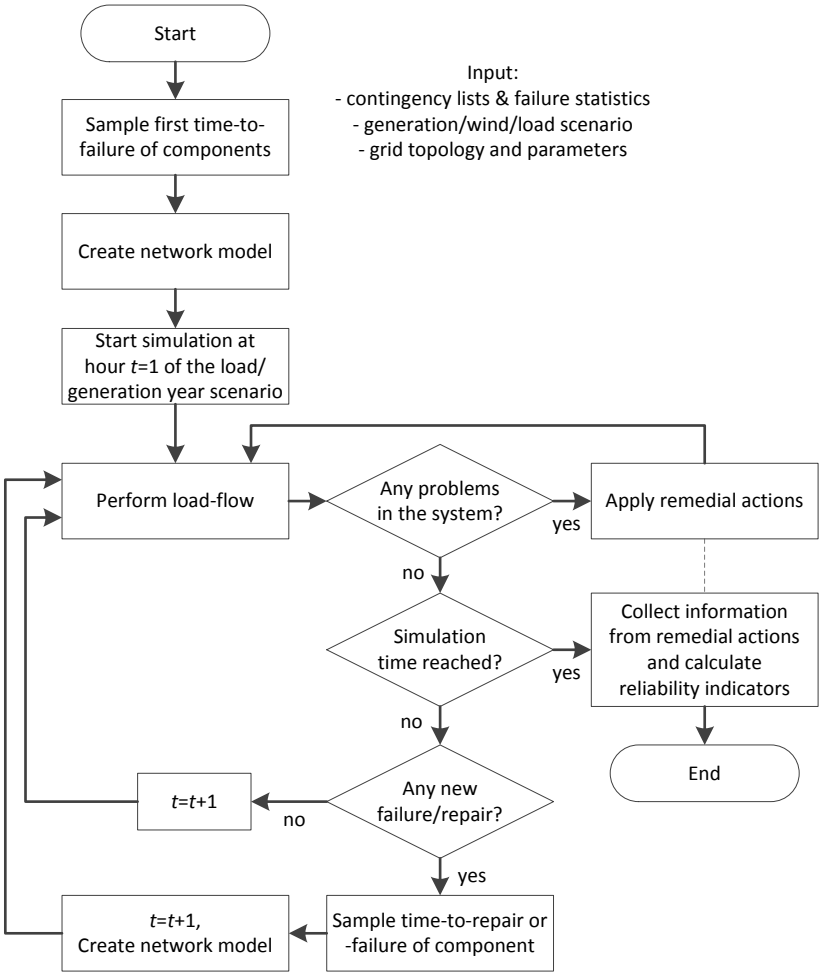

Figure 2.18: Typical algorithm of (sequential) Monte Carlo simulation.

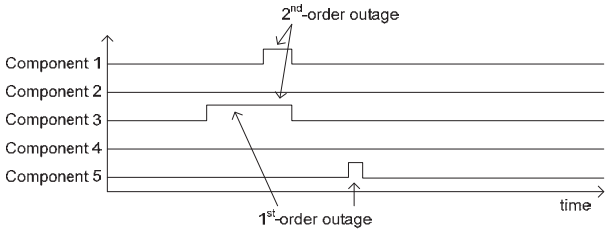

Figure 2.19: Monte-Carlo simulation.

A typical algorithm for (sequential) Monte Carlo simulation is shown in figure 2.18. The algorithm starts by sampling the first times-to-failure of the system components. It is assumed that all components are working when the simulation starts. The network model is then created and the simulation starts. Because a long simulation time is required to obtain reasonable accuracy, it is common to simulate the same year multiple times. The load/generation scenario then follows a loop until the Monte Carlo simulation ends. During the Monte Carlo simulation, results from the remedial actions are collected. Reliability indicators are then calculated from these results. It is also possible to calculate the reliability indicators during the simulation to show the progress of the simulation.

2.6. CONCLUSION

In this chapter, the main approaches followed in probabilistic reliability analysis of power systems were discussed. Reliability analysis can roughly be divided into two processes. The first process is the actual reliability analysis. This can for example be deterministic n-α contingency analysis or probabilistic state enumeration. The second process is the core calculation within the reliability analysis. For power system reliability analysis, this can e.g. be a dc load flow or a connectivity study. The choice for a certain approach always depends on the characteristics of the specific study. For a substation, a combination of fault/event tree and connectivity analysis is often used. And for large transmission networks, a combination of state enumeration and dc load flow is a suitable option. The approaches discussed in this chapter are used to analyze the reliability impact of EHV underground cables and offshore networks for wind energy in the next chapters.

3

RELIABILITY OF EHV UNDERGROUND CABLES

3.1. INTRODUCTION

As already mentioned before in the introduction, traditional overhead lines (OHLs) are facing more opposition from local society and therefore, underground cables (UGCs) become a preferred alternative for future grid extension. Currently in the Netherlands, EHV underground cables are applied in the Randstad380 project [9]. In Randstad380 Zuid, 11 km of EHV UGCs has been placed. Another, partially-cabled, UGC connection is located in the Randstad380 Noord corridor. In total, more than 20 km of underground cable will be in service from 2018. Due to its location in the west of the Netherlands, Randstad380 will play a significant role in the transmission of offshore wind energy to the load centers in the future as a significant expansion of offshore wind capacity is expected in the west of the Netherlands.

Whereas there is much experience with underground cables at HV and lower voltage levels, EHV UGCs are a relatively new technology and not much is known about their behavior in large, heavily-loaded transmission networks yet. Most existing studies concentrate on particular aspects. For example, the diagnosis of cables was studied in [33–35], and fault localization in [36–38]. A method to include the aging process of MV XLPE cables into reliability analysis was presented in [39]. The effects of thermal stress and thermal transients on the expected life of cables was studied in [40]. The costs of the end-of-life risk were considered in [41]. The reliability of line-cable-line configurations was studied in [42]. An overall cost comparison of overhead lines and underground cables is described in [43]. For the Randstad380 project, various aspects like resonant behavior [10], transient performance, and the issue of reliability are under study [12].

As far as reliability is concerned, the focus of the research published so far is on the components of cable circuits. The cables themselves, the joints and terminations contribute significantly to the overall unavailability of an UGC connection [44, 45], because of the much longer repair time of a cable circuit compared to an OHL circuit. The possi-

bilities for reducing the failure frequency and the repair time of UGC connections were reported in [46] and [45] respectively. In [47], it was concluded that the configuration of a cable circuit influences the reliability considerably. Still, a comprehensive approach to assess the reliability of UGC connections and to analyze the impact on the reliability of large transmission networks is missing.

It is therefore of interest to assess the reliability of underground cables and to investigate which factors are of influence. Furthermore, the possible solutions to increase the reliability and their effect should be analyzed. The UGC connections of Randstad380 will serve as case study in this research. Special attention will be paid to the collection of accurate failure statistics because the availability of failure statistics of EHV cables is limited. Using the models described in the previous chapter, first the reliability of an UGC connection is assessed. Once the reliability of an UGC connection is known, the impact on the reliability of large transmission networks can be investigated. Here, special attention will be paid to how the impact of UGC connections on the reliability of large transmission network can best be assessed. This will also provide insight into the maximum cable length that can be allowed in transmission networks, and under what conditions.

This chapter is organized as follows. First, section 3.2 defines some terminology and nomenclature that is used in this chapter. Then, the failure statistics of underground cables are discussed in detail in section 3.3. In section 3.4, the reliability of UGCs and OHLs is analyzed and compared. Underground cables in the Randstad380 region are studied in section 3.5. Section 3.6 studies the effects of UGCs on the amount of failures in large transmission networks. The risk of further cabling in the EHV transmission network is discussed in section 3.7. General conclusions are drawn in section 3.8.

3.2. TERMINOLOGY

In this chapter, the reliability of underground cable connections is discussed and compared with the reliability of overhead line connections. To avoid confusion, this section describes some terminology that is used in this chapter.

Typically, an *overhead line (OHL)* consists of several aluminum *conductors*, reinforced by steel cores, carried by a *tower*. The part of the overhead line between two towers is called a *line section*. An overhead line can consist of one or more *circuits*, each circuit consisting of three *phases*. To increase the transmission capacity at higher voltage levels (because of the electromagnetic field and the skin effect), a single phase can consist of a *bundle* of multiple conductors.

An *underground cable (UGC) connection* also can consist of one or more circuits. At higher voltage levels (380 kV), a *separate cable* is needed per circuit phase. To increase the transmission capacity, a circuit phase can consist of more (e.g. 2 in Randstad380) separate cables. An underground cable circuit consists of a series of *cable parts* connected by *joints*. At both ends of a cable circuit, *terminations* are installed to connect the underground cable to overhead lines.

3.3. FAILURE STATISTICS

As the total length of EHV underground cables in operation is still limited, the amount of available failure statistics is small. Most of the available statistics stem from UGCs at lower voltage levels and are therefore not suitable. Available statistics can be less useful as well because of different technologies (like oil-filled instead of XLPE) and constructions (like three-core cables instead of single-core cables). Failure statistics from some useful surveys are illustratively depicted in figure 3.1.

For example, the figure shows failure statistics from the Dutch NESTOR database [48] and the German FNN database [49]. Although these are statistics from actual databases, the number of EHV underground cable failures reported in these databases is rather modest. Because of this scarcity, in Cigré Technical Brochure 379 [44] failures of UGCs specifically were reported. Still, the number of cable failures at higher voltage levels (380-500 kV) was limited. In a survey among European TSOs [45], failures of these higher voltage UGCs were studied specifically. High and low estimations of the failure frequencies of UGC components were calculated and are shown in table 3.1. The high estimation probably is more accurate as it is based on failure statistics of only these particular TSOs that responded to the survey. For the low estimation, it was assumed that the TSOs that did not report any failures, did not experience any UGC failures. From the values of table 3.1, the failure frequency per circuit-kilometer-year of a Randstad380 UGC was derived using the calculation approach as explained later in this chapter. High and low estimations of the repair time were obtained with an exponential curve fit. The resulting values are included in figure 3.1 as well.

As indicated by the ellipse in figure 3.1, the failure statistics from different sources cover a large range, especially the repair times. Although individual repair times of thousands of hours have been reported in [45], an average of 730 h (1 month) seems a rea-

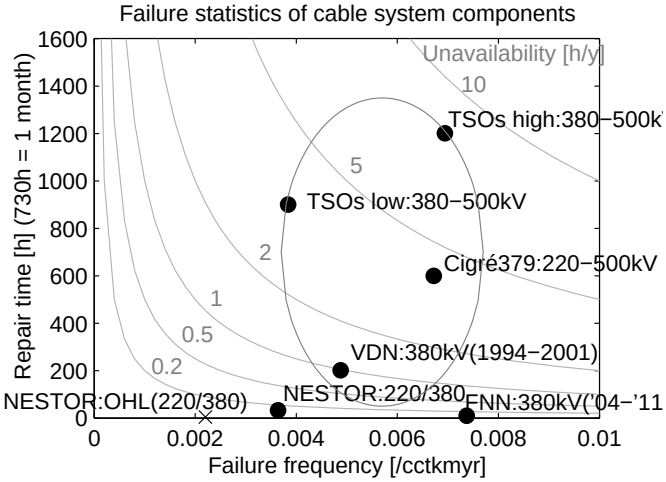

Figure 3.1: Failure statistics of underground cable components (i.e. cables, joints and terminations). Sources: the Dutch NESTOR database (OHL: overhead lines and 220/380kV cables) [5]; FNN Germany statistics (380kV cables) [6]; Cigré report 379 (220-500kV) [1]; and the survey among European TSOs (high/low) [2].

Table 3.1: Cable failure statistics from various sources.

	Cigré379 [44]		TSOs high [45]		TSOs low [45]	
Component	**Failure frequency**		**Failure frequency**		**Failure frequency**	
Cable	0.00133[a]	[/cctkm·y]	0.00120[a]	[/cctkm·y]	0.00079[a]	[/cctkm·y]
Joint	0.00048[b]	[/comp·y]	0.00035[b]	[/comp·y]	0.00016[b]	[/comp·y]
Termination	0.00050[b]	[/comp·y]	0.00168[b]	[/comp·y]	0.00092 [b]	[/comp·y]
Cable circuit	0.00672[c]	[/cctkm·y]	0.00694[c]	[/cctkm·y]	0.00384[c]	[/cctkm·y]
Repair time	600[d]	[h]	1200[d]	[h]	900[d]	[h]

[a] The failure frequency of the cable, measured in [/circuit-kilometers·year], is the failure frequency of a single cable circuit with one individual cable per circuit phase.
[b] The failure frequency of the joints and terminations, measured in [/component·year], is the failure frequency of individual components. For a 3-phase circuit consisting of one individual cable per circuit phase, sets of three joints (and terminations) are required.
[c] The total failure frequency of a cable circuit, measured in [/circuit-kilometers·year], is based on a 10km cable circuit with the Randstad380 configuration.
[d] The repair times of the TSOs research were obtained by an exponential curve fit of the repair times of the recorded failures. However, extremely long repair times of 6600h (3/4 year) have been reported as well.

sonable assumption for calculations. As a comparison, the failure frequency and repair time of overhead lines is also shown in table 3.1 and figure 3.1 (as NESTOR:OHL) [48]. Whereas the failure frequency of UGCs is 2-3 times larger than the failure frequency of OHLs, the repair time is about 100 times larger.

It is expected that UGC connections will be applied more often in the future. To obtain more accurate reliability calculations, it is important to collect failure statistics of these connections. It is also recommended to collect additional information like the cable type, the cable configuration, the voltage levels and the used component technology. This will give more insight into the reliability of different kinds of UGCs. As the application of EHV cables is still limited, the collection of failure statistics can better be done at a regional level (e.g. European) than nationally. Moreover, the occurrence of dependent failures and the repair time of independent and dependent failures can be analyzed in more detail then.

3.4. RELIABILITY OF OVERHEAD LINE AND UNDERGROUND CABLE CONNECTIONS

3.4.1. RELIABILITY CALCULATION

The reliability of overhead line and underground cable circuits can be calculated using the failure statistics of the components. For this calculation, the rules for series connections of components as described in chapter 2 are used, together with the nomenclature as shown at the beginning of this thesis. In this section, this is done for single circuit and double circuit failures. A derivation of the equations using Markov models is shown in appendix C.

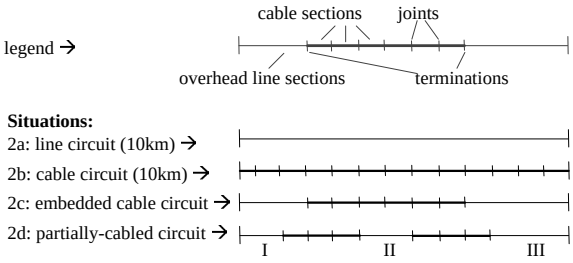

Figure 3.2: Illustration of the 4 studied situations. The layouts show the locations of the cable parts, joints and terminations. The total connection length is 10km in all situations. In situation c and d, the total cable length is 5km.

For a single overhead line circuit (as illustrated in figure 3.2a), the failure frequency and unavailability are:

$$f_{l1} = l_{total} f_{line} \; [/y] \tag{3.1}$$

$$U_{l1} = f_{l1} \frac{r_{line}}{8760} = l_{total} f_{line} \frac{r_{line}}{8760} \; [-] \tag{3.2}$$

Where:
f_{l1} = failure frequency of a single OHL circuit [/y]
l_{total} = total connection length [km]
f_{line} = failure frequency of an OHL circuit [/cctkm·y]
U_{l1} = unavailability of a single OHL circuit [-]
r_{line} = repair time of an overhead line [h]

To calculate the reliability of a fully-cabled circuit (as illustrated in figure 3.2b), all the components of the cable circuit (i.e. cable parts, joints and terminations) must be included. As indicated in figure 3.2b, joints are installed between the cable parts and terminations are present at both ends of the cable circuit. The failure frequency of a cable circuit then becomes:

$$f_{c1} = n_{ic} l_{total} f_{cable} + 3 n_{ic} \left(N_{cpart} - 1\right) f_{joint} + 3 \cdot 2 n_{ic} f_{term} \; [/y] \tag{3.3}$$

Where:
f_{c1} = failure frequency of a single UGC circuit [/y]
n_{ic} = number of individual cables per circuit phase [-]
l_{total} = total connection length [km]
f_{cable} = failure frequency of an underground cable (single circuit, one cable per phase) [/cctkm·y]
N_{cpart} = number of cable parts [-]
f_{joint} = failure frequency of a single joint [/comp·y]
f_{term} = failure frequency of a single termination [/comp·y]

If all cable parts have the same length (l_{cpart} [km]), the failure frequency of a single UGC circuit can be calculated by:

$$f_{c1} = n_{ic} l_{total} f_{cable} + 3 n_{ic} \left\lceil \frac{l_{total}}{l_{cpart}} - 1 \right\rceil f_{joint} + 6 n_{ic} f_{term} \; [/y] \tag{3.4}$$

The unavailability of a cable circuit then becomes:

$$U_{c1} = n_{ic} l_{total} f_{cable} \frac{r_{cable}}{8760} + 3 n_{ic} \left\lceil \frac{l_{total}}{l_{sec}} - 1 \right\rceil f_{joint} \frac{r_{joint}}{8760} + 6 n_{ic} f_{term} \frac{r_{term}}{8760} \; [-] \tag{3.5}$$

Where:
$\lceil x \rceil$ = rounding x to the nearest integer towards infinity
U_{c1} = unavailability of a single cable circuit [-]
r_{cable} = repair time of a cable (part) [h]
r_{joint} = repair time of a joint [h]
r_{term} = repair time of a termination [h]

When calculating the reliability of an UGC connection, it is often assumed that all UGC components have the same repair time. As the amount of available failure statistics is limited, it is not possible to accurately calculate the difference in repair times. As shown in appendix C, with the same repair time it becomes possible to simplify the Markov model of a cable circuit to a two-state model, which simplifies further reliability calculations.

Probabilities, unavailabilities and availabilities are normally dimensionless. In order to obtain more feeling for unavailabilities and other probabilities, annualized values (measured in hours/year) can be calculated. For example, for the single UGC circuit, this annualized unavailability can be calculated as:

$$U^*_{c1} = 8760 U_{c1} \; [h/y] \tag{3.6}$$

Where:
U_{c1} = unavailability of a single UGC circuit [-]
U^*_{c1} = annualized unavailability of a single UGC circuit [h/y]

The annualized values will be often used to express probabilities in this thesis.

The occurrence of failures in double circuits can be derived from equations 3.1-3.2 and 3.4-3.5. The failure frequency and unavailability of independent double circuit failures in overhead lines are:

$$f_{l2ind} = \binom{2}{1} U_{l1} f_{l1} = 2 \frac{f_{l1} r_{line}}{8760} f_{l1} = \frac{2}{8760} f_{l1}^2 r_{line} \; [/y] \tag{3.7}$$

$$U_{l2ind} = U_{l1}^2 = \left(f_{l1} \frac{r_{line}}{8760} \right)^2 = f_{l1}^2 \frac{r_{line}^2}{8760^2} \; [-] \tag{3.8}$$

Where:
f_{l2ind} = failure frequency of independent double circuit failures in overhead lines [/y]
U_{l2ind} = unavailability of independent double circuit failures in overhead lines [-]

The failure frequency and unavailability of independent double circuit failures in UGC connections are:

$$f_{c2ind} = 2U_{c1}f_{c1}\ [/y] \tag{3.9}$$

$$U_{c2ind} = U_{c1}^2\ [-] \tag{3.10}$$

Where:
f_{c2ind} = failure frequency of independent double circuit failures in UGC connections [/y]
U_{c2ind} = unavailability of independent double circuit failures in UGC connections [-]

Because of the limited amount of failure statistics of EHV cables, it is not possible to calculate different repair time for the components of a cable connection. If it is assumed that all components of the UGC connection have the same repair time (r_{cable}), these equations become:

$$f_{c2ind} = 2U_{c1}f_{c1} = 2\frac{f_{c1}r_{cable}}{8760}f_{c1} = \frac{2}{8760}f_{c1}^2 r_{cable}\ [/y] \tag{3.11}$$

$$U_{c2ind} = U_{c1}^2 = \left(f_{c1}\frac{r_{cable}}{8760}\right)^2 = f_{c1}^2\frac{r_{cable}^2}{8760^2}\ [-] \tag{3.12}$$

To calculate the failure frequency and unavailability of dependent double circuit failures, a dependent failure factor (c_{cc}) is defined. The dependent failure factor is the ratio between the failure frequency of dependent double circuit failures and the single circuit failure frequency. The failure frequency and unavailability of dependent double circuit failures then become:

$$f_{l2dep} = c_{cc}f_{l1}\ [/y] \tag{3.13}$$

$$U_{l2dep} = f_{l2dep}\frac{r_{line}}{8760} = c_{cc}f_{l1}\frac{r_{line}}{8760}\ [-] \tag{3.14}$$

$$f_{c2dep} = c_{cc}f_{c1}\ [/y] \tag{3.15}$$

$$U_{c2dep} = f_{c2dep}\frac{r_{cable}}{8760} = c_{cc}f_{c1}\frac{r_{cable}}{8760}\ [-] \tag{3.16}$$

Where:
f_{l2dep} = failure frequency of dependent double circuit failures in OHL connections [/y]
c_{cc} = dependent failure factor [-]
U_{l2dep} = unavailability of dependent double circuit failures in OHL connections [-]
f_{c2dep} = failure frequency of dependent double circuit failures in UGC connections [-]
U_{c2dep} = unavailability of dependent double circuit failures in UGC connections [-]

The failure frequency and unavailability of dependent double circuit failures are a direct result of the dependent failure factor. This dependent failure factor is assumed to be the same for both overhead lines and underground cables. In reality, there are several factors that may cause a dependent failure. And these factors are different for underground cables and overhead lines. In table 3.2, some of these factors are listed. Because of the limited amount of failure statistics of underground cables, it is difficult to determine whether the dependent failure factor is higher or lower than for overhead

Table 3.2: Causes of dependent failures in UGC and OHL connections.

OHL connections	UGC connections
Weather effects	New technology
External origin	Movement of the soil
Hoisting works	Excavation works
Protection system	Protection system

lines. Therefore, in this research the same dependent failure factor is assumed for both overhead lines and underground cables.

Another assumption of this model is that the repair time is the same for double circuit failures and single circuit failures. In reality, these repair times can be different. Again, because of the limited amount of failure statistics, and also because of modeling simplicity, both repair times are assumed to be the same in this research.

3.4.2. FAILURES IN THE RANDSTAD380 ZUID CABLE CONNECTION

Using equations 3.1-3.16, the failure frequency and probability of failures in a double circuit connection can be calculated. The Randstad380 Zuid UGC connection, with a length of 11 km, is studied. In this configuration, 2 individual cables are applied per circuit phase to facilitate transport capacity ($n_{ic} = 2$). Furthermore, the length of the cable parts is about 900 m ($l_{cpart} = 0.9$). As indicated in figure 3.2b, in this case joints are installed at 12 locations and terminations are present at both ends of the connection. The high estimation of the failure frequencies from table 3.1 is used together with a repair time of 730 h. It is supposed that the dependent failure factor is 0.1, for both underground cables and overhead lines. This value is based on failure statistics from databases [48]-[49].

First, failures of a single circuit are studied. Table 3.3 shows how the individual components contribute to the total reliability of a single circuit. As can be seen from the table, the cable circuit will fail about once every 14 years. The (annualized) unavailability in 52 h/y then. All the components of the cable circuit contribute to the total failure fre-

Table 3.3: Failure frequency and (annualized) unavailability of one circuit of the 11km Randstad380 cable connection using the TSOs high estimate of the failure frequency.

Component	Amount	Fail.freq.[a]	f_{c1} [/y]	U^*_{c1} [h/y]
Cable	11 km	0.00120 (x2)	0.026	19.3
Joints	72	0.00035	0.025	18.4
Terminations	12	0.00168	0.020	14.7
Total			**0.071**	52.4
Line	*11 km*	*0.00220*	*0.024*	*0.2*

[a] As the failure frequency of the cable is measured per circuit kilometer with a single cable per circuit phase, this value must be doubled for an UGC configuration with two cables per circuit phase.
f_{c1} is the total failure frequency of one circuit. U^*_{c1} is the annualized unavailability, in hours/year. The repair time of the cable connection is assumed 730h.

Table 3.4: Occurrence of failures in double circuit connections.

Failure type	Failure freq. [/y]		Probability* [h/y]	
	Line	Cable	Line	Cable
Single circuit failures	0.048	0.142	0.4	104.8
Independent double circuit	1.1e-6	8.3e-4	4.3e-6	0.31
Dependent double circuit	2.4e-3	7.1e-3	0.02	5.2

quency and unavailability. As comparison, the total failure frequency of an 11 km long overhead line circuit is calculated. This overhead line circuit will fail only once every 42 years. As can be seen, the cable circuit fails about three times as often as the overhead line circuit. This is mainly caused by the two individual cables per circuit phase and the additional joints and terminations. The unavailability shows a large difference between the overhead line and the underground cable circuit, which is mainly caused by the difference in repair times.

Table 3.4 shows the occurrence of failures in double circuits. The failure frequency and (annualized) probability of single circuit failures is double the value as shown in table 3.3, because there are two single circuits in a double circuit.

Because of the long repair time of UGC connections, the unavailability of a single circuit is larger and it becomes more likely that the second circuit (independently) fails during repair of the first circuit. Table 3.4 shows that independent double circuit failures occur considerably more often in the cable connection than in the overhead line connection (8.3e-4 vs. 1.1e-6 /y). Also, the probability of having an independent double circuit failure differs considerably (0.31 vs. 4.3e-6 h/y).

For dependent double circuit failures, the table shows that these occur about three times as often in underground cable connection as in overhead lines (7.1e-3 vs. 2.4e-3 /y). This is similar to the difference found for single circuit failures. Also, the difference in probability is comparable (5.2 vs. 0.02 h/y). This is because the same dependent failure factor is assumed for underground cables and overhead lines.

It is interesting to compare the failure frequencies of dependent and independent double circuit failures. Whereas this difference is several orders of magnitude for overhead lines (2.4e-3 vs. 1.1e-6 /y), this difference becomes smaller for underground cables (7.1e-3 vs. 8.3e-4 /y). Within UGC connections, independent double circuit failures become more frequent because of the relatively long repair time and it becomes more likely that the second circuit fails independently during the repair of the first circuit.

This effect is studied in more detail for increasing connection lengths. Figure 3.3 shows the Mean Time Between Failures (MTBF = 1/failure frequency) and probability (annualized to h/y) of double circuit failures in cable connections. As can be seen, from about 110 km independent double circuit failures will occur more often than dependent double circuit failures. This can be explained by equations 3.11 and 3.15. These equations show that the failure frequency of dependent double circuit failures increases linearly with the single circuit failure frequency (and the connection length) whereas the failure frequency of independent double circuit failures increases quadratically with the single circuit failure frequency (and the connection length). The right graph shows that

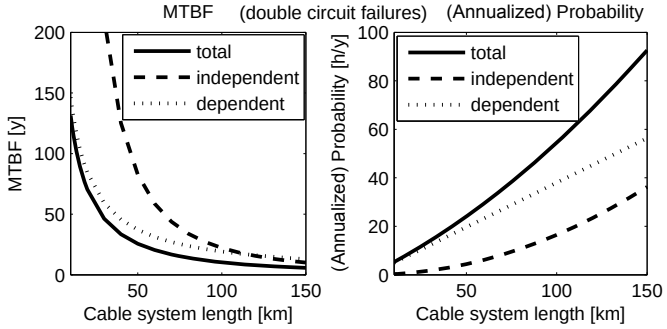

Figure 3.3: Mean time between double circuit failures and annualized probability of double circuit failures in cable connections.

independent failures then contribute significantly to the total probability of having a double circuit failure. For overhead lines, double circuit failures are almost always dependent failures.

This can have consequences for the planning and operation of large transmission networks. In general, in transmission networks, it is assumed that single circuit failures are relatively likely to occur. Dependent double circuit failures occur less often and independent double circuit failures are rare. If more and longer cable connections are installed in the network, independent double circuit failures will happen more frequently. This is in line with the findings of [47]. Possible independent double circuit failures that include a cable circuit should therefore be studied in more detail during system design and observed closely during system operation.

3.4.3. SOLUTIONS TO IMPROVE THE RELIABILITY

There are several possible solutions to improve the reliability of a cable connection. Reducing the repair time or failure frequency of the components, partially-cabling and alternative cable configurations are the studied solutions in this section.

REDUCING THE FAILURE FREQUENCIES AND REPAIR TIME

In the previous calculations, the reliability of underground cable connections was calculated. Whereas the failure frequency of a cable circuit does not differ significantly from the failure frequency of an overhead line circuit, the repair time of a cable connection is about hundred times as long. Probably the best way to increase the reliability of transmission networks with underground cables is to reduce the repair time of cable connections. In [45], the repair process of underground cables was analyzed. Figure 3.4 shows the activities that contribute to the total repair time. As can be seen, the actual repair of the cable connection takes 1-2 weeks. However, activities like cleaning the site, getting spare/new parts, and arranging technical people can cause a much longer repair time.

If the repair process is more optimized, the total repair time can be reduced significantly. This is illustrated in figure 3.5. Some repair activities can be planned before a failure occurs. For example, a permission to perform future repairs can be arranged on beforehand. Also, spare parts of most components can be made available for the case a

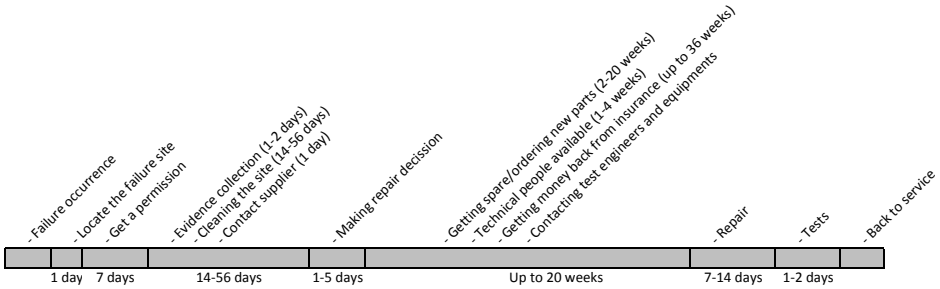

Figure 3.4: Scheme of the repair time of cable connections [45].

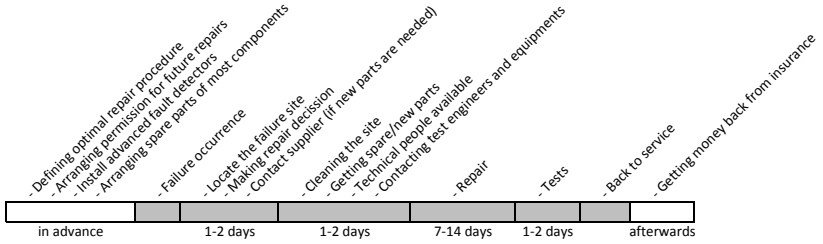

Figure 3.5: Improved scheme of the repair time of cable connections.

failure occurs. Furthermore, with advanced fault detection, it becomes easier to localize the fault within limited time. Other activities like getting money back from the insurance can be managed after the cable connection is repaired. In this way, the repair time can be reduced to about 2 weeks (336 h), although exceptions are still possible.

Another possibility to increase the reliability of UGC connections is to reduce the failure frequency of the components [46]. Advanced installation and testing techniques are possibilities to reduce the failure frequencies.

The effects of smaller failure frequencies and a shorter repair time can be studied by using the equations from the previous section with the low failure frequencies from table 3.1 and a repair time of 336 h (2 weeks). The results are shown in table 3.5. As can be seen, the failure frequency and probability of failures within cable double circuits have reduced compared to table 3.4. The difference between independent and dependent double circuit failures in cable connections has increased. But there is still a large difference between overhead lines and underground cables.

As mentioned before, failure statistics show a large range of repair times. The variation in the repair time can cause a large variation in the reliability of larger networks. In order to determine the reliability of the transmission network, well-defined input parameters like accurate failure frequencies are necessary. A guaranteed system reliability performance requires input parameters like guaranteed repair times.

Table 3.5: Occurrence of failures in double circuit connections with a shorter repair time and smaller failure frequencies of the components.

Failure type	Failure freq. [/y]		Probability* [h/y]	
	Line	Cable	Line	Cable
Single circuit failures	0.048	0.080	0.4	58.4
Independent double circuit	1.1e-6	1.2e-4	4.3e-6	0.02
Dependent double circuit	2.4e-3	4.0e-3	0.02	1.3

PARTIALLY-CABLED CONNECTIONS

Another way to improve the reliability of a connection is to limit the use of underground cables. Cables will then only be applied at those locations where they are the most desired. This will lead to a partially-cabled connection. In a partially-cabled connection, one or multiple cable sections can be embedded.

Figure 3.2 shows two examples of partially-cabled connections. Situation 3.2c is an embedded cable circuit. This is the situation in the Randstad380 Zuid connection in the Netherlands, where an 11 km cable section is installed within a connection of 22 km. Situation 3.2d is a partially-cabled connection with multiple embedded cable sections. An example is the Randstad380 Noord connection in the Netherlands, where three cable sections of 2, 3, and 3 km respectively are used within a connection of 45 km.

The failure frequency and unavailability of a partially-cabled connection can be calculated by combining equations 3.1-3.5:

$$f_{pc1} = n_{ic} l_{cable} f_{cable} + 3 n_{ic} N_{csec} \left\lceil \frac{\frac{l_{cable}}{N_{csec}}}{l_{cpart}} - 1 \right\rceil f_{joint} + 6 n_{ic} N_{csec} f_{term} + l_{line} f_{line} \; [/y] \tag{3.17}$$

$$U_{pc1} = \left(n_{ic} l_{cable} f_{cable} + 3 n_{ic} N_{csec} \left\lceil \frac{\frac{l_{cable}}{N_{csec}}}{l_{cpart}} - 1 \right\rceil f_{joint} + 6 n_{ic} N_{csec} f_{term} \right) \frac{r_{cable}}{8760} + l_{line} f_{line} \frac{r_{line}}{8760} \; [/y] \tag{3.18}$$

Where:

$\lceil x \rceil$ = rounding x to the nearest integer towards infinity
f_{pc1} = failure frequency of a partially-cabled circuit [/y]
l_{cable} = total cable circuit length [km]
N_{csec} = number of embedded cable sections [-]
l_{line} = total overhead line length [-]
U_{pc1} = unavailability of a partially-cabled circuit [-]

In these equations, it is assumed that all components of an underground cable connection have the same repair time (r_{cable}). Furthermore, the number of joints is based on the total cable circuit length, the number of embedded cable sections and the average cable part length. Depending on the length of the embedded cable sections, the number of joints might be somewhat different in reality.

The failure frequency and unavailability of double circuit failures then become:

$$f_{pc2ind} = 2 f_{pc1} U_{pc1} \ [/y] \tag{3.19}$$

$$U_{pc2ind} = U_{pc1}^2 \ [-] \tag{3.20}$$

$$f_{pc2dep} = c_{cc} f_{pc1} \ [/y] \tag{3.21}$$

$$U_{pc2dep} = c_{cc} U_{pc1} \ [-] \tag{3.22}$$

Where:
f_{pc2ind} = failure frequency of ind. double cct failures in partially-cabled connections [/y]
U_{pc2ind} = unavailability of ind. double cct failures in partially-cabled connections [-]
f_{pc2dep} = failure frequency of dep. double cct failures in partially-cabled connections [/y]
U_{pc2dep} = unavailability of dep. double cct failures in partially-cabled connections [-]

Using equations 3.1-3.5 and 3.17-3.18, the occurrence of single circuit failures are calculated and shown in table 3.6. It is assumed that the total connection length is 10 km of which 5 km underground cable. As can be seen, for the embedded cable circuit (2c), less joints are required. This leads to a smaller failure frequency and unavailability compared to situation 2b.

It is also possible to divide the underground cables over multiple cable sections at different locations. For example in situation 3.2d, there are two cable sections of 2.5 km each, within a connection of 10 km. As can be seen from table 3.6, the main difference between situations 3.2c and 3.2d is that in the partially-cabled connection, additional terminations are required at 2 locations while one set of joints can be omitted. Compared to situation 3.2c, both the failure frequency and unavailability have increased because of the additional terminations.

It is now interesting to compare the partially-cabled circuit (situation 3.2d) with the fully-cabled circuit (situation 3.2b). Table 3.6 shows that although the unavailability of the partially-cabled circuit is smaller than the unavailability of the fully-cabled circuit (44.4 vs. 50.6 h/y), the failure frequency of the partially-cabled circuit is larger than the failure frequency of the fully-cabled circuit (0.0717 vs. 0.0694 /y). It seems that for some cases, a fully-cabled circuit can perform better than a partially-cabled circuit.

If this is studied into more detail, there can be two cases:

1. A line section is located at the end of a connection (sections I&III, situation 3.2d)

2. A line section is located between two cable sections (section II, situation 3.2d)

Table 3.6: Reliability comparison of partially-cabled circuits.

Situation	Joints	Terminations	Failure freq.	Unavailability*
3.2a	-	-	0.0220 /y	0.176 h/y
3.2b	12 locations	2 locations	0.0694 /y	50.6 h/y
3.2c	5 locations	2 locations	0.0537 /y	31.2 h/y
3.2d	4 locations	4 locations	0.0717 /y	44.4 h/y

If a line section at the end of a connection is replaced with cables, cables and joints are added to the connection while the amount of terminations remains the same. The unavailability of the connection will increase. If a line section in between two cable sections is replaced with cables, the difference is:

- - 2 sets of terminations
- - l overhead line
- + $2l$ underground cable
- + $l/l_{cp} + 1$ sets of joints

When this is compared using the parameters of table 3.1 (high estimation), it is found that the unavailability of 3.6 km overhead line section is equal to the unavailability of 3.6 km cable section. Below 3.6 km, the unavailability of a line section is larger and above 3.6 km, the unavailability of a cable section is larger. It seems therefore better to avoid overhead line sections shorter than 3.6 km.

Because this minimum length of overhead line sections depends on the used input parameters, it is of interest to study the effects of parameter changes. Figure 3.6 shows the result of this sensitivity analysis.

Figure 3.6 shows that the minimum line section length is strongly dependent on the failure frequency and the repair time of the terminations. If these are reduced, the minimum line section length reduces too. If the failure frequency and repair time of the cables and joints are reduced, the minimum line section length increases. If the cable part length increases, the minimum line section lines increases as well.

It is of interest to point out that if the failure frequency and repair time of all the cable connection components (cables, joints and terminations) change, the minimum line section length does not change significantly. Also, changes of the failure frequency and repair time of the overhead line do not lead to a significant difference.

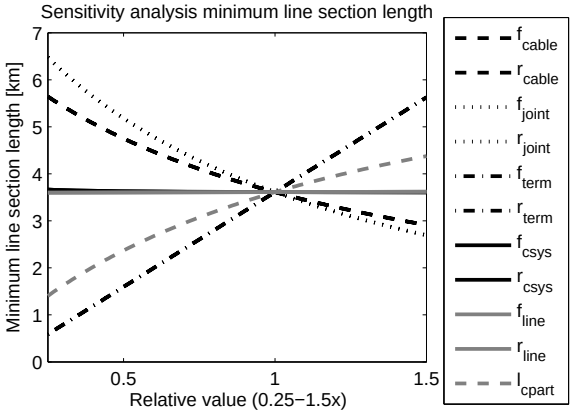

Figure 3.6: Sensitivity of the minimum line section length to input parameter changes. The x-axis shows the relative values of the input parameters (where 1= the parameters as given in table 3.1 (high estimation)). Lines with the same color and pattern are located below each other.

If the minimum line section length is studied for double circuits using equations 3.20 and 3.22, it is found that the minimum line section length remains almost similar. It remains almost similar as well if a cable configuration with only one individual cable per circuit phase is used.

ALTERNATIVE CABLE CONFIGURATIONS

Another option to improve the reliability of a cable connection is to use an alternative configuration [47]. For example, the use of additional disconnectors, circuit breakers or spare cables can be beneficial for the reliability.

In figure 3.7, some alternative configurations for single circuits are shown. Configuration 3.70, a double circuit overhead line, is the reference configuration. Configuration 3.7a is the standard Randstad380 cable configuration (with two individual cables per circuit phase). In case of a cable failure, one circuit is disconnected by the protection system. In configuration 3.7b, an additional spare cable is installed that can be used after a cable failure. A switching time of 24 h is assumed. In configuration 3.7c, additional disconnectors are installed. After a failure, the damaged cable can be isolated and half-a-circuit can be put into operation again. In configuration 3.7d, additional circuit breakers are installed. After a cable failure, the damaged cable can be isolated directly and only half-a-circuit is disconnected.

Underground cable configurations can be effectively modeled by Markov models [15, 16, 42, 47, 50, 51]. Using the Markov models as described in the appendix, the results as shown in table 3.7 are obtained. The results from table 3.3 are included in this table as well. As can be seen, if an additional spare cable is used (configuration 3.7b), the Mean

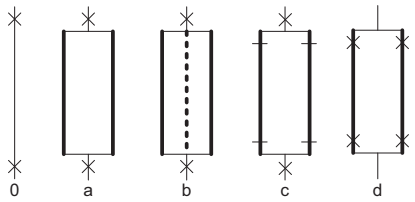

Figure 3.7: Configurations of UGC single circuits. 0 = single line circuit, a = single cable circuit (circuit switching), b = a with additional spare cable, c = single cable circuit with disconnectors (circuit switching), d = single cable circuit with circuit breakers (cable switching).

Table 3.7: Reliability of the alternative single circuit configurations.

	0	**a**	**b**	**c**	**d**
$P^*_{50\%}$ [h/y]	-	-	-	50.4	52.1
$P^*_{0\%}$ [h/y]	0.2	52.4	1.8	1.7	0.1
$f^*_{50\%}$ [/y]	-	-	-	0.071	0.071
$f^*_{0\%}$ [/y]	0.024	0.071	0.071	0.071	2.1e-4
$T^*_{50\%}$ [y]	-	-	-	14	14
$T^*_{0\%}$ [y]	41	14	14	14	4.7e3

$P^*_{50\%}$ / $P^*_{0\%}$ = annualized probability of having 50%/0% transmission capacity available, $f_{50\%}$ / $f_{0\%}$ = frequency of 50%/0% capacity states, $T_{50\%}$ / $T_{0\%}$ = mean time between 50%/0% capacity states. T equals $1/f$.

Time Between Failure remains the same. This is because after a failure, the whole circuit is switched off first. But by using the spare cable, the circuit can be put into operation sooner and the total unavailability of the circuit is reduced. This unavailability is still higher than the unavailability of the line circuit.

If additional disconnectors are used (configuration 3.7c), the Mean Time Between Failures remains the same as well. It is however possible to continue operation at half capacity within a limited switching time. Consequently, the probability of the zero-capacity state is reduced. This half-capacity state is maintained until the damaged cable is repaired. With additional circuit breakers (configuration 3.7d), the cable circuit is switched per cable (half a circuit). The results in table 3.7 show that the old values of the zero-capacity state have now become the new values of the half-capacity state. The probability of having zero transmission capacity has reduced significantly.

For system operation, the different configurations will have different consequences. In configuration 3.7b, it is important that the spare cable can be manually connected in a short time. A good design of the cable circuit and of the repair plan helps to reduce the repair time. In practice, the use of a spare cable causes some problems. In the calculation, it is assumed that the spare cable can replace any other cable of the circuit. In reality, this may be impossible because of the location of the cable and cross-bonding of the cables. Moreover, this spare cable must be tested regularly to guarantee that it can be used whenever needed. A last constraint are the additional costs that are probably larger than the benefits of the higher reliability of the cable circuit.

The configuration with the half-capacity states, 3.7c and 3.7d, have consequences for system operation as well. The main constraint is the possibility of the half-capacity state. For example, when a cable circuit is part of a longer double circuit overhead line circuit, a half-capacity state may cause problems. In case of a single failure, it may be necessary to take measures to reduce the power flow through the remaining circuit. If this is possible, the reliability of the cable circuit can be improved significantly with the investment of additional disconnectors or circuit breakers (and protection systems). Because of the half-capacity state, configuration 3.7d may perform even better than a single circuit overhead line.

A similar study can be performed for double circuits, as illustrated in figure 3.8. Table 3.8 shows the results of the analysis. The results from table 3.4 are included in this table too. Table 3.8 shows that if a configuration with a spare cable is used (configuration 3.8b), the Mean Time Between single Failures ($T_{50\%}$) remains the same while the probability of

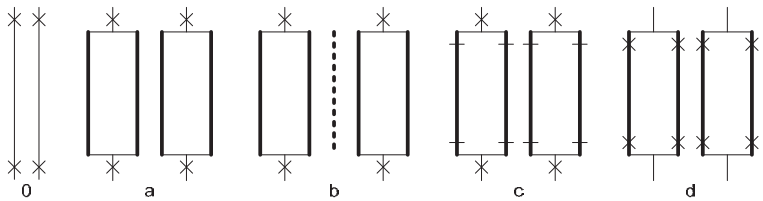

Figure 3.8: Configurations of UGC double circuit. 0 = double overhead line circuit, a = double cable circuit (circuit switching), b = a with additional spare cable, c = double cable circuit with additional disconnectors (circuit switching), d = double cable circuit with additional circuit breakers (cable switching).

Table 3.8: Reliability of the alternative double circuit configurations.

	0	a	b	c	d
$P^*_{75\%}$ [h/y]	-	-	-	103.5	103.5
$P^*_{50\%}$ [h/y]	0.39	103.5	3.87	50.4	0.46
$P^*_{25\%}$ [h/y]	-	-	-	2.1e-2	9.3e-4
$P^*_{0\%}$ [h/y]	4.3e-6	0.31	3.1e-5	1.7	6.9e-7
$f^*_{75\%}$ [/y]	-	-	-	0.14	0.14
$f^*_{50\%}$ [/y]	4.8e-2	0.14	0.14	0.14	1.3e-3
$f^*_{25\%}$ [/y]	-	-	-	8.3e-4	3.8e-6
$f^*_{0\%}$ [/y]	1.1e-6	8.3e-4	3.2e-5	1.3e-6	3.8e-9
$T^*_{75\%}$ [y]	-	-	-	7.1	7.1
$T^*_{50\%}$ [y]	20.7	7.1	7.1	7.1	786
$T^*_{25\%}$ [y]	-	-	-	1.2e3	2.6e5
$T^*_{0\%}$ [y]	9.3e-5	1.2e3	3.1e4	7.9e5	2.6e8

$P^*_{75\%}/P^*_{50\%}/P^*_{25\%}/P^*_{0\%}$ = annualized probability of having 75%/50%/25%/0% transmission capacity available, $f_{75\%}/f_{50\%}/f_{25\%}/f_{0\%}$ = frequency of 75%/50%/25%/0% capacity states, $T_{75\%}/T_{50\%}/T_{25\%}/T_{0\%}$ = mean time between 75%/50%/25%/0% capacity states. T equals $1/f$. Only independent failures are studied here.

single failures ($P^*_{50\%}$) becomes much smaller. Consequently, the MTBF of independent double failures ($T_{0\%}$) increases and the probability of independent double failures ($P^*_{0\%}$) is reduced.

If additional disconnectors are used (configuration 3.8c), the MTBF of the 50% capacity state remains the same ($T_{50\%}$). This is because after a failure, first one circuit is switched off. But because it is possible to continue operation at 75% within a limited switching time, the probability of the 50% capacity state is reduced ($P^*_{50\%}$). The old probability has now become the probability of the 75% capacity state ($P^*_{75\%}$). The MTBF of independent double circuit failures can be increased and the probability ($T_{0\%}$, $P^*_{0\%}$) can be reduced significantly in this way.

With additional circuit breakers (configuration 3.8d), the MTBF of the 50% capacity state ($T_{50\%}$) is increased because after a failure, half-a-circuit is switched off. The probabilities of having 50%, 25% or 0% capacity ($P^*_{50\%}$, $P^*_{25\%}$, $P^*_{0\%}$) become even smaller.

Similarly to the single circuits, the use of a spare cable can cause practical problems in reality. The other configurations may be better alternatives. Whereas the use of additional circuit breakers (and protection systems) leads to higher overall costs, the use of additional disconnectors is a more efficient way to increase the reliability of the cable connection. It must however be studied whether the 75% capacity state is acceptable in the actual transmission network. In practice, a 75% capacity may be acceptable as cable circuits can be overloaded to a certain level and for a certain period. This dynamic loading is however not considered in this thesis.

3.5. UNDERGROUND CABLES IN THE RANDSTAD REGION

3.5.1. UNDERGROUND CABLES IN THE CONNECTION OF MVL380

As already mentioned in the introduction of this thesis, the network around Maasvlakte is a suitable network to study the effects of various new developments. In this section, the effects of underground cables in the connection of MVL380 substation are studied.

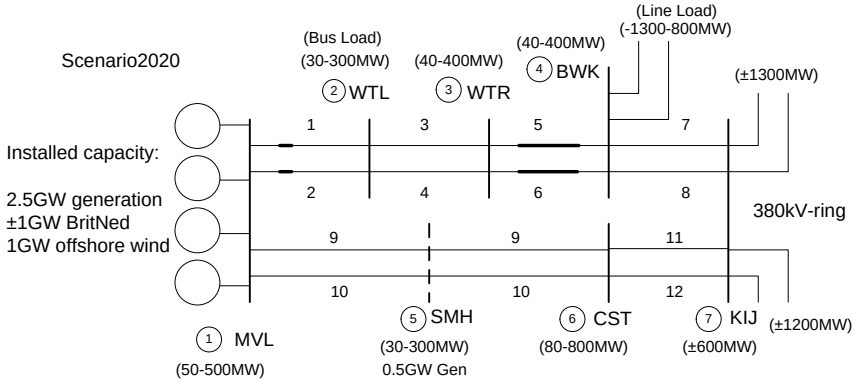

Figure 3.9: Maasvlakte (MVL) region network. In the figure, the bus loads, line loads and installed generation per bus are shown. The locations of the underground cables of Randstad380 Zuid are indicated by bold lines.

RELIABILITY OF THE CONNECTIONS

As shown in figure 3.9, Maasvlakte substation is connected to the main 380kV ring by two connection routes, MVL-WTL-WTR-BWK and MVL-SMH-CST-KIJ. The first route includes the new Randstad380 Zuid connection, with a long cable section of 11 km between WTR and BWK. A smaller cable section of 2 km is located between MVL and WTL to cross a river. The connection MVL-SMH-CST-KIJ is an existing connection, consisting of overhead lines.

To study the reliability of the connections of MVL380, an overview of all the components of these connections can be made. All components (cable sections, overhead lines and substation equipment) are included in the calculations and the failure frequencies and repair times as given in appendix B are used. It is assumed that all the failure frequencies and repair times of the included components contribute to the total failure frequency and unavailability of the circuit. In reality, it may be possible that some component failures do not lead to an interruption of the complete circuit. It may also be possible that the circuit is reconnected within a short time if the failed component can be disconnected.

First, the connection MVL-WTL-WTR-BWK is studied. The results are shown in figure 3.10. It can be seen that one circuit of this connection fails about once every 4 years. In the failure frequency, the overhead lines and the underground cables have the largest contribution and both contribute almost equally. In the cable section, joints and terminations have a relatively large share in the failure frequency. The average unavailability of one circuit of this connection is 77 h/y. This unavailability is almost completely caused by the cable section as its repair time is significantly longer than the repair time of overhead lines. Also in the cable section, joints and terminations have a large contribution to the total unavailability. The contribution of the terminations to the total unavailability is relatively large as the failure frequency of the terminations is large.

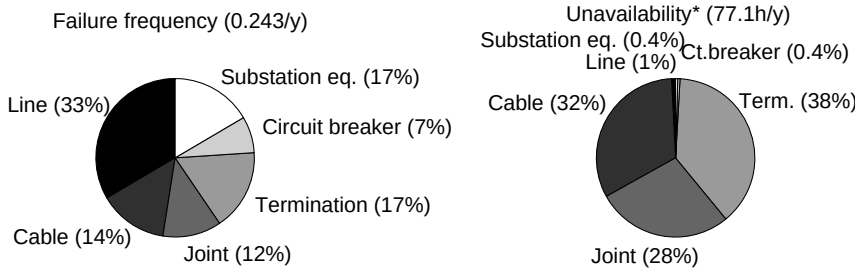

Figure 3.10: MVL-WTL-WTR-BWK: contribution of components to the failure frequency and unavailability.

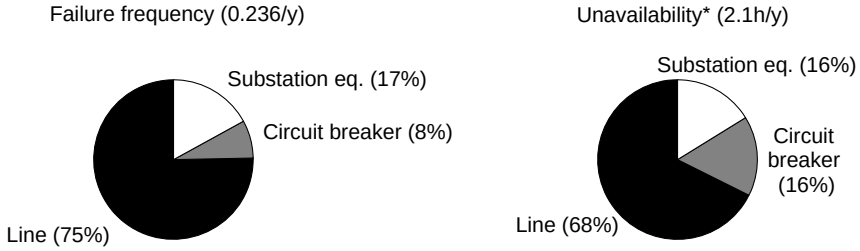

Figure 3.11: MVL-SMH-CST-KIJ: contribution of components to the failure frequency and unavailability.

The same calculation can be performed for the connection MVL-SMH-CST-KIJ. The results are shown in figure 3.11. As can be seen, one circuit of this connection fails almost as often as one circuit of the first connection, although this second connection is longer (80 km) than the first connection (50 km). The failure frequency is mainly the result of overhead line failures.

The average unavailability of this second connection is however significantly smaller than the unavailability of the first connection. In the unavailability of the second connection, overhead line failures contribute the most, although circuit breaker failures and failures of the substation equipment contribute as well. The cable section in the first connection results in a significantly larger average unavailability.

RELIABILITY ANALYSIS MVL REGION NETWORK

The reliability of the network around MVL substation will now be studied by using a state enumeration approach (section 2.5). Several assumptions are made for this study. First, the MVL region network as shown in figure 3.9 is considered, together with a load/ generation scenario for 2020 (scenario2020, appendix A). As shown in figure 3.9, this scenario includes about 2.5 GW installed generation at MVL380. Another 0.5 GW installed generation is located at SMH380. The ranges of the bus loads are as indicated in the figure. The line loads to the main 380kV ring are shown in the figure as well. The bus loads of the substations are relatively small, such that the main load flow is from MVL380 to the main 380kV ring.

The studied network includes the substation SMH380. As SMH380 is a tapping station, a failure in a line connected to SMH380 will lead to a disconnection of the complete MVL-SMH-CST circuit. Therefore, MVL-SMH-CST is regarded as one (double circuit) connection in the model. For simplicity, SMH380 is not considered separately. The load and generation at SMH380 is added to the load and generation at MVL380.

In the load flow calculation, only the MVL region network is considered. The line loads to the main 380kV ring are added to the bus loads of BWK380 respectively KIJ380. The calculations can be performed including the rest of the 380kV network. This does not lead to significantly different results though.

Independent failures as well as dependent double circuit failures are considered in the analysis. For dependent double circuit failures, a dependent failure factor of $c_{cc} = 0.1$ is assumed. For the underground cable sections, the standard configuration (configuration a in figure 3.8) is used. The reliability of the substation equipment is not included in the study. Busbar failures that lead to the disconnection of the two connected circuits can be included, but this does not lead to significantly other results.

Combinations up to 2 failure events are included in the study. Dependent double circuit failures are considered as single failure events, i.e. one failure event that leads to the simultaneous failure of two components. Consequently, the considered failures become: 1 independent single circuit failure, 2 independent single circuit failures, 1 dependent double circuit failure, 2 dependent double circuit failures, 1 independent single circuit failure + 1 dependent double circuit failure.

The reliability of the network is described by the probability of an islanded substation (i.e. a substation is disconnected from the network), the probability of an overloaded circuit in the network and the expected amount of redispatch. These are calculated as described in section 2.5. If a network failure leads to an overloaded circuit and redispatch has to be performed, it is assumed that the generation at MVL380 is decreased and the generation at KIJ380 increased in steps of 100 MW. It is assumed that there is enough reserve capacity available at KIJ380. It is possible to divide the redispatch over the main 380kV ring, but this does not lead to significantly different results either.

BASE CASE

Using scenario2020 (see also appendix A), the reliability of the base case can be studied. In the base case, two underground cable sections are installed in the network, as indicated in figure 3.9. One is the Randstad380 Zuid cable and one is the (2 km) river crossing between MVL380 and WTL380. The results of the analysis are shown in table 3.9.

Table 3.9: Reliability results of the base case.

Probability* of an islanded substation	1.4e-3	h/y
Probability* of an almost islanded substation	7.5	h/y
Probability* of an overloaded circuit	1.3e-5	h/y
Probability* of the n-0 state	0.74	h/y
Expected corrective redispatch	2.6e-3	MWh/y
Expected preventive redispatch	167	MWh/y

The (annualized) probabilities are measured in h/y.

As can be seen, there is a small probability that a substation becomes islanded. The probability of an almost islanded substation, i.e. one more failure will lead to an islanded substation, is larger. As dependent double circuit failures are considered as one failure event, the probability of an almost islanded substation is relatively large. The probability of an islanded substation only depends on the topology of the network, not on the actual load flow within the network. Moreover, the importance of each substation within the network is different. For example, the islanding of a small substation like WTL380 can be manageable as the load of this substation can also be supplied by the 150kV network. The islanding of a large substation containing a substantial amount of generation like MVL380 can be catastrophic though.

In the table, it is shown that the probability of an overloaded circuit is small. Consequently, the expected amount of corrective redispatch (i.e. the redispatch that is needed to restore n-0 redundancy after a network failure) is small as well. The probability of the n-0 state and the expected amount of preventive redispatch (i.e. the redispatch needed to restore n-1 redundancy after a network failure) are larger. This preventive redispatch will cause preventive redispatch costs, which can be a potential financial risk for the TSO. In this base case however, these values are still relatively small.

It must be mentioned that the probability of an almost islanded substation, the probability of the n-0 state and the expected amount of preventive redispatch are all dependent on the definition of a failure event. In this study, dependent double circuit failures are considered as one failure event. Therefore, if one double circuit of a substation fails and a double circuit failure of the other connection will lead to an islanded substation, this substation is regarded as almost in island. Moreover, if there is one single circuit failure in the network and a further double circuit failure will lead to an overloaded circuit, the transmission network is considered to be in the n-0 state. If dependent failures are considered as two failure events, these probabilities become significantly smaller.

UNDERGROUND CABLES AT DIFFERENT LOCATIONS

It is of interest to study the effects of underground cables at different locations within the MVL region network. For this study, first the situation in which the complete network consists of overhead lines is studied. Then, certain overhead line connections within the network are replaced by underground cables, until the complete network consists of underground cables only. For each situation, the reliability of the network is calculated. Three more situations are studied: the base case, the situation in which a short double circuit cable section of 1 km is installed in connection 1-2 (indicated by 1(1km) in the figures), and the situation in which 2 short double circuit cable sections of 1 km are installed in connections 1-2 and 9-10 (indicated by 1,9(2x1km) in the figures).

For multiple cable sections, a distinction between two situations can be made as shown in figure 3.12. Figure 3.12a shows the situation in which two cable sections are located within the same connection route between MVL380 and KIJ380. In figure 3.12b, two cable sections are installed within different connection routes. This distinction will be important for the conclusions of this study.

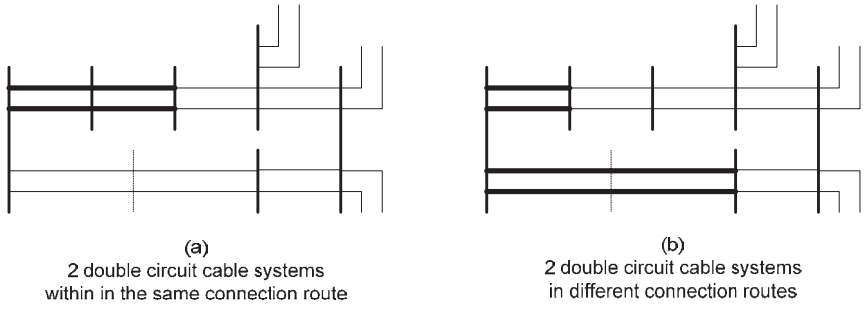

Figure 3.12: Examples of 2 cable sections within the same route and in different routes. As SMH380 is excluded from the study, the connection MVL-SMH-CST is regarded as one double circuit.

PROBABILITY OF AN ISLANDED SUBSTATION

Figure 3.13 (left) shows the probability of an islanded substation in the network. As can be seen, for increasing cable length, the probability of an islanded substation becomes larger. Moreover, the figure shows a clear distinction between 0, 1 and 2 or more cable sections. In the figure, the situation in which two double circuit cable sections of 1 km are installed in connections 1-2 and 9-10 (see figure A.2) is indicated by 1,9(2x1km). According to the figure, it is still better to replace the complete 9-10 double circuit with underground cables than to install two 1 km double circuit cable section within connections 1-2 and 9-10. The relatively large probability of these small cable sections is mainly caused by the terminations of the cable sections.

Another distinction is the difference between multiple cable sections including connection 9-10 and excluding connection 9-10. According to the figure, the long connection 9-10 contributes relatively less to the probability of an islanded substation. This is because the probability of the failure combinations (e.g. two dependent double circuit failures) is smaller for one long cable section than for multiple shorter cable sections. There is no significant difference between multiple cable sections within the same and within different connection routes.

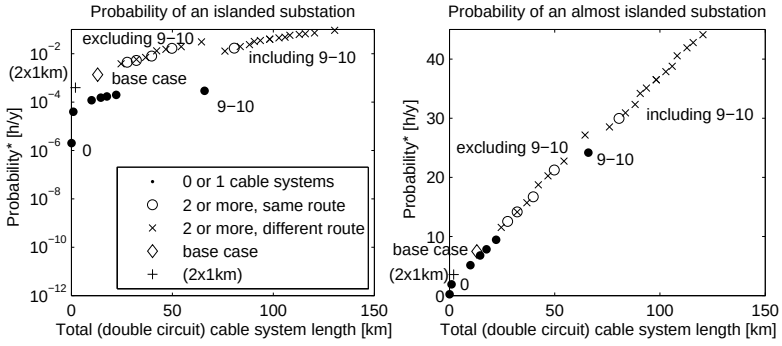

Figure 3.13: Probability of an islanded and almost islanded substation in the MVL380 region network.

Figure 3.13 (right) shows the probability of an almost islanded substation. In the figure, a clear linear relationship between the probability and the total cable length can be seen. This effect is a result of the definition of one failure event. In the studied network, any combination of two dependent double circuit failures leads to an islanded substation. As it is assumed that a dependent double circuit failure is one failure event, the probability of an almost islanded substation becomes the sum of the probabilities of these dependent double circuit failures.

The figure shows a small variation from the linear relationship for multiple cable sections, which is caused by the amount of terminations. There is no significant difference between multiple cable sections within the same and within different connection routes for a certain total cable length. The probability of an almost islanded substation is much larger than the probability of an islanded substation. The probability of an almost islanded substation is relatively large, because of the definition of a failure event, which in this case means that every dependent double circuit failure leads to an almost islanded substation.

1 GW OF WIND CAPACITY AT MVL380

In scenario2020, there is 1 GW offshore wind energy connected to MVL380 substation. Using this scenario, the probability of an overloaded circuit becomes as shown in figure 3.14 (left). As can be seen, the probability of an overloaded circuit is larger for increasing cable lengths. This probability is the largest for multiple cable sections including connections 1-2 and 9-10. The probability of an overloaded circuit is still relatively small. There is no clear difference between multiple cable sections within the same and within other connection routes for a certain total (double circuit) cable length.

However, figure 3.14 (right) clearly shows several groups for the probability of the n-0 state. The group of multiple cable sections including cable sections in both connections 1-2 and 9-10 gives the largest probability. This can be explained as follows. In the studied network, the main load flow is from MVL380 to KIJ380, while some load is connected to the other substations. Therefore, the connections 1-2 and 9-10 are somewhat more loaded and somewhat more likely to become overloaded than the other connections.

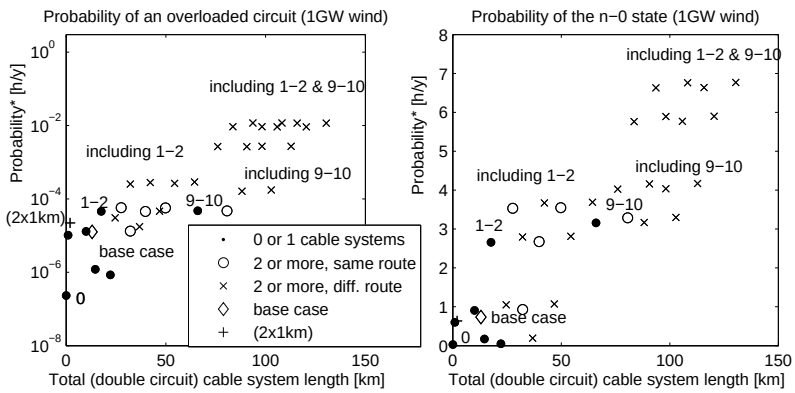

Figure 3.14: Probability of an overloaded circuit and the n-0 state, MVL380 network, 1GW offshore wind.

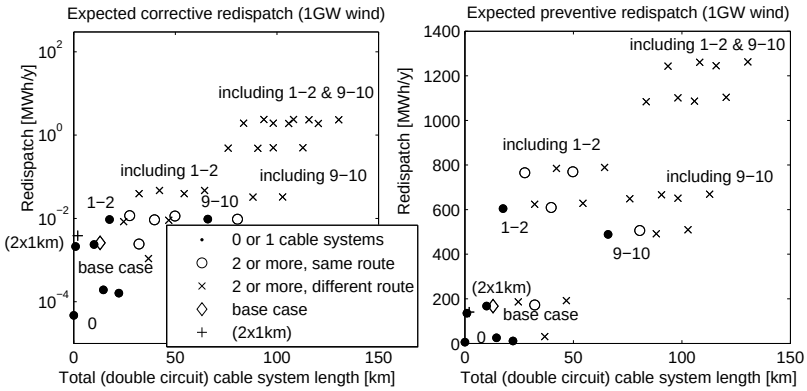

Figure 3.15: Expected corrective and preventive redispatch, MVL380 network, 1GW offshore wind.

More heavily loaded connections will contribute more to the total network unreliability.

The expected amount of corrective and preventive redispatch can be calculated as well. The results are shown in figure 3.15. These graphs look somewhat similar to figure 3.14. The same groups of multiple cable sections can be distinguished. The expected amount of corrective redispatch is small. The expected amount of preventive redispatch is larger, as it is assumed that n-1 security must be restored during a network failure. Again, there is no clear difference between multiple cable sections within the same and within other connection routes for a certain total (double circuit) cable length.

3 GW OF WIND CAPACITY AT MVL380

In the future, MVL380 will be one of the main connection points of offshore wind energy. In scenario2020, 1 GW installed capacity of offshore wind is connected to MVL380 substation. It is of interest to study the effects of larger installed capacities of offshore wind. If the installed capacity of the offshore wind is increased to 3 GW, the maximum generation (minus the load) at MVL380 becomes about 5.2 GW. This is the maximum capacity of the network for which n-1 redundancy is maintained. It is assumed that the additional wind power is absorbed by the main 380kV ring at KIJ380.

Figure 3.16 shows the probability of an overloaded circuit and the n-0 state. As can be seen, the probability of an overloaded circuit has increased compared to figure 3.14. There is now a clear distinction between multiple cable sections within the same connection route and within different connection routes. Multiple cable sections within the same connection have the same result as one cable section. According to this figure, it is even better to install underground cables in one complete connection route than two small cable sections within connections 1-2 and 9-10.

The graph of the probability of the n-0 state shows a linear relationship between the probability of the n-0 state and the total cable length. The probability of the n-0 has increased compared to figure 3.14. The small variation from this linearity is caused by the different amount of terminations of multiple cable sections. There is no significant difference between cable sections within the same and within different connection routes.

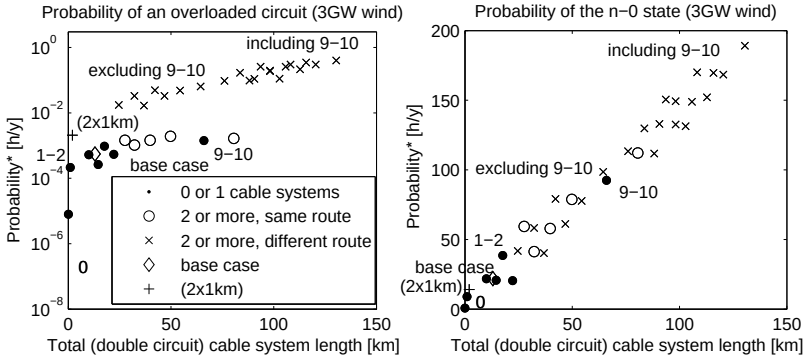

Figure 3.16: Probability of an overloaded circuit and the n-0 state, MVL380 network, 3GW offshore wind.

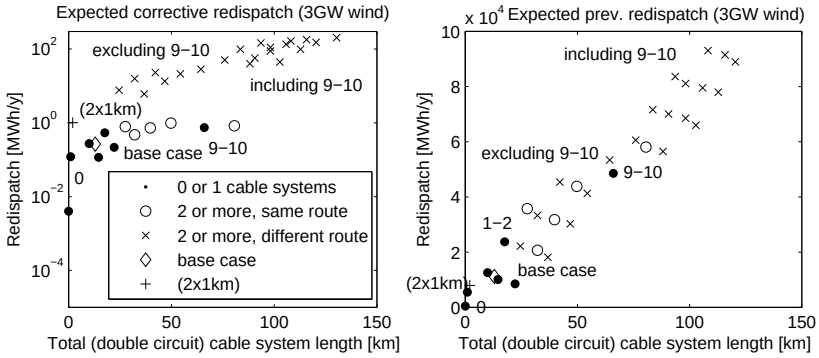

Figure 3.17: Expected corrective and preventive redispatch, MVL380 network, 1GW offshore wind.

Figure 3.17 shows the expected corrective and preventive redispatch. These graphs show comparable effects as figure 3.16. It can be seen that the expected amount of corrective redispatch has increased, especially for longer cable sections within different connection routes. The expected amount of preventive redispatch increases significantly for longer cable sections. This is the result of the definition of one failure event and the assumption that n-1 redundancy must be maintained during network failures. If n-0 redundancy is acceptable during network failures or if dependent double circuit failures are not considered as one failure event, the expected amount of preventive redispatch becomes significantly smaller.

NETWORK RELIABILITY VERSUS THE GENERATION AT MVL380

As the main load flow in the studied network is from MVL380 to the main 380kV ring (KIJ380 and BWK380), it is possible to perform the same analysis for different generation levels at MVL380. This calculation is based on several assumptions. First, it is assumed that the large-scale generation is transmitted by the two connection routes from MVL380 to the main 380kV ring. The load is absorbed at KIJ380 and BWK380 (60% at KIJ380 and 40% at BWK380), such that the power flow is equally divided between the

two connection routes. Furthermore, the generation and load at the other substations are small compared to the amount of generation at MVL380, and can be neglected. Independent single circuit failures as well as dependent double circuit failures are included in the study. If a network failure leads to an overloaded circuit, generation is redipatched between MVL380 and KIJ380.

Figure 3.18 shows the probability of an overloaded circuit and the probability of the n-0 state. As can be seen, for generation levels below 2.5 GW, network failures do not lead to an overloaded circuit in the network. It is however still possible that network failures lead to an islanded substation. Above 2.5 GW, network failures including three circuits can lead to an overloaded circuit. From about 5 GW, some dependent double circuit failures and certain independent single circuit failures will lead to an overloaded circuit and the probability increases. The probability of the n-0 state then becomes 1 (8760 h/y), as some single failure events will lead to an overloaded circuit.

As can be seen in the figures, installing underground cables will lead to increased probabilities of an overloaded circuit and the n-0 state. In the base case, the increase in the probability of an overloaded circuit between 2.5 and 5 GW seems manageable. For higher generation levels, this probability becomes much larger (100s h/y). The probability of the n-0 state becomes larger as well for generation levels between 2.5 and 5 GW (100s h/y).

The expected amount of corrective and preventive redispatch are shown in figure 3.19. For generation levels below 2.5 GW, the redispatch is caused by the islanding of MVL380. From 2.5 GW, network failures including three circuits can lead to redispatch, and from about 5 GW, some dependent and independent failures will require redispatch. From about 10 GW, redispatch is always required as this is the maximum transport capacity of the network.

Underground cables will lead to an increase in the expected amount of corrective and preventive redispatch. Especially the increase in the amount of preventive redispatch is large. The amount of preventive redispatch is dependent on the definition of one failure event and the acceptance of n-0 redundancy during network failures.

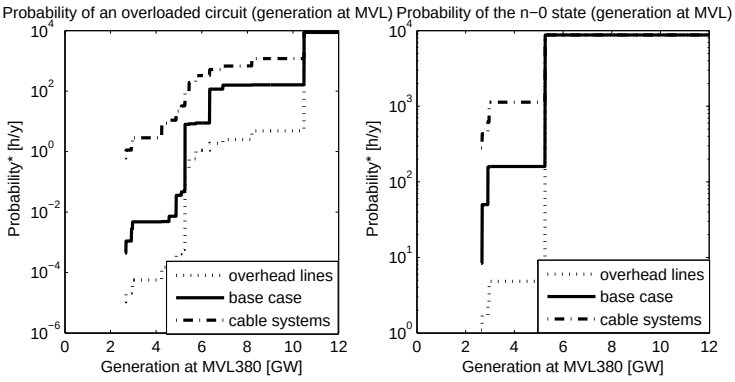

Figure 3.18: Probability of an overloaded circuit and the n-0 state in the MVL380 region network for increasing generation at MVL.

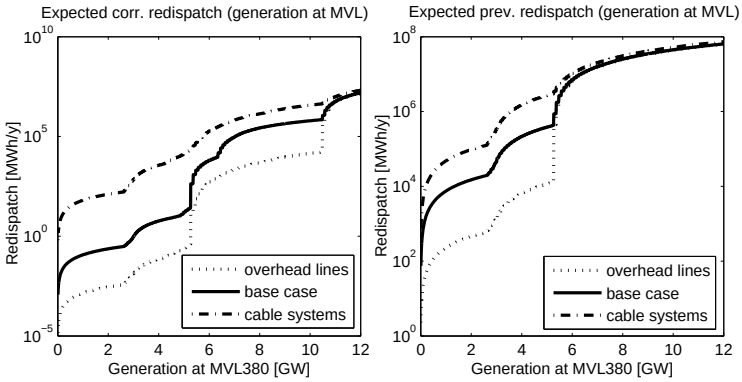

Figure 3.19: Expected corrective and preventive redispatch in the MVL380 network for increasing generation at MVL. For generation levels below 2.5GW, the redispatch is caused by islanding of MVL380.

EFFECT OF MORE WIND GENERATION AT MVL380

It might be interesting to study the effects of more installed offshore wind capacity at MVL380 substation. As mentioned before, in the base scenario there is 1 GW offshore wind capacity connected to MVL380 substation. To study the reliability impact of more offshore wind generation, the installed wind capacity can be increased in the load/ generation scenario (i.e. scenario2020). It is assumed that the extra wind power is absorbed in the 380kV-ring connected to KIJ380. Figure 3.20 shows the results of this reliability analysis. On the x-axis the total installed generation capacity (i.e. wind and conventional) at MVL/SMH is shown, while the y-axis shows the occurrence of various system states (e.g. overloaded or n-0 redundant).

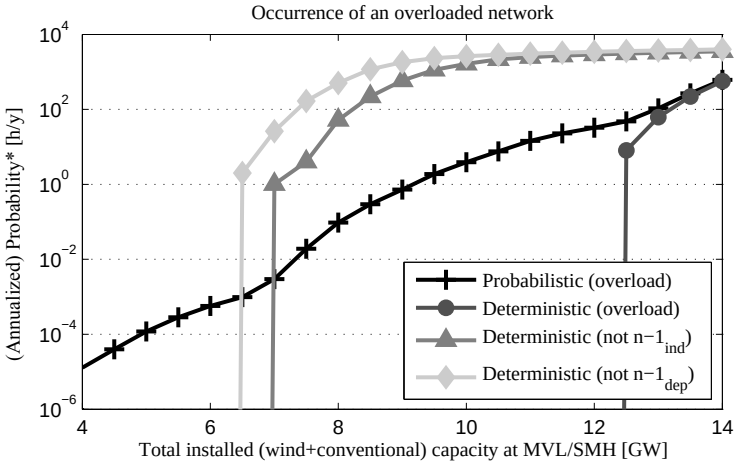

Figure 3.20: Reliability analysis for increasing installed generation capacity at MVL/SMH.

The graph is an illustrative example of the difference between deterministic and probabilistic approaches. The figure shows the probability of an overloaded network (black line, +) and the deterministic occurrence of an overloaded network (dark gray, •). Furthermore, the graph shows how often the network is not deterministic n-1 redundant, if only independent contingencies are considered (light gray triangle), and if both independent and dependent double circuit failures are considered (light gray diamond).

From this graph, it can be concluded that the probability of an overloaded network indeed increases when the loading of the network increases. To compare probabilistic and deterministic reliability indicators, the three deterministic criteria and the probabilistic indicator are shown in one graph. For example, the deterministic overload shows that at about 12.5 GW installed generation capacity, the network will be overloaded for sure for 2 h/y. This because the total load flow in the networks becomes larger than the maximum transport capacity of the network then.

Furthermore, it can be seen that at about 6.5-7.0 GW installed capacity at MVL/SMH, the network is 1 h/y not n-1 redundant. Consequently, the network is in the n-0 state (alert state). However, according to the probabilistic analysis, the network is overloaded for about 1e-3 h/y in this case. In addition, although the deterministic approach shows that the network is 1 h/y in the n-0 state at about 6.5-7.0 GW and 1 h/y overloaded at about 12.5 GW installed capacity at MVL/SMH, according to the probabilistic approach the network will be overloaded for 1 h/y at about 9 GW installed capacity.

The difference between deterministic and probabilistic reliability indicators is illustrated in this example. In the meanwhile, it shows the challenges of interpreting the results of reliability analysis. If it is decided to use a probabilistic criterion, what probability of an overloaded network is acceptable and how much generation capacity can then be installed at MVL380 substation? Of course, this also depends on the remedial actions that are needed to relieve the network overload, i.e. whether generation redispatch will be sufficient or whether load needs to be curtailed.

CONCLUDING REMARKS

These studies showed the influence of underground cables at various locations within a transmission network. For the probability of an islanded substation, the probability of an overloaded circuit and the expected amount of corrective redispatch, there is a clear difference between multiple cable sections within the same connection route and within other connection routes when the network becomes more heavily loaded. According to the results, it is even better to replace one complete connection route by underground cables than to install short cable sections within both connection routes. This effect is strongly dependent on the loading of the network and is the most pronounced if the network is maximally loaded under n-1 redundancy, in this case with 3 GW wind capacity at MVL380. This result suggests that the situation with cable sections within different connection routes (figure 3.12b) should be avoided.

For the probability of an almost islanded substation, the probability of the n-0 state and the expected amount of preventive redispatch, there is a linear relationship between the probability and the total (double circuit) cable length if both dependent and independent failures are considered. The resulting values are dependent on the definition of one failure event and the acceptance of n-0 redundancy during network failures.

3.5.2. UNDERGROUND CABLES IN THE RANDSTAD REGION

A similar study can be performed for the Randstad region network, as illustrated in figure 3.21 (and described in appendix A). The same assumptions as for the MVL380 analysis are made. As BKL and SMH are tapping stations, these stations are excluded from the study. The load of these substations is added to the load of DIM and MVL respectively. It is assumed that at DIM, both circuits OZN-DIM-BKL-KIJ are connected to the substation. Connection 21-22 is part of the main 380kV ring and is considered fully reliable. Table 3.10 gives an overview of the installed generation capacity at the substations in the two scenarios that will be studied.

First, the line loadings in normal operation are determined by using scenario2020. Table 3.11 shows the maximum line loadings in the studied scenarios. As can be seen, connections 13-14 (BVW-OZN) and 15-16 (OZN-DIM) are the most heavily loaded. Consequently, it can be expected that these connections will contribute the most to the total unreliability on the network.

If an n-1 contingency analysis is performed on the network by using scenario2020, it is found that circuit 16 is one hour (per year) overloaded if circuit 15 is out of service. A

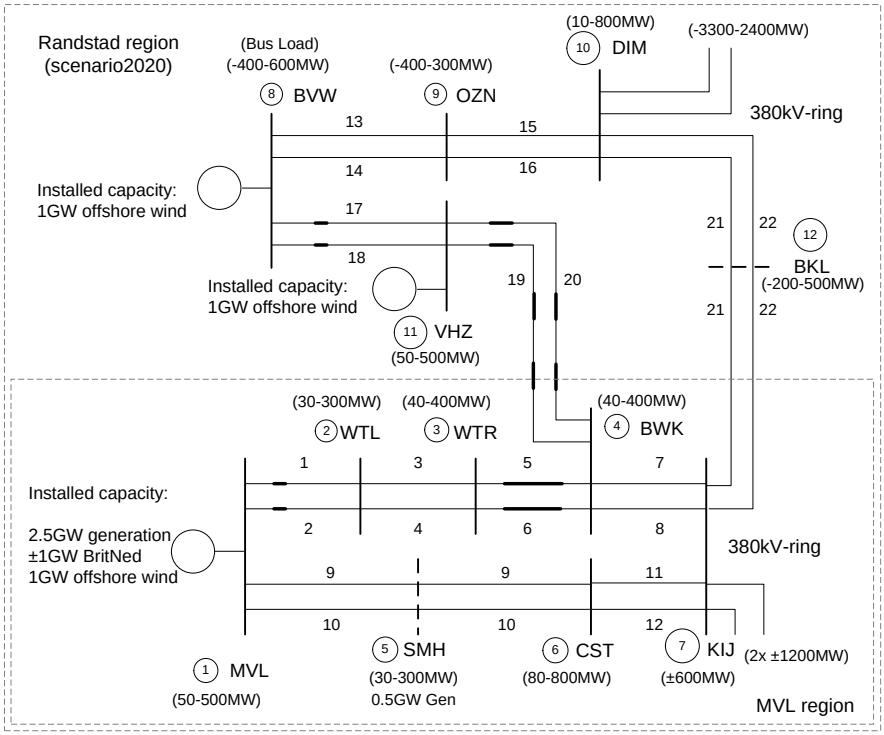

Figure 3.21: Randstad region network. In the figure, the bus loads, line loads and installed generation per bus are shown. The locations of the underground cables of Randstad380 Noord and Zuid are indicated by bold lines.

Table 3.10: Installed capacity according to two scenarios for 2020.

Installed capacity	Scenario 2020	Changed scenario
BVW380 offshore wind	1 GW	2 GW
VHZ380 offshore wind	1 GW	2 GW
MVL380 conventional gen.	2.5 GW	2.5 GW
MVL380 BritNed	± 1 GW	± 1 GW
MVL380 offshore wind	1 GW	3 GW
SMH380 conventional gen.	0.5 GW	0.5 GW

Table 3.11: Maximum line loadings in the used scenarios.

Connection	Scenario 2020	Changed scenario
1-2	34%	47%
3-4	31%	44%
5-6	24%	40%
7-8	25%	56%
9-10	32%	55%
11-12	28%	47%
13-14	55%	52%
15-16	57%	53%
17-18	17%	17%
19-20	23%	39%
21-22	40%	38%

Table 3.12: Reliability of the network based on an n-1 contingency analysis.

Connection 15	Unavailability [-]	h/y overloaded [h/y]	Network overloaded [h/y]
Overhead line	3.07e-5	1	3.07e-5
Cable section	7.82e-3	1	7.82e-3

failure of circuit 16 however does not cause an overload of circuit 15, because of a slight difference in the rated capacities. Other single circuit failures and dependent double circuit failures do not lead to any overloaded circuits. With this information, a first guess of the network reliability can be made. As can be seen in table 3.12, the unavailability of circuit 15 is 3.07e-5 if it is an overhead line and 7.82e-3 if it is an underground cable connection. As a result, it can be expected the probability of an overloaded circuit within the network is around 3.07e-5 h/y if circuit 15 is an overhead line and around 7.82e-3 h/y if this circuit is an underground cable. Next, the probability of an islanded substation and an overloaded network is calculated including the higher-order failure states and the results will be compared.

PROBABILITY OF AN ISLANDED SUBSTATION IN THE NETWORK

For the Randstad region network, the probability of an (almost) islanded substation is shown in figure 3.22. Due to space limitations, in the figures only some connection numbers are shown. Three clouds can be distinguished. The probability of an islanded substation is the smallest when the network consists of overhead lines only, or when

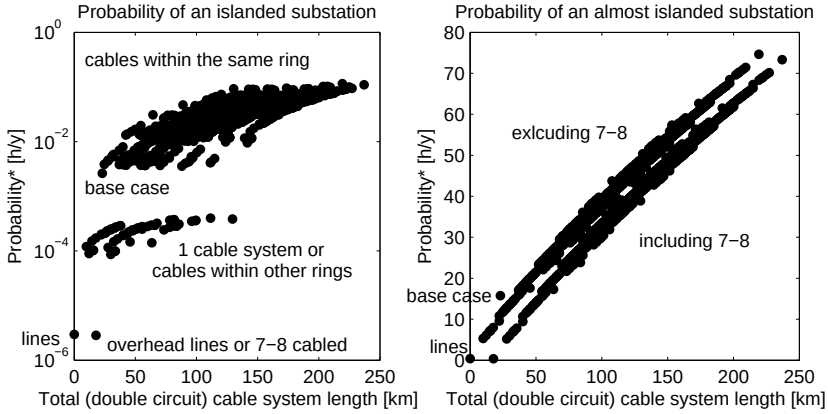

Figure 3.22: Probability of an islanded and almost islanded substation, Randstad region network.

connection 7-8 is replaced by underground cables. As can be seen in figure 3.21, cabling connection 7-8 does not contribute much to the probability of an islanded substation as three double circuit (including 7-8) failures are required for an islanded substation.

In figure 3.22, the cloud in the middle consists of these situations in which one double circuit cable connection is installed in the network or when multiple double circuit cable connections are installed within different network rings. The upper cloud consists of the situations in which multiple cable sections are installed within the same network ring. Because in this latter case, certain substations are connected in between two double circuit cable sections, the probability of an islanded substation is the largest.

Figure 3.22 (right) shows the probability of an almost islanded substation. As can be seen, there is an almost linear relationship between the total (double circuit) cable length and the probability of an almost islanded substation. A small deviation from this linearity is caused by the total amount of terminations of the cable connections. As connection 7-8 does not contribute significantly to the probability of an (almost) islanded substation, actually two lines can be distinguished (including 7-8 and excluding 7-8). As the probability will saturate at 8760 h/y, the lines are slightly curved.

NETWORK RELIABILITY USING SCENARIO2020

The probability of an overloaded circuit and the probability of the n-0 state using scenario2020 are shown in figure 3.23. Previously, it was suggested that connections 13-14 and 15-16 will contribute the most to these probabilities. Furthermore, it was estimated that the probability of an overloaded circuit is 3.07e-5 h/y if circuit 15 is an overhead line and around 7.82e-3 h/y if this circuit consists of underground cables.

In figure 3.23, the probability of an overloaded circuit is shown. Several clouds can be distinguished in the figure. As can be seen, the probability indeed is around 3e-5 h/y if circuit 15 is an overhead line and around 8e-3 h/y is this circuit consists of underground cables. The figure also shows that the probability of an overloaded circuit increases if connection 1-2 is a cable connection. Although it was shown before that connection 1-2 is a heavily-loaded connection, this connection was not overloaded in the n-1 contin-

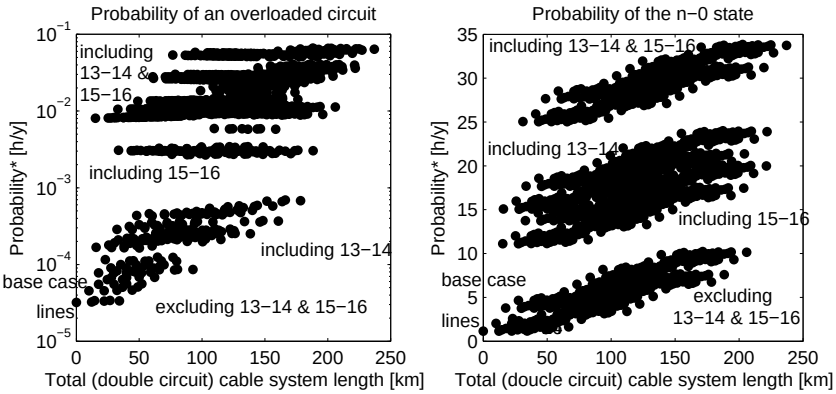

Figure 3.23: Probability of an overloaded circuit and the n-0 state, Randstad region network, scenario2020.

gency analysis. If the higher-order failure states are included in the reliability analysis, the contribution of these states to the probability of an overloaded circuit can be studied. As a result, several clouds can be distinguished in figure 3.23, which mainly depends on whether connection 13-14 and 15-16 are cabled.

In figure 3.23 (right), several clouds can be distinguished as well. As can be seen, the probability of the n-0 state is the largest if both connections 13-14 and 15-16 are replaced by underground cables. It can be concluded that the probability of an overloaded circuit and the probability of the n-0 state are strongly dependent on the actual loading of the network. Heavily-loaded connections will contribute significantly more to these probabilities if these connection are replaced by underground cables. Connections that are less loaded have a minor contribution to these probabilities.

NETWORK RELIABILITY USING A CHANGED SCENARIO

To study the effects of a more heavily loaded network and a more equally divided load flow, the study is performed again using an alternative scenario (see also table 3.10). In this changed scenario, several assumptions are made. First, it is assumed that the capacity of all the circuits is 2635 MVA. Furthermore, the impedance of connection 1-2 is increased to three times its previous value to get a more balanced load flow within the Northern ring of the Randstad region network. This could be realized by installing additional series impedance like in Randstad380 Zuid. As a result, the installed offshore wind capacities can be increased to 2 GW, 2 GW, and 3 GW at BVW, VHZ and MVL respectively. The additional power is absorbed at DIM and KIJ (the main 380kV ring). Although these assumptions may be somewhat extreme, it is the intention of this study to show the effects of a more balanced load flow and a more heavily loaded network.

Table 3.11 shows the line loadings of this changed scenario. As can be seen, the load flow is more equally divided over the different connections and most connections are maximally loaded at about 50%. Only connection 17-18 is considerably less loaded and is expected to contribute less to the total network unreliability.

The probability of an overloaded circuit is shown in figure 3.24 (left). If this figure is compared with figure 3.23, a significant increase in the probability of an overloaded

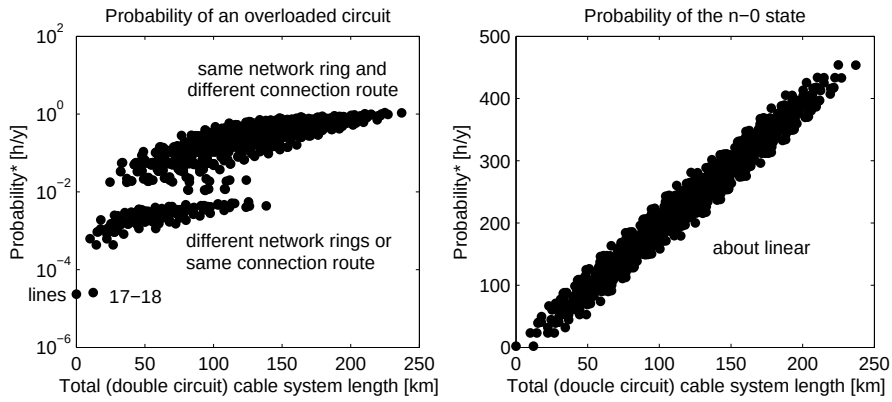

Figure 3.24: Probability of an overloaded circuit and the n-0 state, Randstad region network, changed scenario2020.

circuit can be seen. Furthermore, three clouds can be distinguished. The lowest probability is obtained when the network consists of overhead lines only or when only connection 17-18 is replaced by underground cables. As connection 17-18 is considerably less loaded, the contribution to the probability of an overloaded circuit can be neglected.

The middle cloud consists of situations in which only one (double circuit) cable is installed within the network. Another possibility is that multiple cable sections are installed within different network rings or within the same connection route within the same ring. The upper cloud consists of situations in which multiple cable sections are installed within different connection routes within the same network ring. As can be seen in the figure, these will cause the largest probability of an overloaded circuit.

Figure 3.24 (right) shows the probability of the n-0 state. As can be seen, the probability of the n-0 state increases almost linearly with the total (double circuit) cable length. Again, this depends on the definition of a failure event (i.e. whether dependent double circuit failures are considered as one failure event or not). A small variation is caused by the total amount of terminations within the network. Compared with figure 3.23 (right), the probability of the n-0 state has increased significantly. This is because the network is more heavily loaded.

CONCLUDING REMARKS

Comparing the results of the Randstad and MVL380 region networks, several conclusions can be drawn regarding the reliability of underground cables in transmission networks. These are summarized in table 3.13. A rather trivial conclusion is that it is better to replace a weakly-loaded connection with underground cables than a heavily loaded connection. Although trivial, this can easily result in a misinterpretation of the reliability analysis. For example, it is possible that in a certain reliability analysis with a certain load flow scenario, a cable connection is weakly-loaded and does not contribute significantly to the network unreliability. Later, when the load flow in the network changes because of other load patterns, new generation units or renewable sources, this cable connection will become heavily-loaded and will contribute significantly to the network unreliability.

(Almost) islanded substation	Overloaded network / n-0 state
The probability of an (almost) islanded substation is independent of the load flow within the network.	The probabilities of an overloaded circuit and the n-0 state are strongly dependent on the load flow within the network.
There is a step in the probability of an islanded substation for 0, 1 or 2 or more cable sections within the same network ring.	**It is better to replace a weakly-loaded connection with cables than a heavily-loaded connection.**
For the probability of an islanded substation, it is better to limit the number of cable connections to maximum one per network ring.	There is a step in the overload probability for no underground cables, cable sections within the same connection route, and cable sections within different connection routes.
The probability of an almost islanded substation increases linearly with the total (double circuit) cable length within the network ring.	The probability of the n-0 state increases linearly with the total double circuit cable length.
In larger transmission networks, it is better to divide cable sections over different network rings with maximum one cable section per network ring.	**For multiple cable sections, it is better to have cable sections within the same connection route than within different connection routes within the same network ring.**

Table 3.13: Conclusions reliability of underground cables in transmission networks.

According to the studies, the network reliability is dependent on whether the cable sections are within the same network ring and within the same connection route. The latter one being a series of connections with relatively small load at the substations on the connection route (such that the load flow is roughly the same over the connection route). For the probability of an islanded substation, it is better to limit the number of cable sections to one per network ring. For the probability of an overloaded network, it is better to avoid cable sections within different connection routes. More cable sections (also partially-cabled) within the same connection route will have a similar effect as one long cable section.

3.6. AMOUNT OF FAILURES IN LARGE TRANSMISSION NETWORKS

In the previous section, the effects of underground cables in the connection of MVL380 substation and in the Randstad region were studied. In reality, underground cables will be part of a larger transmission network. The reliability of the cable connections will influence the reliability of this larger network. As there is a trend to install more underground cables, it is of interest to study the impact on the reliability of the transmission network as a whole.

In the current operational practice, n-1 redundancy is an essential criterion. Single failures should not lead to a failure of the transmission network. Moreover, possible dependent double failures, like dependent double circuit failures, may not lead to a failure of the transmission network as well. Therefore, during system operation, the possible single contingencies (and certain dependent double contingencies) are carefully mon-

itored. In case of a failure, n-1 redundancy will give the system operator time to take corrective actions to restore secure operation. It is therefore important to know how often single, double, and even triple contingencies might happen.

In this section, it is estimated how often failures will happen in practice if more and longer cable connections are installed in the transmission network. For this study, the main ring of the Dutch 380kV transmission network is used as a study case (appendix A). This main ring is designed for n-1 redundancy during maintenance activities. The main 380kV ring consists of 26 line circuits ranging from 20 to 70 km. For the calculation, certain double line circuits are replaced by underground cables. Although it is not the intention to replace these line circuits by cables, it provides insight into the influence of underground cables on the reliability of large transmission networks. The mean time between single, two, three and four contingencies and their probabilities are calculated for this main ring.

3.6.1. PROBABILITY AND FREQUENCY OF FAILURE STATES

With the state enumeration described in appendix D, the probabilities and frequencies of the different system failure states can be calculated. First, the range of the probabilities and frequencies of the individual failure states are calculated. The results are shown in figure 3.25. In the figures, the minimum, average and maximum values of the individual state probabilities and frequencies are shown by the lines with dots. The large dots indicate the total probability and frequency of the particular failure states.

As can be seen, there is a large decrease in the probability and frequency for higher-order states. There is no overlap between the ranges of state probabilities and frequencies. Moreover, the probabilities and frequencies of independent failure combinations are an order of magnitude smaller than for dependent failures. For this reason, it is often sufficient to observe only the lower-order contingencies (i.e. 1 independent, 2 dependent, sometimes 2 independent) during system operation and planning. Higher-order states are rare and often not considered.

A similar study can be performed for a network including a 10 km underground cable section. For this study, an underground cable section is assumed to be installed within a line connection of medium length. Figure 3.26 shows the results. As can be seen, the ranges of state probabilities and frequencies have now increased as the maximum values have become significantly larger. The minimum values are unaltered because the shortest connections in the network are still overhead lines. The ranges of the state frequencies of single and dependent double failures have not changed because these frequencies are not dependent on the repair time.

Although the average and total state probabilities and frequencies have become larger, there is still a strong decrease in the probabilities and frequencies of higher-order states. In this case, it is probably still sufficient to observe the lower-order states only. The overlap between the ranges suggests that special attention should be paid to higher-order contingencies that include the cable sections.

For the extreme scenario in which the complete 380kV main ring is replaced by underground cables, the results of this study are as shown in figure 3.27. The state probabilities and frequencies have now increased significantly. Consequently, there is only a weak decrease in these probabilities and frequencies for higher-order states. There is an

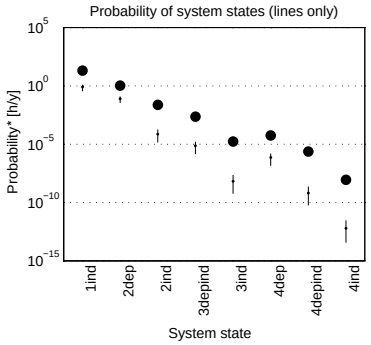

(a) **Probability**

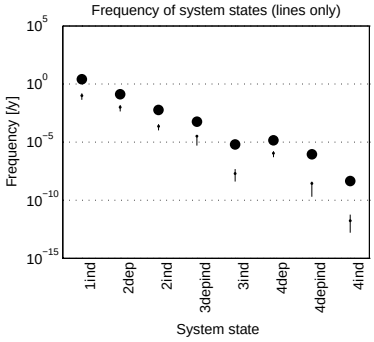

(b) **Frequency**

Figure 3.25: Probability and frequency of system failure states if the 380kV ring consists of lines only.

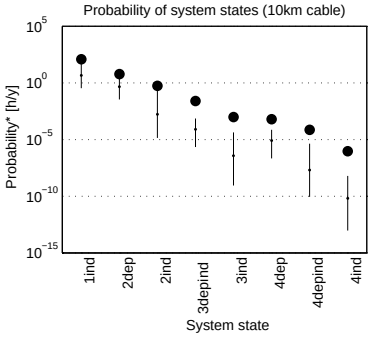

(a) **Probability**

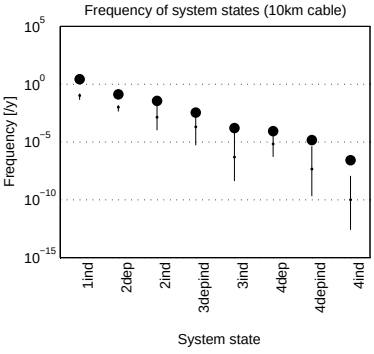

(b) **Frequency**

Figure 3.26: Probability and frequency of system failure states if a 10km cable section is installed in the 380kV ring.

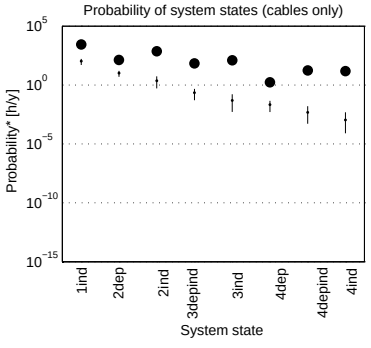

(a) **Probability**

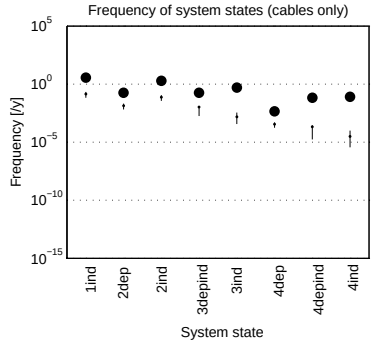

(b) **Frequency**

Figure 3.27: Probability and frequency of system failure states if the 380kV ring consists of underground cables only.

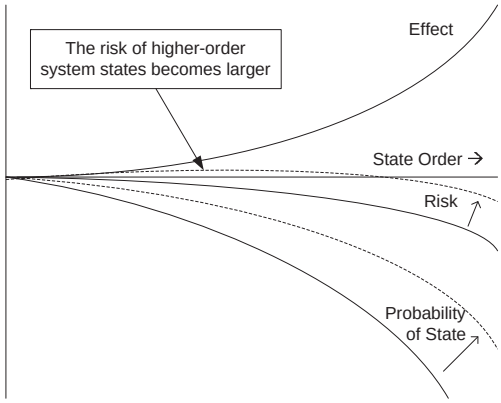

Figure 3.28: Increasing risk when more unreliable components are included in the network. The solid lines indicate the risk, state probabilities and effects in the current situation. The dashed lines indicate the increased state probabilities and risk when more unreliable components are included.

overlap between most of the system failure states and (more complex) combinations of independent failures become more likely than (more logical) dependent failures.

This principle is also illustrated in figure 3.28. For higher-order states, the state probability becomes smaller. The effects however increase for these higher-order states. The total risk is defined as the product of the probability and the effect [16]. As normally the decrease of the probability is stronger than the increase of the effects, the total risk per state order decreases for higher-order states.

Now, if the decrease of the state probabilities is weaker, the total risk increases as well. As shown by the dashed lines, the result can be that certain states (e.g. 2 independent failures or the combination of 1 dependent and 1 independent failure) will have a larger total risk than lower-order states. Consequently, these states will highly influence the total reliability of the network and must be considered in system planning and operation.

For larger transmission networks, the minimum, average and maximum probabilities and frequencies of the individual failure states do not change much. Actually, these become a bit smaller because the product of the availabilities of the other components decreases for larger networks. The total probabilities and frequencies of the states will increase though. The probability and frequency of independent higher-order failures will increase even faster because of the larger amount of independent failure combinations. In larger transmission networks this does not need to be a problem, as independent failures are less likely to be in the same area.

When the transmission network is large enough, it is probable that it is normally in a higher-order state, i.e. there are always some failed connections under repair. Using an approximation of the model, described in appendix D, it is possible to study the effects of larger transmission networks on the probability of the system failure states. The results are shown in figure 3.29. The figure on the left shows the situation in which 10% of the connections are underground cables. It can be seen that for larger transmission

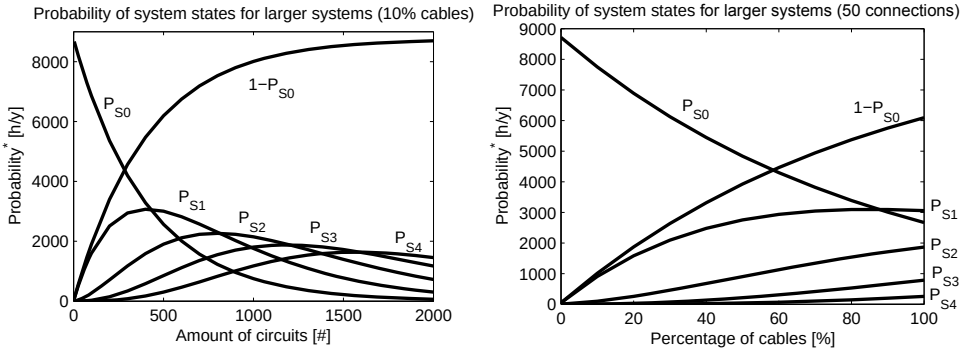

(a) 10% underground cables **(b) Percentage of underground cables.**

Figure 3.29: Influence of the network size on the state probabilities (left) and increasing percentage of underground cables (right). P_S, P_{S1}, etc. indicate the probabilities of having 0,1, etc. failures. $1-P_{S0}$ indicates the probability of having one of more failures. An average line length of 50 km is assumed. The repair time of cable connections is assumed 730 h and the repair time of overhead lines is assumed 8 h. The dependent failure factor is 0.1. Higher-order states (than P_{S4}) are not shown. In the left figure, a percentage of cables of 10% is assumed and in the right figure, it is assumed that the network consists of 50 connections. For the calculation, the mathematical approximation of the state model is used (D).

networks, it indeed becomes more likely that the network is in a higher-order state.

Something interesting is the fact that the probabilities of the higher-order states are so close to each other. Normally in small networks, there are no failures. Single failures can happen, double failures are less likely and higher-order failures can almost be neglected. In a very large transmission network (of about 1000 circuits), it is likely that there are two failures. However, it is almost as likely that there are one or three failures in the network. There is even a large probability that there are zero or four failures. And probably, the higher-order failures cannot be neglected as well. This will make reliability analysis of very large (or very unreliable) networks even more complex.

In figure 3.29b, the effect of more cables in the transmission network is shown. A repair time of cable connections of 730 h is assumed. It is shown that for increasing percentages of cabling, the probability of higher-order failure states increases. Therefore, for a certain repair time, the maximum percentage of underground cabling in the transmission network might be limited as well.

3.6.2. INFLUENCE OF THE FAILURE FREQUENCY AND REPAIR TIME

As already discussed before for underground cable connections, the failure frequency and the repair time are two parameters that influence the reliability. In this section, the effect of the failure frequency and the repair time on the amount of failures in large transmission networks is studied. Again, the Dutch main 380kV-ring is considered and the model as discussed in appendix D is used. For this first study, one cable section of 10 km is included in the 380kV-ring.

Figures 3.30 to 3.32 show the results of this study. In the figures, the failure frequency (measured in /cctkmyr) is assumed to include the joints and terminations as well. Figure 3.30 shows the probability of having no failures in the network. As can be seen, this

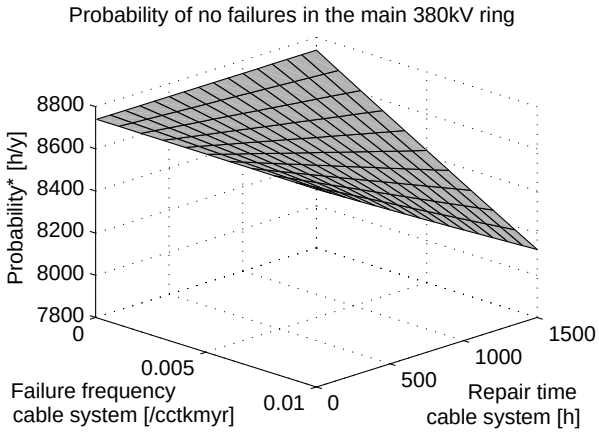

Figure 3.30: (Annualized) probability of no failures in the main 380kV ring. The indicated failure frequency is measured in /cctkm·yr. It is assumed that this value includes the failure frequencies of the joints and terminations as well. For this calculation, one double circuit cable section of 10 km is included in the network.

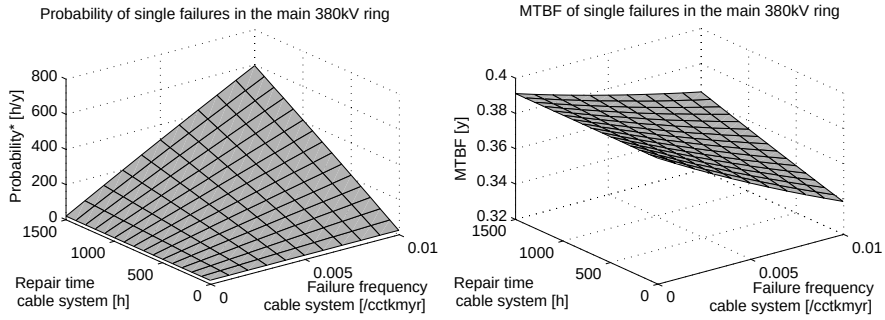

(a) P1 **(b) MTB1F**

Figure 3.31: (Annualized) probability and MTB1F of single failures in the main 380kV ring.

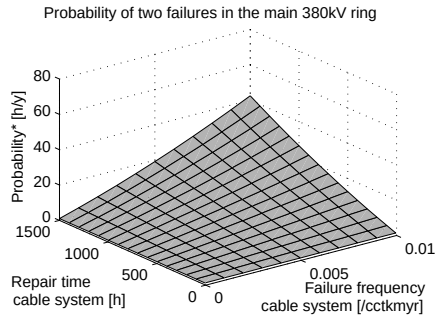

(a) P2

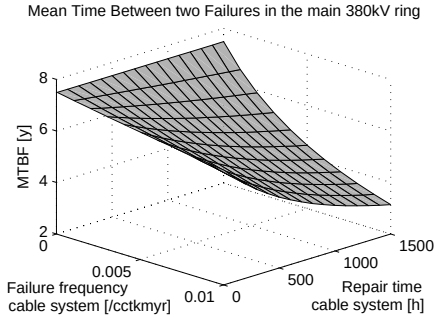

(b) MTB2F

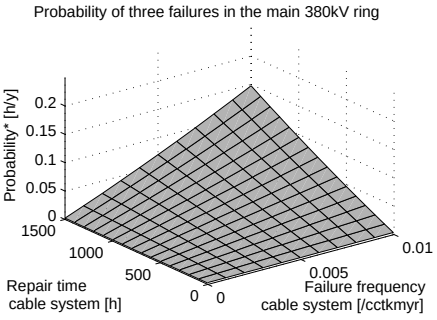

(c) P3

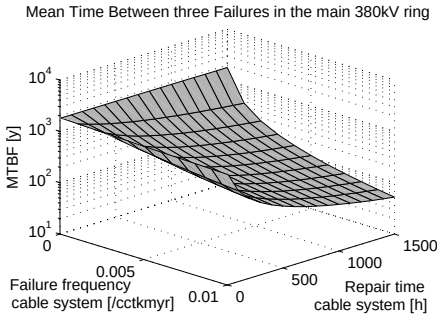

(d) MTB3F

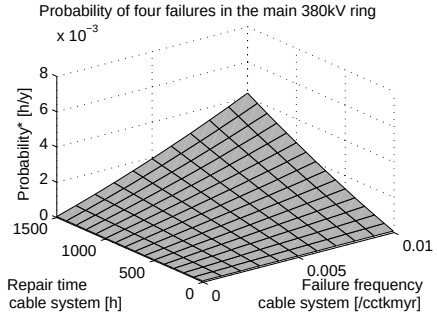

(e) P4

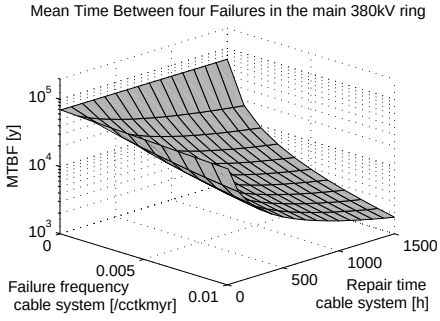

(f) MTB4F

Figure 3.32: (Annualized) probability and MTBF of higher-order failures in the main 380kV ring.

probability decreases for increasing failure frequencies and repair times. From figure 3.31, it can be seen that the probability of single failures is almost linearly proportional to the failure frequency and repair time. This is logical as the unavailability of a component is the product of its failure frequency and repair time. The MTB1F decreases more or less linearly for increasing failure frequencies, while the influence of the repair time is smaller. Actually, there is a small increase for larger repair times. This is because in this case, the higher-order failure states become more possible.

Figures 3.32a and 3.32b show the results for two failures in the network. In the left figure, a significant increase in the probability of two failures can be seen. For example, for a failure frequency of 0.005 /cctkmyr and a repair time of 730 h, it is expected that there will be two failures in the network for about 20 h/y. In the right figure, the reduction in the MTB2F can be seen. For a failure frequency of 0.005 /cctkmyr and a repair time of 730 h, there will be two failures in the network about once every 5 year. The relative increase of the probability is much larger than the decrease in MTB2F. This is caused by the large difference in repair time of overhead lines and underground cables.

The other figures show the probabilities and MTBF of three and four failures. Although the probability of these higher-order contingencies increases, the probability is still relatively small. This can be explained as follows. Because for this study, one double circuit cable section is included in the network, higher-order (3 and 4) contingencies always include an overhead line. As the repair time of this overhead line is small, the total probability of these higher-order states is small as well. The figures of the MTBF however show a significant decrease for larger failure frequencies and longer repair times. In general, these figures show that the reliability of the larger transmission network can be improved by both reducing the failure frequency or the repair time of cable connections.

3.6.3. INFLUENCE OF THE TOTAL CABLE LENGTH AND REPAIR TIME

The length is another parameter that influences the reliability of a cable connection. It is of interest to study the effects of changes in the total underground cable length and the repair time of the occurrence of failures in large transmission networks. This is done in this section. For the study, it is assumed that there is one cable section in the network. The failure frequencies from table 3.1 (TSOs high) are used.

Figures 3.33 to 3.35 show the results of this study. As can be seen in figure 3.34, the probability of single failures increases significantly for longer cable connections and longer repair times. This larger probability is mainly caused by the longer repair time of the cable connection. The MTB1F is less sensitive to the total cable length as the difference between the failure frequency of underground cables and overhead lines is smaller. The small increase for longer repair times in the MTB1F is because in this case, the probability of higher-order states becomes larger.

In figures 3.35a and 3.35b, the effects on the occurrence of two failures in the network is shown. These figures show a large increase in the probability and a decrease in the MTB2F of two failures. Figures 3.35c to 3.35f show the consequences for three and four failures. For longer cable connections and longer repair times, the MTB3F and MTB4F decrease significantly. The MTB2F decreases from once every 2,000 years to once every 300 years, while the MTB4F decreases from once every 70,000 years to once every 1,000 years. The increase in the probabilities is limited as it is assumed that there is only one

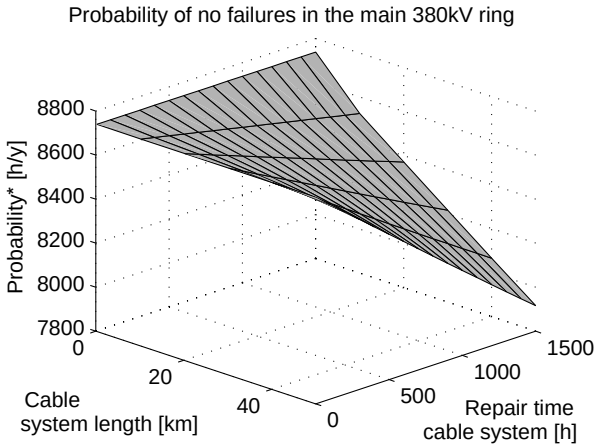

Figure 3.33: (Annualized) probability of no failures in the main 380kV ring.

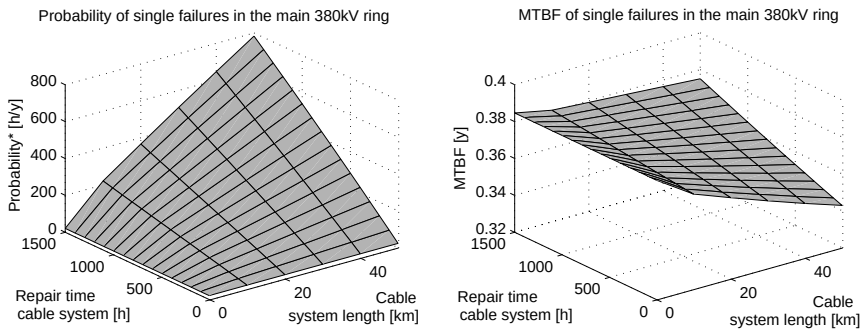

(a) P1 **(b) MTB1F**

Figure 3.34: (Annualized) probability and MTB1F of single failures in the main 380kV ring.

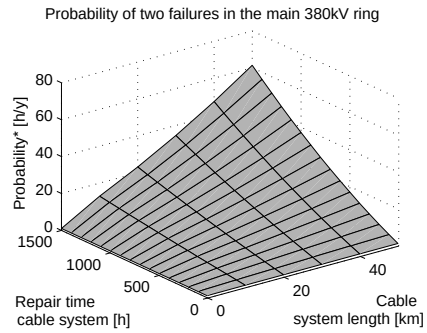

(a) P2

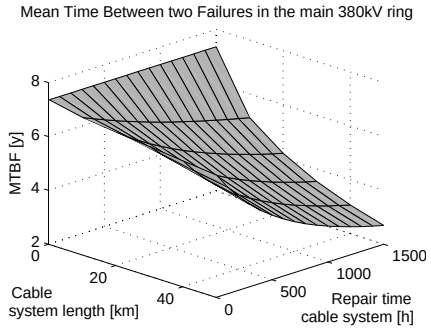

(b) MTB2F

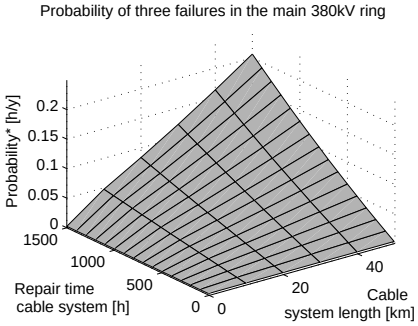

(c) P3

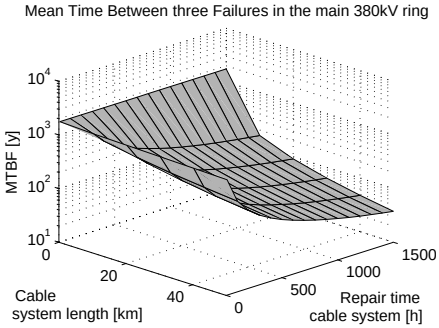

(d) MTB3F

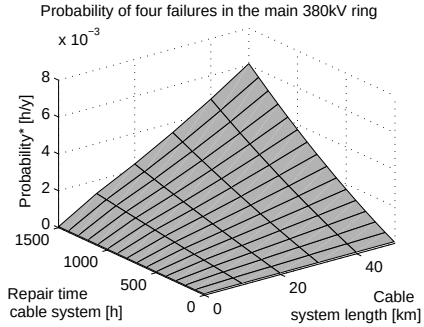

(e) P4

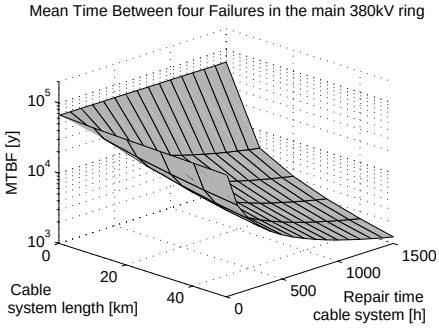

(f) MTB4F

Figure 3.35: (Annualized) probability and MTBF of higher-order failures in the main 380kV ring.

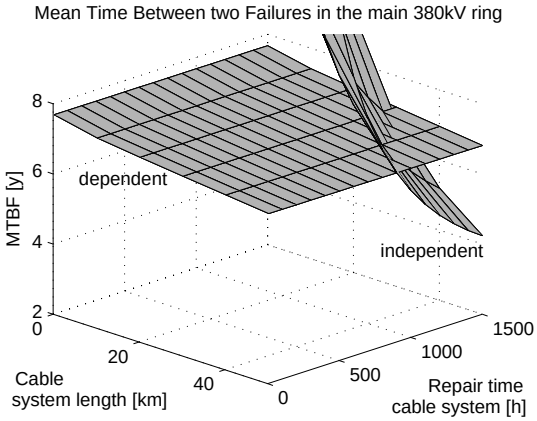

Figure 3.36: MTBF of two independent and dependent failures in the main 380kV ring.

double circuit underground cable in the network. Therefore, in three and four failures always an overhead line is included and the probability of these states is limited by the repair time of the overhead line.

An interesting effect that was also mentioned before is that independent higher-order failure will happen more frequently if longer cable connections are installed in the network. This effect can be studied for increasing cable lengths and longer repair times as well. The result is shown in figure 3.36. As can be seen, for longer cable connections and repair times, independent double failures will occur more often. At some point, independent double failures will become even more frequent than dependent double failures. The same effect can be found for independent and dependent higher-order failures, although this will not happen within the studied ranges of the cable connection length and the repair time.

3.6.4. INFLUENCE OF THE LENGTH AND NUMBER OF CABLE CONNECTIONS

In the future, more underground cables will be installed in the transmission network. The number of cable connections can influence the reliability of the transmission network as well. Therefore, it is of interest to study the effects of more and longer cable connections on the occurrence of failures in the transmission network. For this study, the failure frequencies from table 3.1 (TSOs high) together with a repair time of 730 h are used. Figures 3.37 to 3.39 show the results of this study.

As can be seen, the number of cable connections will have only a small influence on the probability of single and two failures. This because the difference between the repair times of overhead lines and underground cables is already large. The influence on the MTB1F and MTB2F is somewhat larger, because of the additional terminations. Also, the step between no underground cables and a short cable connection is caused by the terminations.

The number of cable connections has a similar impact on the MTB3F and MTB4F. The main difference can however be seen in the probabilities of 3 and 4 failures (P3/P4).

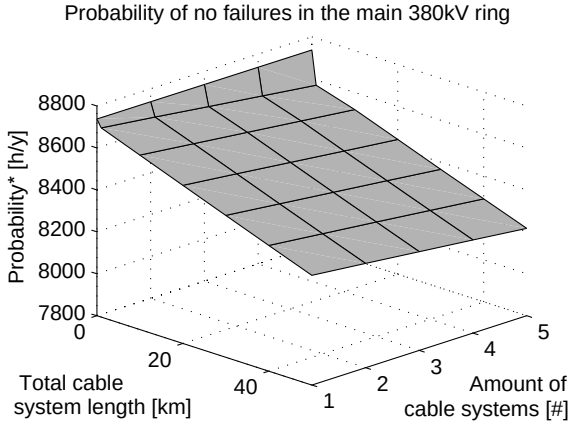

Figure 3.37: (Annualized) probability of no failures in the main 380kV ring. A repair time of 730 h is assumed for underground cables.

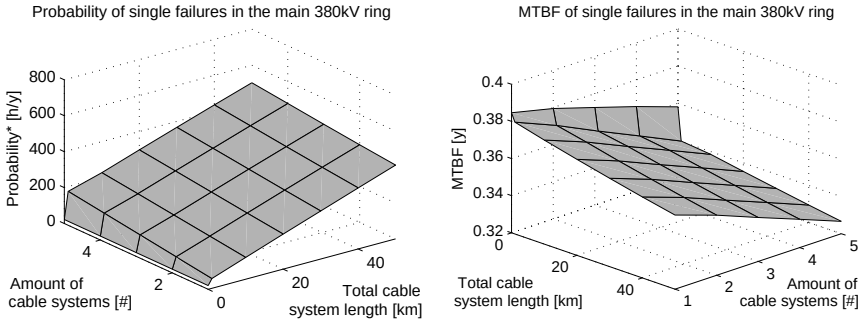

(a) P1 **(b) MTB1F**

Figure 3.38: (Annualized) probability and MTB1F of single failures in the main 380kV ring.

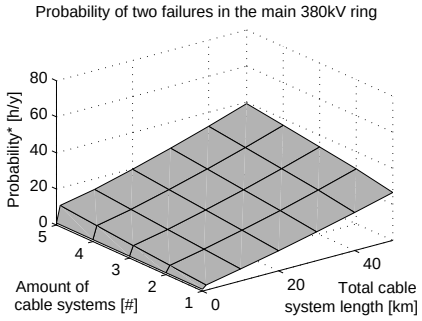

(a) P2

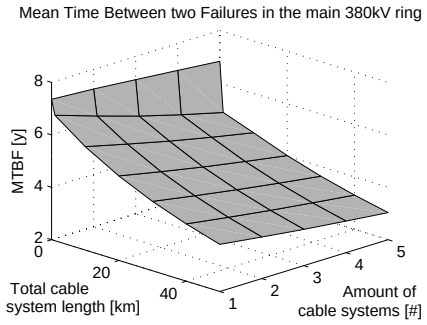

(b) MTB2F

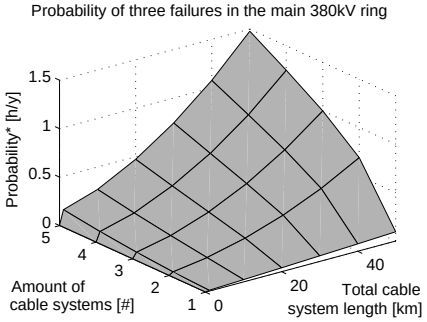

(c) P3

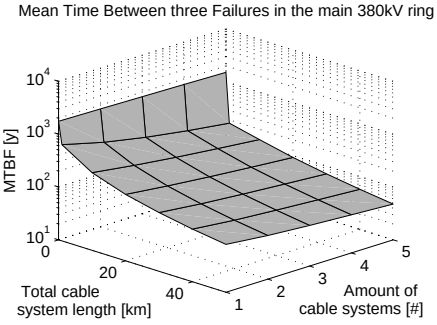

(d) MTB3F

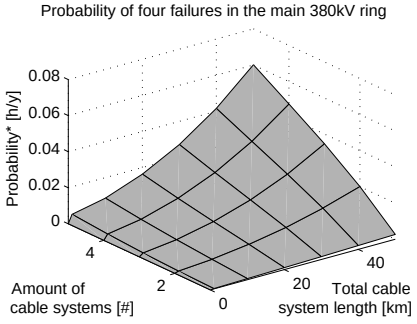

(e) P4

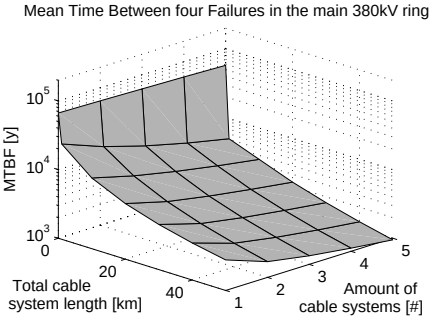

(f) MTB4F

Figure 3.39: (Annualized) probability and MTBF of higher-order failures in the main 380kV ring.

There is a significant increase in these probabilities for an increasing number of cable connections. This can be explained as follows. In the previous studies, it was assumed that there is only one double circuit cable connection in the transmission network. With three and four failures, there was always an overhead line involved and the probabilities of these states was limited by the repair time of the overhead line. With two double circuit underground cables in the transmission network, it is likely that in three and four failures only cable connections are involved. The result is a step in the probability between one and two cable connections and an increase in probability for even more cable connections. The reliability of the transmission network can therefore be improved by limiting the number of cable connection per network ring.

3.7. RISK OF FURTHER CABLING IN TRANSMISSION NETWORKS

Underground cables will have an impact on the reliability of large transmission networks, not only on the number of failures that occur but eventually also on the expected amount of load curtailment and generation redispatch. In this section, the impact of underground cables on the reliability of the complete Dutch EHV transmission network is analyzed [31, 52]. Again, a state enumeration approach (chapter 2) will be followed. This reliability analysis includes various remedial actions (national generator redispatch, cross-border redispatch and load curtailment) and calculates various reliability indicators. Combined, these indicators give a better understanding of the reliability of the transmission network.

Three possible locations for underground cable connections are selected to study the reliability impact. These will be called connection I, II and III in this section. First, the relative loading of these connections in the load flow scenario2020 is studied. The result is shown in figure 3.40. As can be seen, connection I is the least loaded, while connection III has the highest relative loading. This will be important later when discussing the results of the reliability analysis.

The reliability of the transmission network is now analyzed. Remedial actions are included, and the probability of load curtailment is chosen here to represent the reliability.

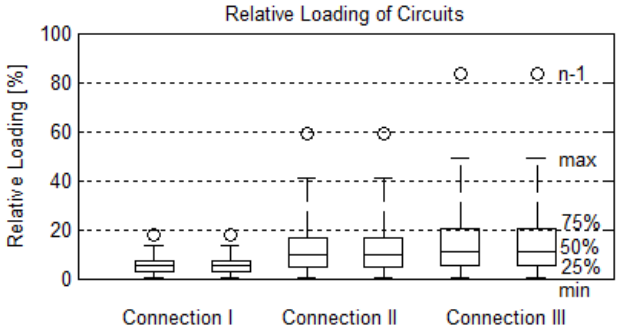

Figure 3.40: Relative loading of the circuits of connections I, II and III.

Within the studied connections, the total length of the underground cables is varied between 0% and 100% of the total connection lengths. The results are shown in figure 3.41.

As can be seen, the probability of load curtailment does not change if underground cables are applied in connection I, whereas this probability increases if cables are installed in connection II. The probability of load curtailment increases considerably if underground cables are located in connection III. This difference is mainly caused by the different loading of the three connections. As connection I is only weakly loaded, the impact of underground cables is small. As connection III is highly loaded, underground cables will have a strong impact on the network reliability. If one of these connections will be fully cabled, then fully cabling connection II instead of connection III gives an improvement of a factor 100, while fully cabling connection I instead of III gives an improvement of a factor 125.

As the probability of load curtailment does not show any difference for connection I, it is also possible to study other reliability indicators. Figure 3.42 shows the probability of

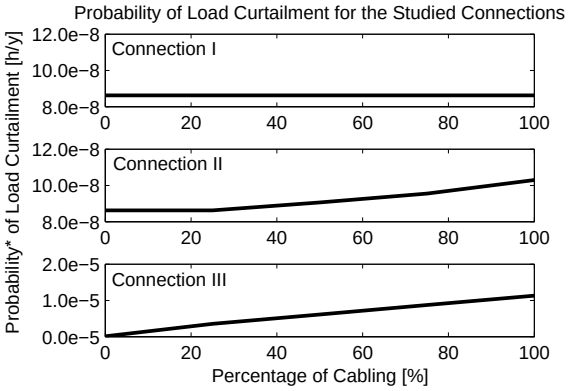

Figure 3.41: Probability of load curtailment for underground cables in the three studied connections.

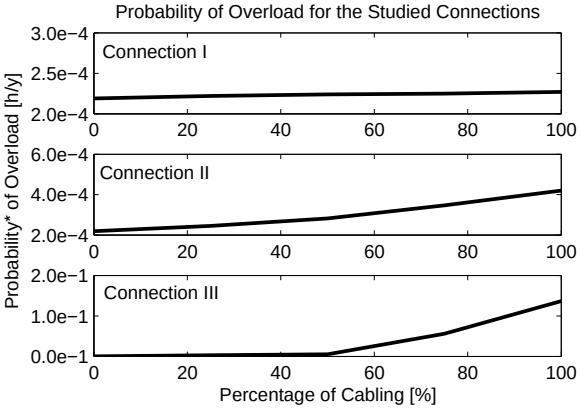

Figure 3.42: Probability of an overloaded network (probability of redispatch) for underground cables in the three studied connections.

an overloaded network, which in fact is equal to the probability of redispatch because the overload must be solved by redispatch first. It can be seen that the probability increases only slightly if underground cables are installed in connection I. The increase is more significant for connection II, and extreme for underground cables in connection III. The difference is mainly caused by the different loadings of the three connections (see also figure 3.40). Comparing figures 3.42 and 3.41, it can also be concluded that generation redispatch is an effective remedial action to prevent load curtailment.

Several factors can influence the reliability of underground cables. The actual loading of a connection was already mentioned before. Another factor is the application of series impedance compensation. Underground cables have a smaller impedance than overhead lines. Series impedance can be applied to better divide the load flow over the network. In [31, 52], it is found that the increase in probability of load curtailment of connection II is completely caused by the impedance difference. In contrast, series compensation of connection III does not give any improvement in the probability of load curtailment. It is therefore worth to study the effect of series impedance compensation for future UGC projects.

The sensitivity to various input parameters if 50% of connection III is cabled is shown in table 3.14. As can be seen, series impedance compensation does not have any effect in this case. The network reliability could be increased by cabling only 25% of connection III, which leads to an improvement of about a factor 2. Other options are to reduce the failure frequencies or the repair time (both give ±factor 2 improvement). If only half the transmission capacity is sufficient, the reliability can be improved by about a factor 2 by using only 1 cable per circuit phase. If 2 cable sections instead of 1 are installed in connection III, the reliability decreases by 11%. The other way around holds as well: if 2 cable sections are installed, the reliability can be improved by about 11% by using only 1 cable section. Table 3.14 also shows that if the dependent failure factor for cables is 0.05 instead of 0.1, the probability of load curtailment reduces by about a factor 2 as well.

From these options, reducing the repair time probably is the most promising. This gives an improvement of about a factor 2, and the repair time can be reduced considerably by using a more optimized repair scheme. Although reducing the failure frequencies

Table 3.14: Sensitivity to input parameters: connection III 50% cabled.

Scenario	Probability of load curtailment [h/y]	Improvement factor [-]
Standard situation	6.11e-6	0
With impedance compensation	6.11e-6	0
25% of connection cabled	3.53e-6	2
TSO low failure frequencies	3.38e-6	2
Repair time 336h (2 weeks)	3.06e-6	2
1 cable per circuit phase[a]	3.06e-6	2
0.05 dependent failure factor	3.06e-6	2
2 cable sections instead of 1	6.79e-6	0.9

[a] Here, it is assumed that half the transmission capacity is acceptable while the impedance of the connection does not change significantly.

gives about the same improvement, it is challenging to reduce these by 50%. Limiting the amount of underground cables by a shorter cable length, less cable sections, and less cables per phase results in a better reliability, but these must be in line with the other requirements for a specific underground cable project.

3.8. CONCLUSION

In this chapter, the reliability of underground cables was studied. Starting with failure statistics, the reliability of underground cable connections was analyzed and compared with the reliability of overhead line connections. Then, the impact on the reliability of transmission networks was studied.

As 380kV underground cables are a relatively new technology, the amount of failure statistics available is limited. Most studies are based on cables of lower voltage levels. Two useful sources are a survey by Cigré [44] and the update by the European TSOs [45]. In general, the failure statistics show a large range of failure frequencies and, especially, repair times. For future reliability research, it is important to collect more failure statistics for underground cables. This will lead to more accurate results in the sense of more accurate reliability indicators. Furthermore, events like the occurrence of dependent double circuit failures can be considered in more detail in the analysis.

If the reliability of EHV underground cables is compared with the reliability of EHV overhead lines, it is found that cables are less reliable. The failure frequency of an underground cable connection is about three times the failure frequency of an overhead line connection. This is caused by the failure frequencies of the joints and terminations and the fact that two individual cables are used in the studied Randstad380 configuration. The difference in the unavailabilities is larger as the repair time of underground cables is about hundred times the repair time of overhead lines. Double circuit failures were studied using a dependent failure factor. For overhead lines and shorter cable connections, double circuit failures are mainly dependent failures. For longer cable connections (than about 110 km), independent double failures will happen more often than dependent double failures depending on the connection length.

The reliability of underground cables can be improved in several ways. First, the failure frequencies and repair times can be reduced. The failure frequency could be reduced by advanced testing and monitoring techniques. As the repair time is much larger than the repair time of overhead lines, much improvement can be obtained by reducing this repair time. Activities like getting permission, arranging technical personnel and the availability of spare or new parts all contribute to the total repair time. Most of these activities can be arranged on beforehand, such that the repair process becomes more optimized. The studies in this chapter showed that a large range of the repair time causes a large range of the network reliability (i.e. the reliability indicators). An accurate network reliability assessment requires input parameters like accurate failure frequencies and well-defined repair times.

A second option to improve the reliability of a cable connection is partial-cabling, where cables are only installed at those locations in a connection where they are the most desired. Short line sections (shorter than 3.6 km in the studied situation) should be avoided. The third option to increase the reliability is by using another cable configuration. The use of an additional spare cable gives theoretically the best improvement,

but this configuration will cause practical challenges with cross-bonding, testing and the extra costs. The use of cable switching (half-a-circuit) with circuit breakers (and protection systems) will lead to an increase in the reliability as well, although the costs of the additional circuit breakers can be an issue. The most economical solution is the use of additional disconnectors, which can isolate the damaged cable (half-a-circuit) after a cable failure. It must however be studied whether a 75% capacity state is acceptable in the operation of the power system, as the division of the load flow over the remaining cables depends on the impedances of the connected overhead lines in the case of an embedded cable section. Also, this solution might require immediate operational actions in case of a next failure.

A comparison of cable sections at different locations in the MVL380 region and Randstad region networks showed that the reliability of the network strongly depends on the location of the cables. For the probability of an islanded substation, it is better to avoid the connection of a (critical) substation by cables only. The probability of an overloaded circuit depends on the load flow in the network, and a cable section in a heavily-loaded connection has a much higher impact than a cable section in a less heavily loaded connection. Furthermore, there is a large difference in the reliability between a cable section within one connection route and multiple cable sections within different connection routes connecting a large-scale generation center. It is found that one long cable section within one connection route can still be better than two short cable sections within different connection routes.

With state enumeration, the occurrence of failures in larger transmission networks was studied. The influence of different input parameters was studied. An increase in the failure frequency or repair time of cable connections leads to an increase in the probability and frequency of higher-order states. For longer cable connections, the probability and frequency of these states increase significantly. For longer cable connections and longer repair times, independent double failures will happen more frequently than dependent double failures. This can have consequences for the planning and operation of power systems as these independent failures now require special attention. For an increasing number of cable connections, the probability and frequency of the system states increase as well. Especially the probability of having three and four failures will increase as more combinations of three and four cable failures become possible.

A study on the risk of further cabling in the Dutch EHV transmission network showed that various factors affect the final reliability of the network. The actual loading of a connection influences this reliability significantly. In some cases, the application of series impedance compensation can cancel out the reliability impact of underground cables completely. Other influencing factors are the failure frequencies, the repair time, the total cable length and the number of cable sections in a partially-cabled connection. This study also showed that the reliability of transmission networks is better understood if multiple reliability indicators are used.

All the studies in this chapter showed that, generally, underground cables negatively influence the reliability of EHV transmission networks. The studies also showed that there is not one single reliability indicator that completely describes the reliability of a transmission network. Not only the probability of load curtailment, but also the probability of generation redispatch can be important reliability indicators for a TSO. The

Table 3.15: Effectiveness (indicated in •) of various design measures.

Design measure	Effect
Avoid underground cables in heavily-loaded connections	•••
Avoid cables in multiple connection routes supplied by one generation center	•••
Prevent islanding by connecting substations not only by cables	•••
Apply series impedance compensation, if applicable	•••
Use a configuration with disconnectors, if acceptable in system operation	•••
Reduce the failure frequencies of underground cable components	••
Reduce the repair time of underground cable components	••
Use only one cable per circuit phase, compared to Randstad380	••
Reduce the underground cable length within a (partially-cabled) connection	••
Install less cable sections in a partially-cabled connection	•

location of an UGC within the grid topology influences the network reliability considerably. Highly-loaded connections contribute relatively much to the total (un)reliability, such that underground cables should be avoided in crucial, highly-loaded connections.

The possible measures and remedial actions to reduce this impact can be listed and quantified as shown in table 3.15. The most effective measures are related to heavily-loaded connections, underground cables within the same or different connection route(s), islanding of substations, and series impedance compensation. Other measures are reducing the repair time or failure frequency, using only one cable per circuit phase, and reducing the total cable length by 50%. New reliability-based design criteria can be developed for underground cables in large transmission networks from these results. As many factors are of influence on the final reliability of transmission networks with underground cables, future cable projects should be studied individually. In this way, the possibilities to reduce the impact can be studied per individual project.

4

RELIABILITY OF OFFSHORE/ONSHORE TRANSMISSION NETWORKS

4.1. INTRODUCTION

As already mentioned in the introduction of this thesis, in the future an offshore network will be built to connect large-scale offshore wind energy and to enable international trade in electricity. In this chapter, the reliability of offshore networks is investigated, as well as the impact on the reliability of onshore power systems.

Many studies have been devoted to the connection of large-scale offshore wind to the onshore power system. For example, the reliability of offshore wind farm topologies has been discussed in [22, 53–58]. In some other studies, the most optimal configuration for the connection of offshore wind farms was considered [22, 59, 60]. For offshore networks, it is often discussed whether these should be $n-1$ redundant, like the onshore transmission network. It therefore remains as an open research task to study whether and when it is economical to apply redundancy in offshore networks.

The impact of offshore networks on the reliability of onshore power systems must be studied as well. Whereas this impact might be small for limited amounts of offshore wind [22, 61], this can be different for larger offshore wind capacities. As sudden capacity outages of offshore wind can endanger the electricity supply onshore, it is of interest to study how severe these capacity outages are, also in comparison to other possible capacity outage causes. For example, the variability of wind power and the accuracy of wind forecasts are important factors for large-scale offshore wind energy too [62]. When the penetration level of wind energy increases, the need for operating reserve might increase as well [63]. Therefore, the study presented in this chapter also considers the possibility to arrange redundancy for offshore networks alternatively.

The case study in this chapter is based on the expected development of the Dutch offshore transmission network. In the Netherlands, the Dutch TSO TenneT will be re-

sponsible for the construction and management of the offshore network [64]. It is expected that this offshore grid will be connected to the national power system by several connection points [65]. Most of these connection points are located in the west of the Netherlands, where the main load centers are. But large amounts of wind energy will also be transported to the rest of the country and to the neighboring countries.

This chapter starts with a description of some characteristics of offshore wind in section 4.2. Then, failure statistics of components for offshore networks are studied in section 4.3. Section 4.4 describes the concept and benefits of a hub-at-sea for offshore configurations. The reliability of several feasible near-shore network topologies is analyzed in section 4.5. A study on various causes of power imbalance is performed to study whether the onshore power system is strong enough to cope with failures of the offshore network in section 4.6. Finally, conclusions are drawn in section 4.7.

4.2. OFFSHORE WIND

Some characteristics of the variability associated to offshore wind energy are illustrated in figure 4.1. A typical graph of the power production of an offshore wind farm is shown top left. As can be seen, the maximum power of 250 MW is produced for certain periods while the power fluctuates at other moments. In general, the power production of offshore wind farms is larger than the power production of onshore wind farms. This is indicated by the capacity factor, which is defined as the total production of the wind farm in one year divided by the total production that would be obtained when the wind farm would produce maximum power throughout the year. The capacity factor of an offshore wind farm typically is about 0.45, whereas it is typically about 0.35 onshore.

If the power production for every hour of one year is sorted from the largest to the smallest value, a Power Duration Curve (PDC) like shown top right is created. This PDC

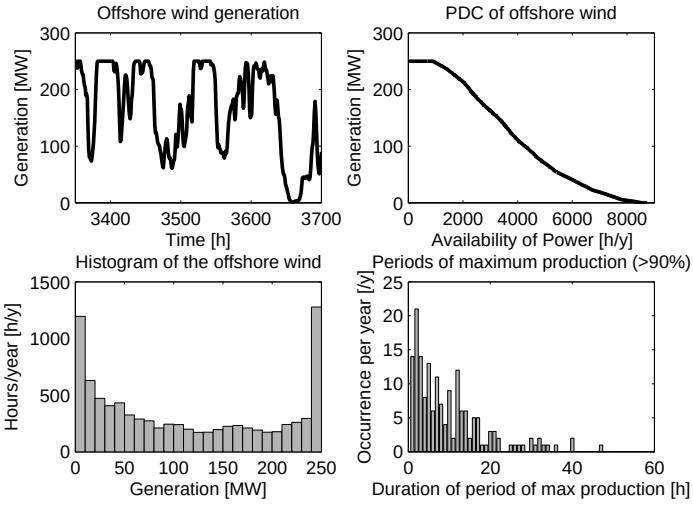

Figure 4.1: Characteristics of offshore wind energy.

shows the amount of hours/year that a certain power production is realized. For example, for 1000 h/y the maximum power of 250 MW is produced and for 4000 h/y the production is larger than 100 MW. Moreover, the PDC gives information about the capacity factor and the smoothing of the wind power (if a wind farm covers a larger area).

Another way to show the production of a wind farm is the histogram shown in figure 4.1 (down left). The histogram shows the probability of having a certain power production. In the figure, the probability is scaled (annualized) to h/y. As can be seen in the histogram, for a significant amount of time, the wind power is either 0 or 250 MW. This means, the wind farm is not producing power or providing maximum capacity. At other times, the wind power is in between these values. Both Power Duration Curves and histograms will be used in the following sections to study the reliability of offshore networks, because these have proven to be useful to illustrate the impact of possible failures of offshore networks for wind energy.

Offshore wind differs from onshore wind because of the differences in landscape. Generally, there is more wind offshore and wind speeds are more stable than onshore. Periods of maximum wind production will therefore occur more frequently offshore than onshore. To study this, the graph shown in figure 4.1 (down right) can be made. The figure shows how often periods of maximum production (i.e. a production larger than 90%) occur. For example, the figure shows that 21 times a year the wind production is larger than 90% for 2 subsequent hours. The figure also shows that periods of 30 to even 48 hours of maximum production can occur.

4.3. FAILURE STATISTICS OF SUBMARINE CABLES

In chapter 3, it was mentioned that the amount of failure statistics of EHV underground cables is limited. For submarine cables, failure statistics are even more scarce.

In Cigré report TB379 [44], the failure frequencies of submarine cables are studied as well. These failure frequencies are listed in table 4.1. As can be seen, the limited amount of statistical data leads to a large range of failure frequencies, especially for specific voltage ranges. For example, some values are 0.0 or NA, while other values are as large as 1.9/100cctkm·y. For EHV DC - MI (DC Mass Impregnated, like BritNed and NorNed), a failure frequency of 0.0998/100cctkm·y is reported. The repair time of submarine cables is also discussed in the Cigré report. In general, long repair times up to several months are reported for all cable types. Excluding the extremes and unknowns, the average reported repair time of submarine cables is approximately 60 days. This is two times the repair time of onshore EHV underground cables (730 h), and 180 times the repair time of

Table 4.1: Failure frequency (all failures) of submarine cables [44].

Component	**Failure frequency** [/100cctkm·y]		
	60-219kV	220-500kV	All voltages
AC - HPOF cables	1.9183	0.0000	0.7954
AC - SCOF cables	0.1277	0.0738	0.1061
AC - XLPE cables	0.0705	NA	0.0705
DC - MI cables	0.1336	0.0998	0.1114
DC - SCOF cables	NA	0.0346	0.0346

Table 4.2: Failure frequency and repair time of submarine cables [66, 67].

Component	Failure frequency		Repair time	
AC circuit breaker (ACB)	0.025	[/comp·y]	168	[h]
AC harmonic filter (ACF)	0.2	[/comp·y]	6	[h]
Coupling reactor (COR)	0.116	[/comp·y]	256	[h]
Converter unit (valves & capacitors) (COU)	0.5	[/comp·y]	4	[h]
Control & protection system (CPS)	0.088	[/comp·y]	6.05	[h]
Converter transformer (CTR)	0.037	[/comp·y]	1580	[h]
DC equipment (DCE)	0.3	[/comp·y]	6.4	[h]
DC cable (DCL)	0.0706	[/100cctkm·y]	1440	[h]

an onshore overhead lines (8 h).

In another source [66, 67], the failure frequencies and repair times of offshore DC connections are discussed as well. Table 4.2 shows these failure frequencies and repair times. As can be seen, the failure frequency of the DC cable is 0.0706/100cctkm·y with a repair time of 1440 h (about 2 months).

Compared with onshore EHV cables, the failure frequency of offshore cables is somewhat smaller. For EHV underground cables, the high estimation of the failure frequency was 0.120/100cctkm·y and the low estimation 0.079/100cctkm·y (see also table 3.1). This is excluding the joints and terminations. The failure frequency of submarine (DC) cables can be smaller than the failure frequency of onshore cable because of their single-cable construction. Moreover, less joints are needed because of the significantly longer length of the cable parts.

Actually, the failure frequency of submarine cables must be smaller than the failure frequency of onshore cables because of their longer total lengths. Whereas onshore cable connections (AC, like Randstad380) usually have lengths up to tens of kilometers, offshore connections (DC, like BritNed and NorNed) can be hundreds of kilometers. According to the failure statistics of table 3.1, a cable connection with the Randstad380 configuration of hundreds of kilometers would fail several times a year.

Table 4.2 also shows the failure frequencies and repair times of the other components of a submarine connection. The repair time of the DC cable as shown in table 4.2 (1440 h) is comparable with the 60 days mentioned by Cigré.

4.4. HUB-AT-SEA CONFIGURATIONS

4.4.1. HUB-AT-SEA CONCEPT

In the future, the number of offshore wind farms is expected to increase significantly. These offshore wind farms must be connected to the onshore power system by submarine cables. Traditionally, offshore wind farms are connected individually to the onshore grid. As the capacity of offshore wind farms increases and the distance to the shore becomes longer, it is better to collect the power of multiple offshore wind farms and to transport the power to the shore by one connection. For this purpose, offshore substations (hubs-at-sea) are installed. These offshore substations contain the necessary substation and/or converter equipment.

The use of hubs-at-sea can be more economical than individual connections, especially for longer distances. Because of the reactive power losses of AC cables, DC connections are preferred for longer distances. The required converter stations may however be too expensive for smaller individual wind farms. For larger (or multiple smaller) offshore wind farms, a single DC connection can therefore be an economical solution.

Another advantage of a hub-at-sea is the possibility to increase the reliability. This can be explained with an example. In the example, it assumed that 4 offshore wind farms of 250 MW each are connected to the onshore grid. If the PDCs of these wind farms are studied, a graph as shown in figure 4.2a can be created. The graph shows the four PDCs of the wind farms added to one total PDC of all wind farms. As can be seen, each wind farm has a total year production of 990 GWh. It is assumed that the wind farms are located in the same area, such that the power production of the wind farms are equal.

If the four wind farms are connected individually to the onshore grid, a failure of a connection will directly lead to the disconnection of one wind farm. Using figure 4.2a, if there are only three wind farms, the total PDC becomes one PDC-part (of 990 GWh) less. Multiplying this 990 GWh by the unavailability of a connection gives the expected lost energy because of (single) connection failures. For example, if the unavailability of a connection is 100 h/y, the expected lost energy per year becomes:

$$E_{lost} = 990 \cdot \frac{100}{8760} \cdot 4 = 45 \; [GWh] \tag{4.1}$$

The factor 4 in the equation is because of the four connections that possibly can fail. If it is now assumed that the power of the four wind farms is collected by a hub-at-sea and transported by four cables to the shore, the situation becomes as illustrated in figure 4.2b. In case of a cable failure, still three cables are available. Consequently, still a maximum of 750 MW can be transported to the shore (if the individual cable capacities is assumed 250 MW).

As can be seen from figure 4.2b, two situations are possible. First, the total production of the wind farms is smaller than 750 MW and the total power can still be transported

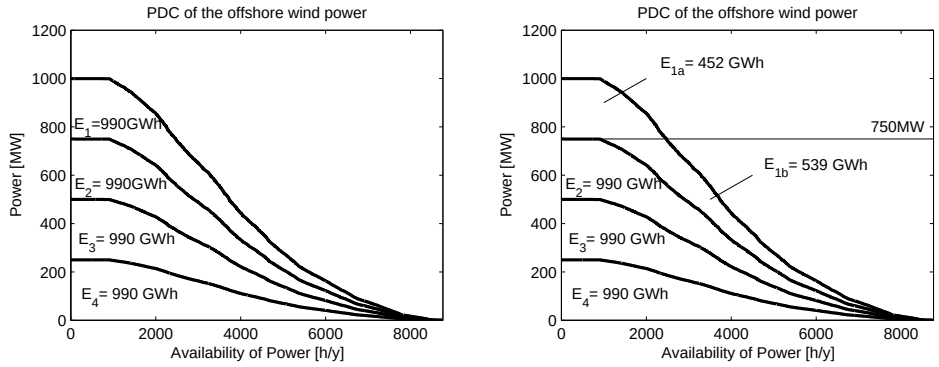

(a) Without hub-at-sea. **(b) With hub-at-sea**

Figure 4.2: Power duration curve of four offshore wind farms.

to the shore. In the graphs, this is the $E_{1b} = 539$ GWh-area. Secondly, the total production of the wind farms is larger than 750 MW and the total power cannot be transported to the shore, indicated as the $E_{1a} = 452$ GWh-area. This power is lost if only three connections are available. If this value is multiplied by the unavailability of a single connection, the expected lost energy per year now becomes:

$$E_{lost} = 452 \cdot \frac{100}{8760} \cdot 4 = 21 \ [GWh] \tag{4.2}$$

Which is less than half the previously calculated value.

This example illustrates the possibility to increase the reliability of the connection by using a hub-at-sea configuration. Of course, the total reliability of the connection depends on more factors (like all network components, cable lengths, the network configuration and higher-order failure states). In the following sections, the reliability of different network topologies is studied in more detail.

4

4.4.2. AC CONFIGURATIONS

Smaller wind farms and near-shore wind farms are often connected to the onshore power system by AC networks. In this section, the reliability of the AC connection of offshore wind farms is studied into detail.

Typically, offshore wind farms are connected to the shore by an AC connection as shown in figure 4.3. As can be seen, this connection consists of two circuit breakers, a step-up transformer and an AC cable. The transformer is needed to increase the voltage of the turbines to the voltage of the connection. If the voltage of the connection differs from the voltage of the onshore network, a second transformer is required onshore.

Using the failure statistics from table 4.2, the reliability of the AC connection can be calculated. A connection length of 50 km is assumed. The results are shown in table 4.3

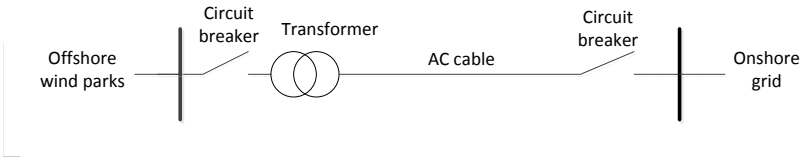

Figure 4.3: Scheme of the AC connection.

Table 4.3: Failure frequency and (annualized) unavailability of a 50km AC connection.

Component	Amount	Fail.freq.	f_1 [/y]	Repair [h]	U_1^* [h/y]
AC cable (/100cctkm)	50	0.071	0.036	1440	51.8
Transformer	1	0.037	0.037	1580	58.5
AC circuit breaker	2	0.025	0.050	168	8.4
Total			**0.123**		**118.7**

For the calculations, the failure statistics from tables 4.1 and 4.2 are used. f_1 is the total failure frequency of one cable connection. U_1^* is the annualized unavailability of one connection in hour/year.

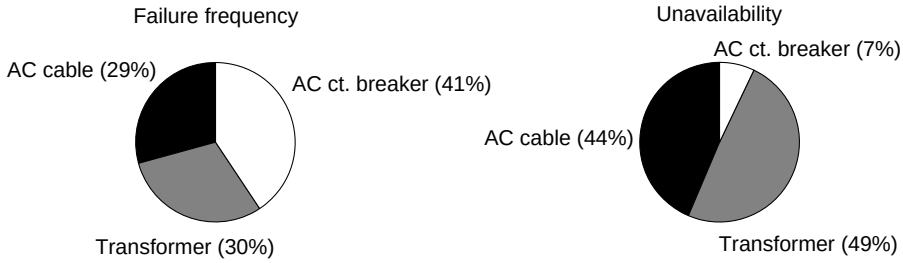

Figure 4.4: Contribution of connection components to the failure frequency and unavailability.

and figure 4.4. As can be seen, all components (cable, transformer and circuit breakers) contribute to the total failure frequency. On average, this connection will fail once every 8 years. Regarding the unavailability of the connection, the AC cable and the transformer contribute the most as these components have large repair times. On average, it can be expected that the connection is 118.7 h/y unavailable.

If multiple smaller offshore wind farms are located within the same area, it can be an option to install an offshore substation. This can be beneficial for the reliability. Four situations will be studied, as shown in figure 4.5. In the first situation (4.5a), four wind farms of 250 MW each are connected individually to the shore. In the second situation (4.5b), a hub-at-sea collects the power of the four wind farms. The hub-at-sea is connected to the shore by four AC cables of 250 MW each. It is possible to create redundancy by installing a fifth AC cable, like in situation 4.5c. Situation 4.5d is a possibility to reduce the costs by installing only three cables (of 333 MW each).

For each situation, the effects of connection failures can be studied. This will give insight into the probability and frequency of loosing a particular amount of wind power, as well as the total lost wind energy because of connection failures. For this purpose, a typical wind generation pattern is assumed. Each wind farm has an installed capacity of 250 MW. The standard AC cable capacity is 250 MW, apart from situation 4.5c where the cable capacity is 333 MW. The failure statistics from table 4.2 are used. It is assumed that the offshore substation is fully reliable. The distance from the wind farms to the shore is assumed 50 km (10 km from the wind farms to the hub-at-sea and 40 km from the hub-at-sea to the shore).

First, the probability of loosing a particular amount of wind power is studied. The results are shown in figure 4.6. As can be seen, for individual connections, there are two peaks in the probability. The figure shows a similar pattern as the histogram in figure 4.1. One peak (around 0 MW capacity outage) is the case when there is no wind production during a connection failure. The other peak (around 250 MW capacity outage) is the case when there is full wind production during a connection failure. The probability of loosing a wind capacity in between these values is smaller. The probability of loosing a wind capacity larger than 250 MW can be neglected as now two connections must fail. The expected lost wind energy is 53 GWh/y, 1.3% of the total wind production.

If a hub-at-sea with four AC cables is used, part of the lost wind power can be saved. As shown in figure 4.6, the probabilities are now a bit smaller. The peak around 250 MW capacity outage stays about the same. Because the wind farms are located within the

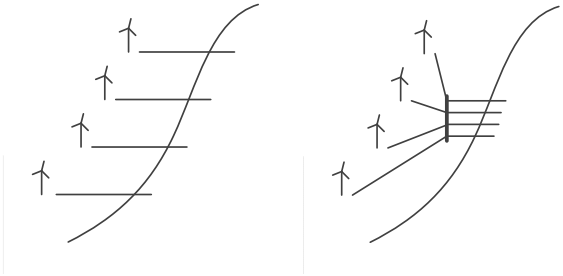

(a) configuration AC1 (b) configuration AC2

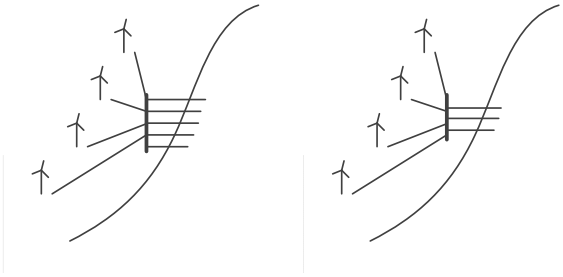

(c) configuration AC3 (d) configuration AC4

Figure 4.5: Hub-at-sea configurations (AC).

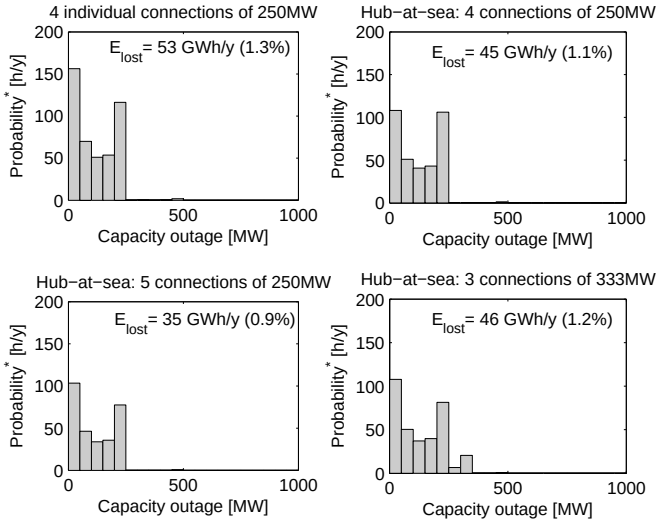

Figure 4.6: Probability of lost power for the AC configurations.

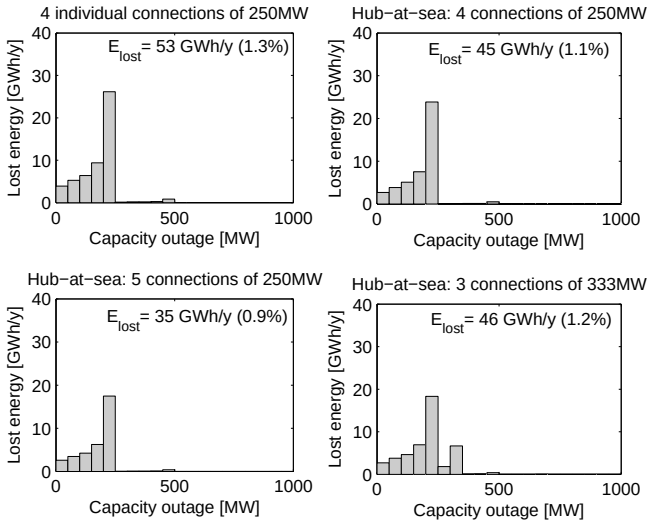

Figure 4.7: Expected lost energy versus lost power for the AC configurations.

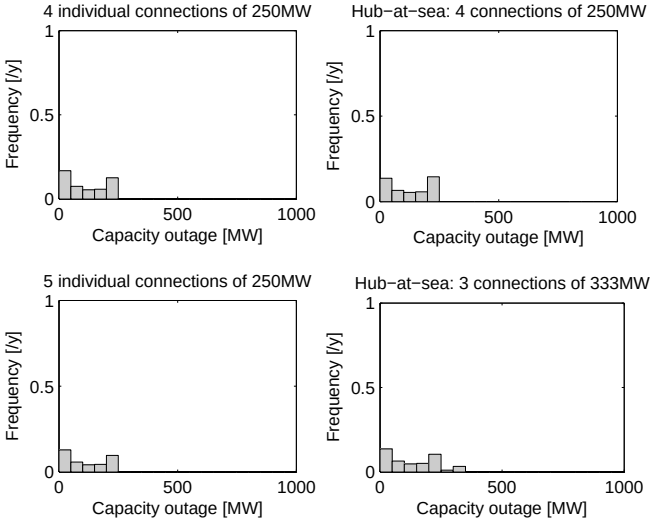

Figure 4.8: Frequency of occurrence of lost power for the AC configurations.

same area, it is likely that all wind farms produce full capacity (or other capacities) simultaneously. In the case of full capacity production, the failure of one AC cable still leads to a capacity outage of 250 MW. The total lost wind energy has reduced to 45 GWh/y now, 1.1% of the total wind production.

With a fifth AC cable, more redundancy is created in the network. As can be seen from figure 4.6, the probabilities have reduced somewhat more and the total lost energy becomes 35 GWh/y (0.9%). The reason why the change in probabilities is such small is because the wind farms are still connected individually to the hub-at-sea. It is assumed that each wind farm has its own step-up transformer. Because of these connections between the wind farms and the hub-at-sea, it is still possible that wind farms are disconnected individually because of component failures.

The last situation is the situation where the hub-at-sea is connected to the shore by three AC cables of 333 MW each. Because of the three cables, it becomes more likely to lose up to 333 MW wind power. This can be seen in figure 4.6 as well. The expected total lost wind energy is 46 GWh/y, 1.2% of the total wind production.

If the probabilities are multiplied by the capacity outage, an indication can be given about how much certain capacity outages contribute to the total lost wind energy. This is shown in figure 4.7. As can be seen, the larger capacity outages (around 250 MW) will contribute the most to the total expected lost wind energy.

For some studies (like generation reserve studies) it may be of interest to know how often a particular amount of wind capacity is lost. This can be calculated by using the failure frequencies of the components of the connection. The result is shown in figure 4.8. For example, it is shown that for the situation with the individual connections, 250 MW wind capacity is lost about once every 5 years.

4.4.3. DC CONFIGURATIONS

For wind farms located farther away from the shore, AC connections are less suitable because of the reactive power losses. In these cases, the wind farms can be connected by HVDC. As the capacity of offshore HVDC cables can be larger than the capacity of offshore AC cables, it is possible to connect multiple smaller wind farms (or one large wind farm) by one HVDC connection to the shore.

Figure 4.9 shows a typical scheme of an HVDC connection. As can be seen, converter units are located at both ends of the DC cable. For the DC connection, also other additional components like DC equipment, control/protection systems, coupling reactors

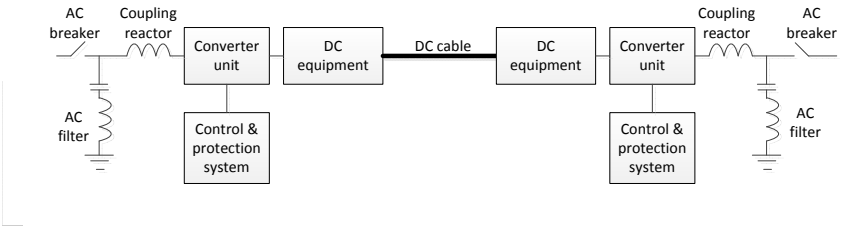

Figure 4.9: Scheme of an HVDC connection [66].

and AC filters are required. These are placed at both ends of the connection.

Using the failure frequencies and repair times from table 4.2, the expected total failure frequency and unavailability of the DC connection can be calculated. Again, a connection length of 50 km is assumed. Table 4.4 and figure 4.10 show the results.

Compared to the AC connection (table 4.3), the DC connection fails much more frequently. This is mainly caused by the converter units, but also by the other additional equipment. The contribution of the DC cable to the total failure frequency can be neglected. The expected unavailability of the DC connection is about twice as large as the expected unavailability of the AC connection. The largest contributors are the DC cable, the converter transformers and the coupling reactors. These components have the largest repair times. It is interesting that the components which contribute the most to the total failure frequency, do not contribute significantly to the total unavailability.

In this study, two possible HVDC configurations are considered. These are illustrated in figure 4.11. In the first situation (4.11a), four wind farms of 250 MW each are connected to the shore by one DC cable of 1 GW. In the second situation, two DC cables of 500 MW each are used to connect the offshore substation to the shore. In the same way as done for the AC connections, the probability of loosing a certain wind capacity can be calculated. Again, it is assumed that the distance between the wind farms and the hub-at-sea is 10 km. The distance from the hub-at-sea to the shore is 40 km.

Figure 4.12 shows the probability of loosing a certain wind capacity. As can be seen

Table 4.4: Failure frequency and (annualized) unavailability of a 50km DC connection.

Component	Amount	Fail.freq.	f_1 [/y]	Repair [h]	U_1^* [h/y]
DC cable (/100cctkm)	50	0.071	0.036	1440	51.8
Converter transformer	2	0.037	0.074	1580	116.9
AC circuit breaker	2	0.025	0.050	168	8.4
AC harmonic filter	2	0.2	0.400	6	2.4
Coupling reactor	2	0.116	0.232	256	59.4
Converter unit	2	0.5	1.000	4	4.0
Control & protection system	2	0.088	0.176	6.05	1.1
DC equipment	2	0.3	0.600	6.4	3.8
Total			**2.568**		**247.8**

For the calculations, the failure statistics from table 4.2 are used. f_1 is the total failure frequency of one cable connection. U_1^* is the annualized unavailability of one connection in hour/year.

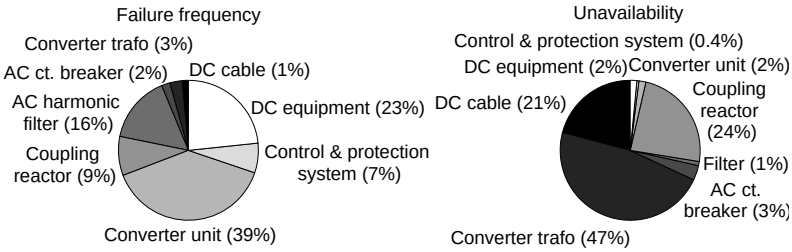

Figure 4.10: Contribution of system components to the failure frequency and unavailability.

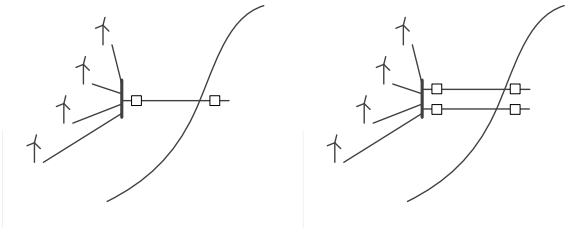

(a) configuration DC1 **(b) configuration DC2**

Figure 4.11: Hub-at-sea configurations (DC).

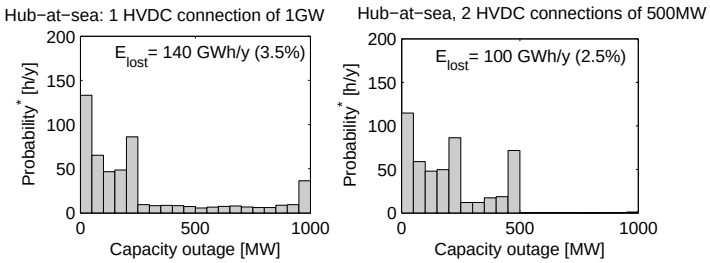

Figure 4.12: Probability of lost power for the DC configurations.

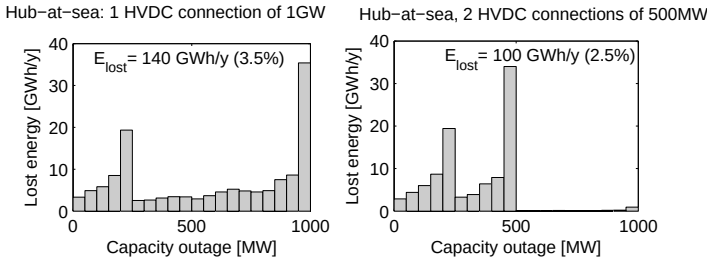

Figure 4.13: Expected lost energy versus lost power for the DC configurations.

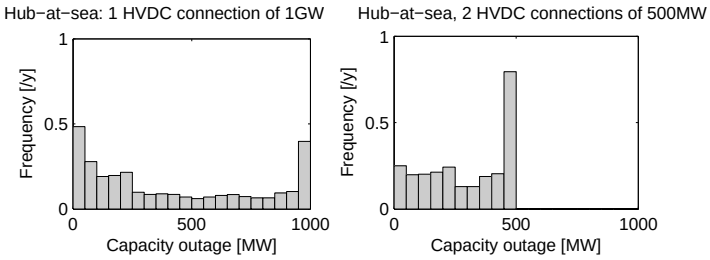

Figure 4.14: Frequency of occurrence of lost power for the DC configurations.

for the first connection situation, the probability of loosing 0-250 MW wind capacity shows a similar pattern as the individual AC connections (figure 4.6). These probabilities are caused by the connections between the wind farms and the hub-at-sea. Furthermore, figure 4.12 shows probabilities of loosing up to 1 GW wind capacity. This is caused by failures of the DC connection.

The expected amount of lost wind energy is 140 GWh/y. This is about three times the value found for the AC connection situations. Figure 4.13 shows how the lost wind capacities contribute to the total expected lost wind energy. As can be seen, the larger wind capacities (250 MW & 1 GW respectively 250 MW & 500 MW) contribute the most to the total lost wind energy.

For the second connection situation (two DC cables), the expected amount of lost wind energy is 100 GWh/y. Because of the two DC connections, the probability of loosing all the wind production is reduced. In case of one cable failure, up to 500 MW can still be transported through the second DC cable. In this way, the lost wind energy can be reduced significantly. In reality, most HVDC connections use a bipolar configuration. This means that if one DC cable or converter fails, it is still possible to operate the connection at half its capacity. Therefore, bipolar HVDC connections with two cables can be considered as connection situation 2 in this study.

For some studies, it may be of interest to know how often a certain wind capacity is lost. The frequency of loosing certain wind capacities is shown in figure 4.14. As can be seen, for the first connection situation (one DC cable) about once every 2 years 1 GW wind capacity is lost. For the second connection situation (two DC cables), about every year 500 MW wind capacity is lost.

In general, it can be concluded that due to the components required for an HVDC connection, a DC connection will fail more frequently than an AC connection. The unavailability will be larger too. In the case of AC connections, a hub-at-sea does not lead to a significant improvement of the reliability. If the reliability of the offshore substation is included into the calculations, the improvement of the reliability becomes even smaller. In the case of a DC connection, the lost wind energy can be reduced significantly by using two DC cables. It must be studied further whether this is an economical solution.

4.4.4. ECONOMICAL COMPARISON

In order to determine whether the alternative configurations are economically feasible, the economics must be studied. First, the value of the lost offshore wind energy is determined. Then, the costs of redundancy in the offshore network are calculated.

In The Netherlands as well as other European countries, wind energy is subsidized. The subsidy guarantees a certain price for the generated wind energy. Depending on the average energy price on the market and the location of a wind farm, the amount of subsidy per generated MWh is determined [68]. With the subsidy, the owner of the wind farm will earn about 100 euro per generated MWh. Using this amount, the value of the lost wind energy can be calculated. Table 4.5 shows the results. As can be seen, the 4 individual AC connections will cause 5.3 mln euro/y of lost wind energy. For a lifetime of 20 years, in total 106 mln euro will be lost. The losses of the DC configurations are larger. For example, the configuration with 2 HVDC connections of 0.5 GW will cause 10 mln euro/y of losses, and in total 200 mln euro.

Table 4.5: Value of the expected lost wind energy per connection configuration.

Configuration	Lost energy [GWh/y]	Value /year [mln euro/y]	Total value [mln euro]
AC1: 4 individual connections of 250MW	53	5.3	106
AC2: hub-at-sea, 4 connections of 250MW	45	4.5	90
AC3: hub-at-sea, 5 connections of 250MW	35	3.5	70
AC4: hub-at-sea, 3 connections of 333MW	46	4.6	92
DC1: 1 HVDC connection of 1GW	140	14	280
DC2: 2 HVDC connections of 0.5GW	100	10	200

The value of the lost wind energy is assumed 100 euro/MWh. The assumed life time of the offshore network is 20 years.

The amount of lost wind energy can be reduced by creating more redundancy in the offshore network. For example, more cables can be added to the network as illustrated by the alternative configurations. The costs of these additional cables must be studied to determine whether this redundancy is economically feasible. In [69], an economical model of offshore networks is given. In the model, the costs of offshore cables as well as the costs of offshore substations are specified. The costs are dependent on factors like the power rating of the components and the prices of copper, lead and aluminum.

For AC submarine cables, the price depends on the capacity. For an AC cable of 250 MW (220 kV), a copper conductor cross section of 500 m^2 is required [70]. An AC cable of 333 MW requires a conductor cross section of 1000 mm^2. According to [69], the prices of these cables are then 0.6 mln euro/km and 1.0 mln euro/km respectively. For a DC cable of 1 GW (MI/500 kV), a copper conductor cross section of 2500 mm^2 is needed [71]. A DC cable of 500 MW is assumed to require a conductor cross section of 1400 mm^2 (as the BritNed cable is ±450 kV, 1GW, 2x 1430 mm^2 [71]). The prices of these HVDC cables then become 0.5 mln euro/km and 0.35 mln euro/km respectively [69].

The installation costs of submarine cables depend on several factors as well. The type of the cable, the total cable length and the location all influence the total installation costs. In [69], the rough estimation of the installation costs of AC submarine cables is 275,000 euro/km and the installation costs of two single phase submarine DC cables is estimated at 250,000 euro/km. In the further calculation, it is assumed that the installation costs of one single phase submarine DC cable is 200,000 euro/km.

The costs of offshore substations and converter stations are also studied in [69]. On average, the costs of an offshore (AC) substation is defined as 130,000 euro/MVA. The costs of an offshore converter station is estimated 240,000 euro/MW, while the costs of the onshore converter station are 102,000 euro/MW. The prices of the converter station are extrapolated for the higher voltage level of the HVDC connection is this study.

It must be mentioned that all these costs are rough estimations. Therefore, the results of the cost comparison of the different connection alternatives can only be indicative. For the exact costs of the alternatives, all the details of the connection should be taken into account carefully.

Using the estimated prices of the components of the offshore network, an indication of the total costs can be made. Table 4.6 shows the estimated costs of the different connection alternatives. As can be seen, for the AC connections the individual connections

Table 4.6: Estimated costs of the alternative offshore network configurations.

Costs [mln euro]	AC1	AC2	AC3	AC4	DC1	DC2
AC cable costs	120	120	144	144	24	24
AC cable installation	55	55	66	44	11	11
Offshore substation	-	130	130	130	-	-
Offshore converter	-	-	-	-	240	240
DC cable costs	-	-	-	-	20	28
DC cable installation	-	-	-	-	8	10
Onshore converter	-	-	-	-	102	102
Total costs	175	305	340	318	405	415

AC1: individual connections, AC2: hub-at-sea four AC cables of 250MW, AC3: hub-at-sea five AC cables of 250MW, AC4: hub-at-sea three AC cables of 333MW, DC1: hub-at-sea one DC cable of 1GW, DC2: hub-at-sea two DC cables of 500MW.

have the lowest investment costs. When compared with table 4.5, it can be concluded that the reduction of the lost wind energy due to connection failures is much smaller than the additional investment costs of the alternative connections.

The difference between the investment costs of the DC connection alternatives is much smaller. It was assumed that the converter costs are the same for both DC connection alternatives. This is a reasonable assumption, as most HVDC converters are bipole converters which can operate at half capacity. Compared with table 4.5, it seems an economical solution to use a configuration with two HVDC cables.

OVER-DIMENSIONING OF THE HVDC CONNECTION

Another way to reduce the amount of lost wind energy is by over-dimensioning the connection. For example, for the DC connection with two cables, it is possible to use two cables of 550 MW and a converter with half-capacity 550 MW. In case of a cable failure, the reduction in transport capacity and the amount of lost wind energy are smaller.

The costs of this over-dimensioning can be studied in a cost analysis. For this study, a connection with two HVDC cables is considered (300 kV, [72]). It is assumed that the bipole converters can operate at half capacity. The distance from the offshore substation to the shore is 40 km and the distance from the individual wind farm to the offshore substation is 10 km. The additional investment costs and the value of the lost wind energy are compared using the economical model of [69].

Figure 4.15 shows the costs comparison of the over-dimensioning. The savings on the investment costs are shown together with the costs of the lost wind energy. As can be seen, if the capacity of the connection becomes smaller than 1 GW, the costs of the lost wind energy increase while some costs can be saved on the investments. On the other hand, when the capacity of the connection is increased, the investment costs become larger while the costs of the lost wind energy decrease.

When the capacity of the connection decreases below 1 GW, the costs of the lost wind energy increase dramatically. This is because when the wind farms are producing full capacity, certainly some wind energy is lost. The costs of the lost wind energy are significantly larger than the savings on the investments. For larger connection capacities, the amount of lost wind energy becomes smaller. However, the figure shows that the the investment costs increase faster (more negative savings on the investment costs).

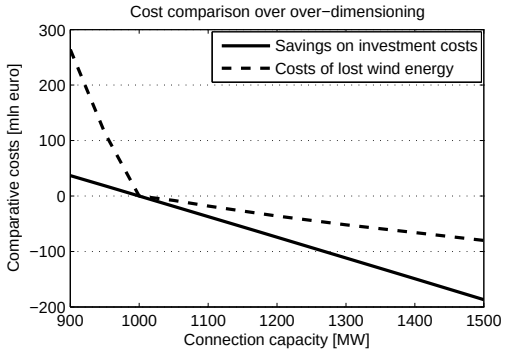

Figure 4.15: Costs comparison of the over-dimensioning of the HVDC connection.

According to this study, there is no economical advantage of creating redundancy in the connection by over-dimensioning. This study was based on assumptions about the costs and the reliability of the components. If the costs of the offshore components (especially the offshore converter) decrease, the line of the investment savings in figure 4.15 becomes less steep. If the components of the connection become more reliable, the decrease in the costs of the lost wind energy becomes less. It seems the best to have a connection capacity equal to the total installed capacity of the wind farms.

4.5. NEAR-SHORE WIND NETWORK CONFIGURATIONS

Whereas HVDC is preferred for wind farms located far from shore, near-shore wind can still effectively be connected by AC technology. In this section, possible near-shore configurations are studied. The options to create offshore redundancy, while increasing the network availability and Net Present Value are investigated [23].

4.5.1. NEAR-SHORE CONFIGURATIONS

In figure 4.16, a possible network configuration for near-shore wind energy is shown. As can be seen, there are two offshore platforms, each connecting 700 MW offshore wind capacity at MV level. On the platforms, the voltage is transformed up to 220 kV. Each platform is connected by two 350 MW cables to an onshore substation.

As indicated in the figure, there are several options to create redundancy in the offshore network. For example, it is possible to install branch couplers between the two connections of a platform. This can be realized on the offshore platform (BC1 & BC2), or in the onshore substation (BC3). In addition, it is possible to interconnect both platforms by hub couplers. These can be between the offshore platforms (HC1 & HC2), or in the onshore substation (HC3). Please, note that BC1 and HC1 are at MV level, while BC2, BC3, HC2 and HC3 are at EHV level.

4.5.2. NET PRESENT VALUE MODEL

The possible configurations as mentioned are now analyzed using a Net Present Value (NPV) approach, as illustrated in figure 4.17 and described in [23]. The NPV model takes

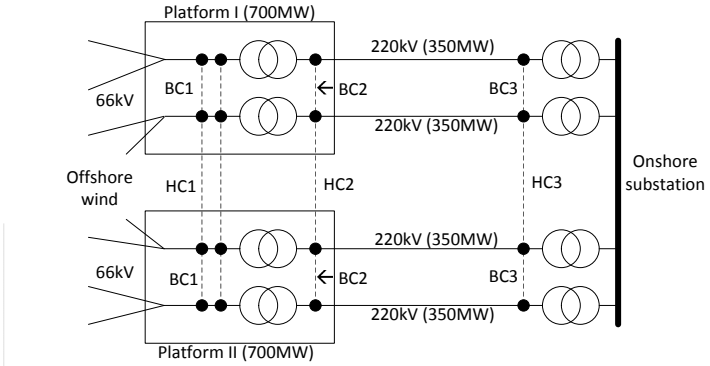

Figure 4.16: Overview of near-shore grid configurations with optional branch and hub couplers [23].

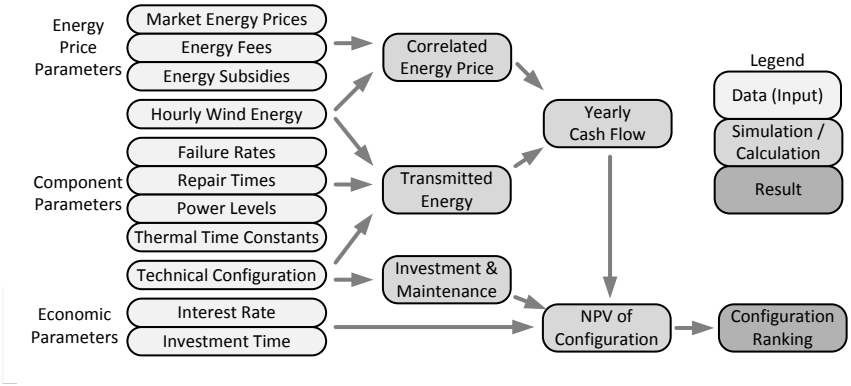

Figure 4.17: Overview of the NPV method [23].

various input parameters into account:

- *Energy price parameters*: These are market energy prices, energy fees and energy subsidies.
- *Hourly wind energy production*: A year scenario is used for the hourly wind production.
- *Component parameters*: These include failure rates and repair times of the components, power rating and thermal time constants of the components.
- *Technical configurations*: These are the possible configurations as mentioned before.
- *Economic parameters*: These are the interest rate and investment time, needed to calculate the NPV.

The NPV model eventually leads to a ranking of possible offshore configurations, based on their NPV.

4.5.3. RESULTS OF THE ANALYSIS

With the NPV model, the reliability of various possible configurations was analyzed and the lost/saved energy and NPV were determined per configuration. From all possible branch and hub coupler combinations, three options were the more realistic and promising: BC1&HC1, BC2&HC2, BC3&HC3. In figure 4.18, it is shown that 14.9 GWH/y of wind energy is lost because of network failures if no branch and hub couplers are installed. It

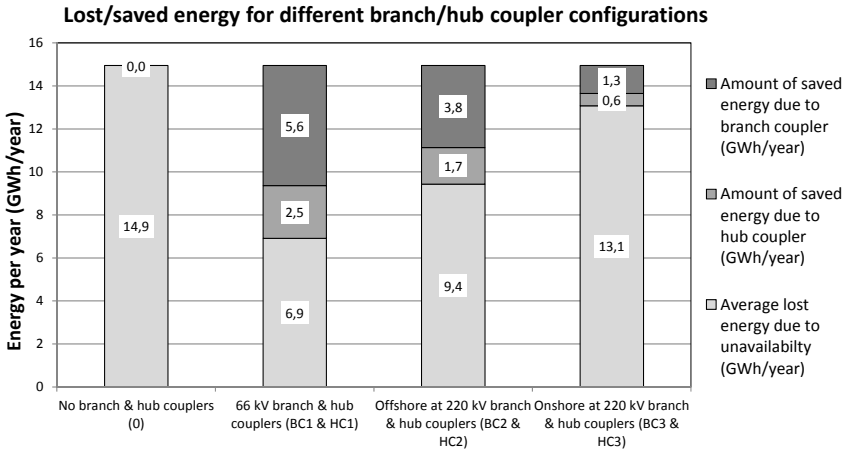

Figure 4.18: Lost and saved energy for different branch and hub coupler configurations [23].

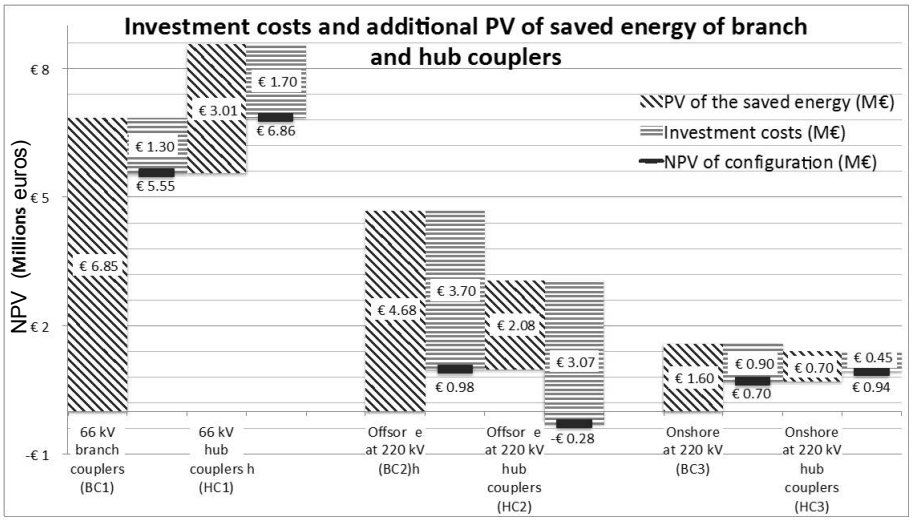

Figure 4.19: NPV of different configurations (per 350 MW connection) [23].

is also shown how much of this energy can be saved by installing branch and hub couplers. As can be seen, BC1 & HC1 have the largest effect. As these couplers are located the closest to the source, they create redundancy for the largest part of the offshore network.

Figure 4.19 shows how the NPV is calculated for the configurations. For example, it can be seen that 6.85 million euro of lost wind energy can be saved by installing branch couplers BC1, at an investment cost of 1.30 million euro. By also installing hub couplers HC1, an extra 3.01 million euro of lost wind energy is saved, at an investment cost of 1.70 million euro. This finally leads to a NPV of 6.86 million euro. From the figure, it can be concluded that this is the most economical solution, as the NPV of the other branch and hub couplers are smaller.

It must be mentioned that other combinations of branch and hub couplers were considered as well. However, these configurations were not realistic (e.g. installing a hub coupler without branch coupler at a certain location is not logical), or not economical (i.e. the NPV is smaller than the NPV of the options shown in figure 4.19).

It was also studied what the most optimal capacity of the branch couplers is [23]. The result is shown in figure 4.20. As can be seen, the amount of wind energy that can be saved increases for branch couplers up to about 175 MW, which is half the capacity of one 220 kV cable. Installing couplers with a larger capacity does not lead to a larger amount of saved wind energy. This can be explained as follows [23]. At 50% of the peak wind power, a 350 MW transformer or 220 kV cable has to process 175 MW from its own branch. In this case, the transformer could thus take up to 175 MW from another branch. At higher wind powers, the transformer can take less power from the other branch because it has to process more power from its own branch and at lower wind speeds, there is simply no need for a branch coupler capacity of more than 175 MW.

As the final NPV depends on many input parameters like the distance to shore and the energy price, a study was performed to determine which combination of couplers

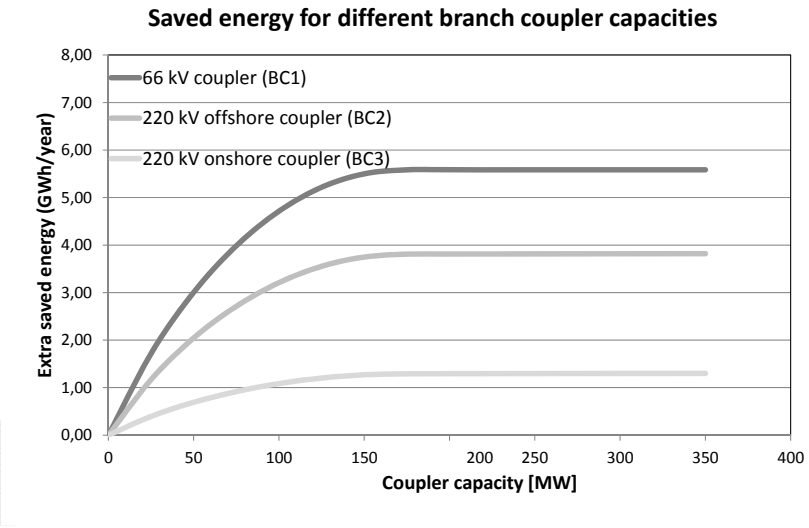

Figure 4.20: Amount of saved energy for different branch coupler capacities [23].

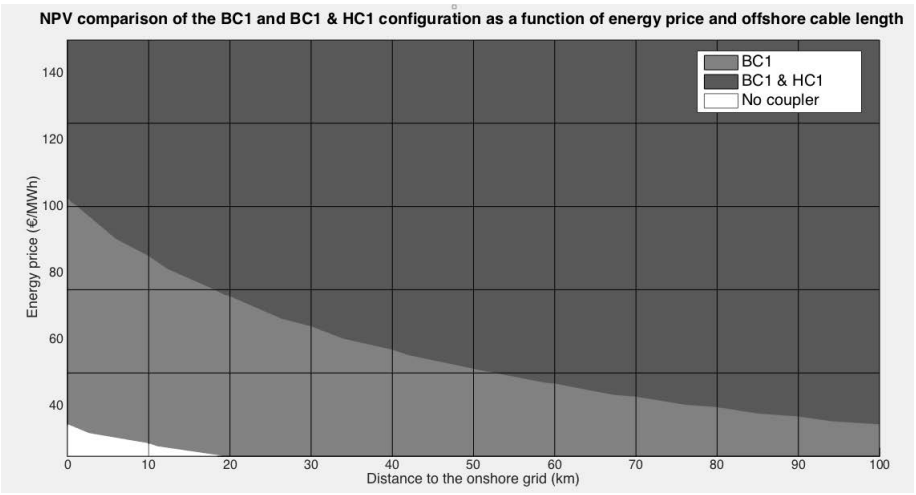

Figure 4.21: NPV comparison of the BC1 and BC1 & HC1 configuration as a function of energy price and offshore cable length [23].

BC1 and HC1 is the most economical in which case. The result is shown in figure 4.21. As can be seen, for short distances to shore and low energy prices, it is the most economical to install no branch and hub couplers. For moderate energy prices and distances to shore, it is the most economical to only install BC1, and for high energy prices and long distances to shore, it is the most economical to install both BC1 and HC1.

This study shows that it can be economical to create some redundancy in offshore networks in specific situations. In the studied offshore network, both the availability of the offshore network and its NPV increased by installing some redundancy. However, creating more redundancy can become uneconomical and full n-1 redundancy is probably not economically feasible. This conclusion probably holds for larger offshore networks as well.

4.6. COMBINED OFFSHORE-ONSHORE POWER SYSTEMS

The studies described in the previous sections showed that offshore redundancy may not be an economical solution from a producer point of view. However, failures of the offshore network can have consequences for the reliability of the onshore power system. For example, the sudden loss of wind capacity could cause power imbalance in the system which can endanger the electricity supply. Onshore, it is common practice to apply n-1 redundancy in the transmission network. For offshore networks, it is questioned whether n-1 redundancy should be applied as well. In this section, an approach to determine and compare the severity of various causes of power imbalance in combined onshore-offshore transmission networks is presented. This approach is used to study a power system with about the size of the Dutch system. It is studied whether n-1 redundancy is required in offshore networks or whether the onshore power system is strong enough to cope with failures of the offshore network.

4.6.1. STUDY APPROACH

GENERAL APPROACH

In this study, the severity of various causes of power imbalance is determined and compared. These causes are generator failures, load and wind forecast errors, failures of submarine interconnections and failures of offshore networks for wind energy.

The severity of the imbalance depends on the capacity of the components in the power system. For instance, if the capacity of the largest generator is 500 MW, it is possible to lose this 500 MW because of a generator failure. And if offshore wind energy is transported to the shore by 1 GW cables, it is possible to lose this 1 GW at once. The power system must be able to withstand such power losses. Thus, the amount of spinning reserve generation is in the order of several GWs in large interconnected power systems, such as the pan-European system. These examples are seen from a deterministic point of view (i.e. worst case scenario). In reality, the severity of power imbalances also depends on the failure probability of the system components and the actual power of the components. This is taken into account in this study as well.

The general approach of this study is illustrated in figure 4.22. As can be seen, the different causes of power imbalance are first studied separately. Then, the results of the individual studies are compared. This study concentrates on the power imbalance from

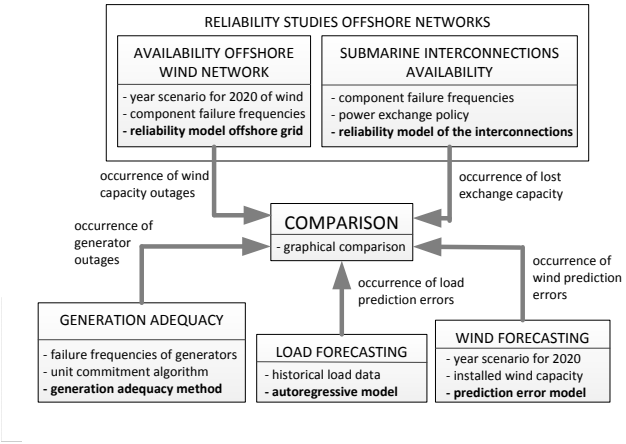

Figure 4.22: Schematic overview of the study approach [73].

a security of supply point of view, i.e. the power imbalance for the system load. In practice, these power imbalances can be solved by remedial actions performed by the TSO to secure the electricity supply. Economical aspects, like whether it is better to invest in network redundancy or to invest in remedial actions and generation reserve, are not considered in this study.

GENERATION ADEQUACY

The analysis of the generation system includes a unit commitment and a generation adequacy study. The generation adequacy study conducted here focuses on a time frame of several hours ahead. Therefore, only spinning reserve is taken into account. With a unit commitment algorithm, the contribution of each generator can be determined, giving:

$P_{gen,n,i}$: production of generator n at hour i

The reliability of the generation system is studied using a generation adequacy approach (chapter 2). Generator failures are not uncommon. An average generator will fail several times a year [74]. This is one of the reasons why there must be enough spinning reserve generation in the power system. Assuming that a failed generator cannot be repaired within a limited time, the probability that a generator has failed after time t, given that it was working at $t = 0$ is given by the unreliability function (chapter 2):

$$U_n(t) = 1 - e^{-\lambda_n t} \approx 1 - e^{-f_n t} \tag{4.3}$$

Under the assumption that:

$$\lambda_n \approx f_n \tag{4.4}$$

Where:
$U_n(t)$ = probability that generator n has failed after time t [-]

t = time [y]
f = failure frequency of generator n [/y]
λ_n = failure rate of generator n [/y]

Using the results of the unit commitment and the generator unreliability functions, it is calculated how often a certain generation capacity outages occur (in [/y]). For example, if generator 12 is planned to produce $P_{gen,12,102} = 100$ MW at time 102 for 1 hour ahead planning, the probability that this generator fails within this time is $U_{12}(1)$. This is also the probability of having 100 MW imbalance at time 1 hour ahead. If this is studied for all generators and a complete year, it can be found how often certain generator capacity outages are expected to occur.

LOAD FORECASTING

The future load can be forecasted up to a certain extent, and there always will be forecast errors. In the planning and operation of the power system, historical loads are often used to predict the future load. Often, loads from 1 day ago, 1 week ago or 1 year ago relative to the considered time horizon are used to study future situations.

There are various mathematical models to predict the load. In this study, an autoregressive model is used to predict the load one hour ahead, based on the hourly loads of the past week (168 h) [17]. In the case study, it was found that this model has a reasonable accuracy in forecasting the load. The autoregressive model is defined as:

$$L_{fore,i} = \alpha_1 L_{i-1} + \alpha_2 L_{i-2} + \ldots + \alpha_{168} L_{i-168} \tag{4.5}$$

Where:
$L_{fore,i}$ = forecasted load at time t [MW]
α_i = autoregression coefficient i [-]

The autoregression coefficients can be found by Matlab. For this model, historical load data is available. The load forecasts are compared with the actual values of this historical load scenario, giving the expected load forecast errors. Also for the load forecast errors, it is studied how often these occur within a year.

OFFSHORE WIND FORECASTING

A third cause of imbalance is the forecast error of the offshore wind power. In [75], it was found that the forecast error of wind power follows a double-sided exponential. This double-sided exponential is described by:

$$P_{error} = \frac{1}{2b} e^{\left(\frac{-|x-\mu|}{b}\right)} \tag{4.6}$$

With:

$$\sigma = \sqrt{2}b \tag{4.7}$$

Where:
P_{error} = probability of the forecast error [-]
x = forecast error [MW]
μ = average forecast error [MW]
σ = standard deviation of the forecast error [MW]

The parameters μ and σ depend on factors like the installed wind capacity, the location of the wind farms and the size of the area covered by the wind farms. This model will be used to determine how often certain wind forecast errors occur.

SUBMARINE INTERCONNECTIONS

The failure of submarine interconnections to other countries can cause a power imbalance as well. The power imbalance caused by failures of submarine connections is strongly dependent on the power exchange policy. For example, during daytime, the full capacity could be used to import power and at night, the full capacity of the submarine interconnection could be used to export power. This was actually the idea behind the NordNed1 cable, where during daytime hydro power from Norway is imported and at night conventional power from The Netherlands is exported. Because of this exchange policy, it is very likely to lose either the full import or export power after a failure. For the case study in this research, an exchange scenario for 2020 based on a market study was provided, listing:

$P_{exch,n,i}$: exchange of connection n at hour i

Long-distance submarine interconnections are mostly HVDC connections with typically the configuration as was shown in 4.9. Using this scheme and failure statistics of the components, the reliability of the submarine interconnection can be calculated. Similarly to the generation system, the probability that a component has failed can be calculated by the unreliability function 4.3-4.4. Again, it is assumed that a failed component cannot be repaired within a short time. According to the calculation rules for reliability networks [16], the reliability of the submarine interconnection is the product of the reliability of the components, as it is assumed that every component in the connection is needed for successful operation.

$$U_{conn}(t) = 1 - \prod_{n=1}^{k} (1 - U_n(t)) \tag{4.8}$$

Where:
U_{conn} = unreliability of the connection [-]
$U_n(t)$ = reliability of component n [-]
k = number of components in the connection [-]

Combining this with the exchange policy, the occurrence of certain power imbalances can be calculated. For example, if the planned import over submarine connection 5 at time 102 for 1 hour ahead planning is $P_{exch,5,102} = 100$ MW, the probability that the submarine interconnection fails within this time is $U_{conn,5}(1)$. This is also the probability of having 100 MW power imbalance. This can now be calculated for all submarine interconnections for one year.

OFFSHORE NETWORK FOR WIND ENERGY

For offshore wind energy networks, the occurrence of power outages is dependent on the power production and the topology of the offshore network. Similar to the submarine interconnection, all the components of the offshore network must be included to

study the reliability. In this study, the offshore wind is connected as was shown in figure 4.11a. Again, it is assumed that the components cannot be repaired within a short time because of the long repair times of offshore components, and the unreliability functions of the components are used (equations 4.3-4.4). For the HVDC connection, the same scheme as was shown in figure 4.9 is used. For both the AC connections and the HVDC connection equation 4.8 holds, realizing that the loss of an AC connection leads to the disconnection of one wind farm while a failure of the HVDC connection leads to the disconnection of four wind farms. All wind farms and their connection are studied to find the occurrence of wind capacity outages due to offshore network failures.

4.6.2. CASE STUDY

TEST CASE DESCRIPTION

The numerical calculations in this research are based on a test power system with a comparable size as the Dutch power system. A schematic overview of the studied system is shown in figure 4.23. This system has a peak load of 15 GW, about 17 GW installed generation capacity, 3 GW installed offshore wind capacity, and submarine interconnection with a total capacity of 3 GW. The offshore wind energy is collected by offshore substations. Each substation of 1 GW combines the power of four 250 MW wind farms and is connected by a DC cable to the shore.

The reliability of the onshore transmission network is not included in this study. In the Netherlands, all substations that include large-scale conventional generation are 4/3 or 3/2 circuit breaker stations and will in the future be connected to the EHV network by two double circuits. Large network failures are very unlikely in these configurations [30]. Therefore, in this study the onshore network can be modeled by a single busbar.

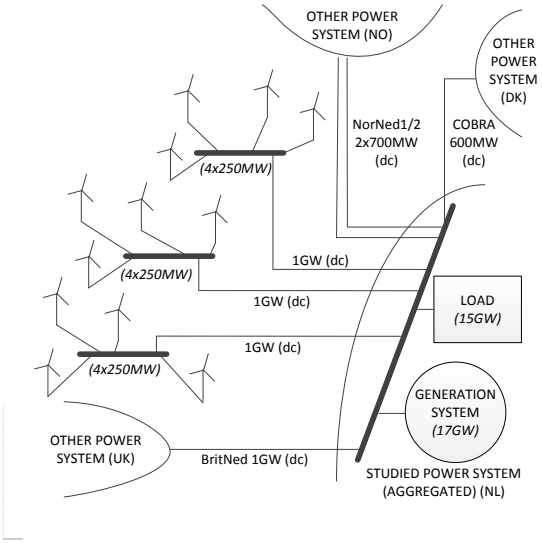

Figure 4.23: Schematic overview of the studied system [73].

Table 4.7: Generation system of the generation adequacy study.

Type	Capacity [MW]	Amount
Coal	600-800	2
Coal	500-600	5
Coal	400-500	2
Gas	600-800	2
Gas	400-600	11
Gas	200-400	15
Gas	0-200	12

GENERATION ADEQUACY

For the generation adequacy study, a generation system as listed in table 4.7 is used. This is comparable to the Dutch generation system. The total installed capacity is about 16 GW. Data concerning failure frequencies of the generators can be found in [74]. In the test case, the production per unit is calculated by a simplified unit commitment algorithm. In this algorithm, the coal plants are always in operation. The gas plants are used if a certain level of production can be guaranteed for several hours. Although this algorithm is very simplistic, it produces a generator behavior realistic enough for this particular study.

The results can be combined to study the expected occurrence of capacity outages. Figure 4.24 shows the result. As can be seen, generation capacity outages up to 700 MW are likely to occur. This is directly related to the installed capacities of the generators and the unit commitment. For example, if the largest (coal) power plant of 700 MW is mostly operated at about full capacity according to the unit commitment, it is possible to lose a generator capacity up to 700 MW. Capacity outages larger than 700 MW are less likely to occur. Because in this study only independent generator failures are considered, these larger capacity outages are only possible if more generators fail within the studied time frame (of 1 to several hours). If dependent failures are included, the large capacity outages will occur somewhat more often.

LOAD FORECASTING

To study the load forecast errors, historical load data from a 150 kV substation in the Netherlands with mainly domestic load is used. The load data is scaled, such that the peak load equals 15 GW, about the total peak load of the Dutch power system. For one year, the occurrence of load forecast errors is studied. The results of this are shown in figure 4.25a.

The figure shows that load forecast errors up to about 500 MW are likely to occur. Load forecast errors larger than 1000 MW are rare. Because forecasts are never exactly right, the total amount of occurrence sums up to 8760 /y. As can be seen, the load forecast error approximately follows a normal distribution (with $\sigma = 268$ MW). With an average forecast error of about 2.5%, this is a relatively accurate forecast. In reality, it may however be possible to obtain more accurate forecasts by using more advanced forecast models. If the time frame of the forecast increases, this distribution becomes wider.

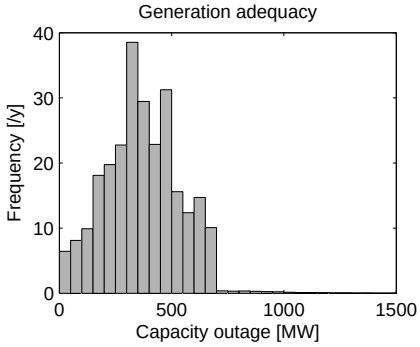

Figure 4.24: Occurrence of generation capacity outages [73].

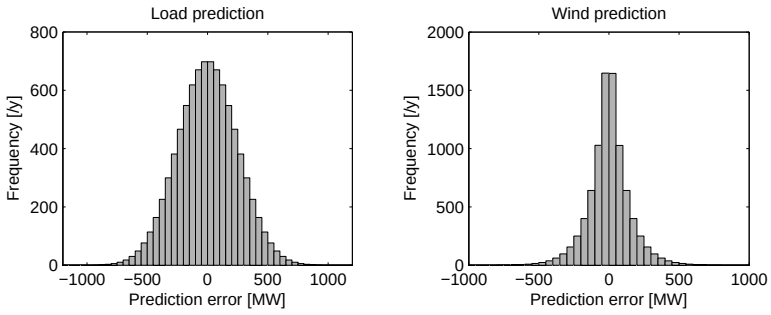

(a) Occurrence of load forecast errors. **(b) Occurrence of wind forecast errors.**

Figure 4.25: Occurrence of load and wind forecast errors [73].

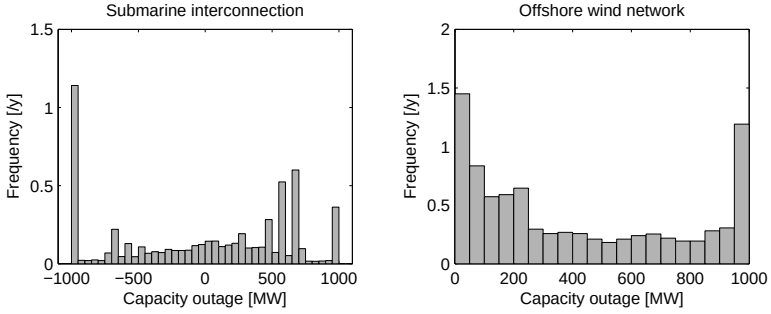

(a) Occurrence of capacity outages of submarine interconnections. **(b) Occurrence of capacity outages caused by the offshore wind network.**

Figure 4.26: Occurrence of capacity outages of submarine interconnections and offshore wind network [73].

OFFSHORE WIND FORECASTING

In [75], the forecast error of about 8 GW of offshore wind in The Netherlands was studied. If a smaller amount of installed wind capacity located within the same area is considered, it seems reasonable to assume that the double-sided exponential can be scaled. If the installed capacity is scaled to the 3 GW of the case study, the occurrence of wind forecast error becomes as shown in figure 4.25b. It can be seen that forecast errors up to 250 MW are frequent and forecast errors up to 500 MW are likely. For different time horizons, the forecast error changes. Large forecast errors become more likely for longer horizons.

SUBMARINE INTERCONNECTIONS

For the power exchange in the test system, a scenario for 2020 (scenario2020, see also appendix A) is used. For the components, the failure frequencies as given in table 4.2 are used. The occurrence of capacity outages are studied and shown in figure 4.26a. The graph is plotted such that it is in line with the generation adequacy study: a positive exchange capacity outage means that power was imported but lost because of a connection failure.

In the graph, several peaks can be distinguished: at -1000, -700, -600, -500, 500, 600, 700, and 1000 MW. These are the installed capacities of the individual submarine interconnections. Because of the exchange policy, it is likely to lose either the full capacity when exporting power or the full capacity when importing power. Capacity outages in between these minimums and maximums are less frequent.

OFFSHORE NETWORK FOR WIND ENERGY

For the power production of the offshore wind farms, scenario2020 is used as well. Figure 4.26b shows the occurrence of capacity outages caused by failures of the offshore wind energy network. As can be seen, it is likely to lose either 0 MW or the total installed capacity (1 GW). This is because wind farms are often producing 0 or the full capacity. Furthermore, capacity outages up to 250 MW occur somewhat more often than capacity outages larger than 250 MW. The first are mainly caused by failures of the connections between the wind farms and the offshore substation, while the latter are mainly caused by failures of the HVDC connection.

4.6.3. COMPARISON AND SENSITIVITY ANALYSIS

COMPARISON OF CAUSES OF POWER IMBALANCE

In the previous section, various causes of imbalance were studied. It is now possible to compare these different causes and to determine which of these causes are the most critical. This is done by combining figures 4.24, 4.25 and 4.26.

Figure 4.27 shows the occurrence of imbalance power caused by various causes. It can be seen that forecast errors of the load and wind are the most frequent. Which is logical, as forecasts are never exactly right. Large load forecast errors (500-1000 MW) are more likely than wind forecast errors of this size. However, the peak load of the studied system is 15 GW while the installed wind capacity is 3 GW. It can be concluded that the predictability of wind is significantly worse than the predictability of the load.

As can be seen in the figure too, imbalance due to generator failures is less common than the forecast errors. Large generator capacity outages of 500-700 MW are relatively

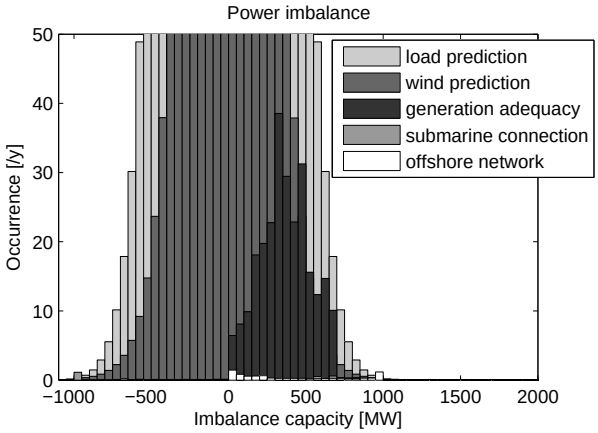

Figure 4.27: Overview of the causes of power imbalance (1h time frame, 3GW installed wind capacity) [73].

frequent, about as frequent as wind forecast errors, but still less frequent than load forecast errors of this size. Enough reserve generation must be available to deal with these load/wind forecast errors and generator failures.

Failures of the submarine interconnection and the offshore wind energy network are significantly less frequent than the other failures. In the figure, these offshore network failures are still in the same range as the forecast errors. This suggests that if in a system of this size enough spinning reserve generation is available to cope with the wind and load variations, there is also enough spinning reserve generation available to cope with generator and offshore network failures. In this way, spinning reserve generation can be seen as a redundancy for the offshore network. Only the large capacity outages of submarine interconnections and offshore wind energy networks (-1000 MW and 1000 MW) are out of the range of the forecast errors. These large capacity outages are probably the most critical.

SENSITIVITY ANALYSIS

As this study is very dependent on input parameters like the amount of offshore wind energy, it is of interest to perform a sensitivity analysis. Two sensitivity analyses will be performed here: in the first, the amount of offshore wind and number of submarine interconnections is changed and in the second, the considered time frame is increased.

The results of the first sensitivity analysis are shown in figure 4.28. The main difference with figure 4.27 is that the wind forecast errors are less severe now, because the installed wind capacity is smaller. As there is less wind power, more conventional generation is needed and generator failures occur somewhat more often. As in this sensitivity analysis the number of submarine interconnections is reduced as well, failures of the offshore network will occur even less often in comparison with figure 4.27.

The results of the second sensitivity analysis are shown in figure 4.29. As the considered time frame is increased from 1 h to 2 h and 3 h now, failures of the generation system and the offshore networks become more frequent. This is because the unreliability function of the components increases with time (equation 4.3). Furthermore, for longer time

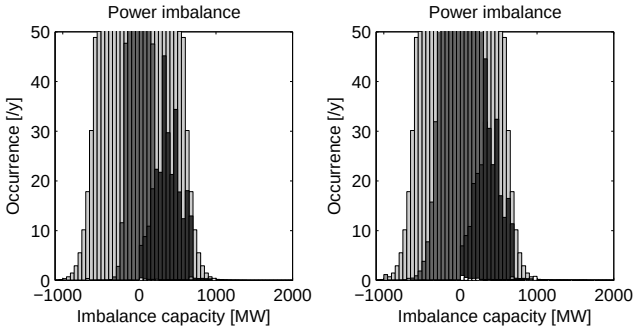

Figure 4.28: Sensitivity analysis: less offshore wind and less submarine interconnections (1h time frame) [73].

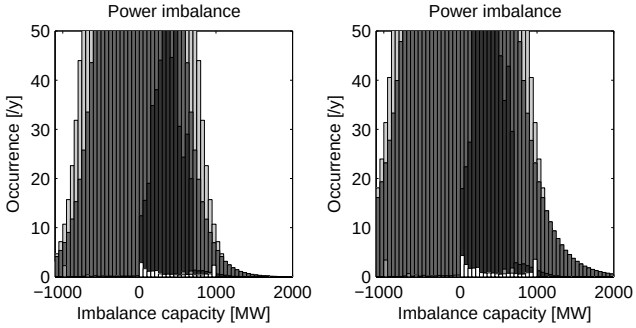

Figure 4.29: Sensitivity analysis: longer time-frame (3GW wind) [73].

frames the load and wind forecasts become less accurate. As can be seen from figure 4.29, load forecasts become somewhat less accurate while wind forecasts become significantly less accurate. Wind forecast errors up to several GWs can occur.

4.7. CONCLUSION

In this chapter, the reliability of offshore transmission networks was described. First, some characteristics of offshore wind were discussed. Then, the failure statistics of offshore network components were investigated. Because offshore networks are a relatively new technology, the amount of available failure statistics is very limited. Two sources of failure statistics were discussed. Both show that transformers and DC cables have the largest unavailability, which is mainly caused by the long repair time of about two months. For future reliability analysis, it would be helpful to collect more failure statistics of offshore components. With these statistics, the results of probabilistic reliability analysis become more accurate. Also, different technologies and voltage levels can be compared and the occurrence of dependent failures can be studied then.

For wind farms located farther from the shore, it is beneficial to collect the offshore wind energy in offshore substations (hubs-at-sea). The availability of an offshore network can be increased by using a hub-at-sea. Several AC and DC configurations were

analyzed. Generally, the unavailability of a DC network is larger than the unavailability of an AC network, because of the additional converter components. Still, transformers and cables contribute the most to the total unavailability of the connection.

Although the expected amount of lost wind energy can be reduced by using a hub-at-sea, the improvement is limited. This is because the wind farms are within the same area and it is likely that all wind farms produce maximum capacity at the same time. A further improvement can be obtained when more redundancy is created in the offshore network (e.g. by installing more cables than needed). For the DC configurations, two variants were studied: one DC cable with the full transport capacity and two DC cables with each half the capacity. Logically, in the first case it is possible to lose the full production while in the second case, it is more likely to lose half the production at a time. Because of the larger unavailability of the DC network, the expected amount of lost wind energy is larger than for the AC cases.

In a simple economical study, all the studied configurations were compared. For the AC networks, the additional costs of a hub-at-sea will be larger than the savings on the lost wind energy. For the DC networks, it seems better to use a configuration with two DC cables of half capacity. In case of a cable failure, the network can continue operation at half capacity. Without installing extra cables, redundancy in the offshore network can be created by over-dimensioning of the cables. It is however found that it is probably the most economical to have a total cable capacity of exactly the installed wind capacity.

In a study on possible network configurations for near-shore wind farms, the collection of wind energy by two platforms connected by AC cables was considered. A Net Present Value approach was followed to determine the most economical offshore network configuration. It was shown that some redundancy in the network is economical. It was also shown that the capacity of the optional (redundant) cables does not need to be larger than half the capacity of the AC cables that connect the platforms to the shore. Full offshore n-1 redundancy is not economical in this case.

When the total offshore wind capacity increases, it becomes more likely to lose a large amount of wind production at a time. It is often questioned whether n-1 redundancy must be applied in offshore networks as well. In a study, various causes of power imbalance were compared. If it is realized that the total peak load in the study was 15 GW while the installed wind capacity was 3 GW, it can be concluded that wind forecast errors are significantly worse than load forecast errors. Generator failures are also common, while failures of submarine interconnections and offshore wind energy networks are less frequent. In a system of about the size of the Dutch power system, wind forecast errors are probably the most severe cause of power imbalance. The onshore system must be strong enough to deal with this. It seems that if there is enough spinning reserve to deal with forecast errors and generator failures, there is also enough spinning reserve to cope with failures of the offshore network. Generation reserve can serve as redundancy for the offshore network in this way.

Large capacity outages of offshore networks can however become more critical for larger-scale offshore networks. If the capacity of a submarine connection or the offshore wind network is 1 GW, it is possible to lose this 1 GW at a time. This can occur more frequently than forecast errors and generation failures, depending on the system size. The sensitivity analyses showed that if the amount of wind energy or the considered time

frame is changed, the severity of the wind forecast errors changes considerably. It is of interest to study in the near future to what extent onshore generation reserve can serve as redundancy for the offshore network and under what conditions. This will provide more insight into the question whether n-1 redundancy must be obeyed for offshore networks.

The studies in this chapter showed that offshore network redundancy is probably not an economical solution. Furthermore, power imbalance caused by wind forecast errors and generator failures is more common and severe than imbalance caused by failures of the offshore network. It is therefore suggested to think differently about offshore network redundancy. For example, onshore generation reserve, energy storage and demand side response can act as redundancy for the offshore network. In future research, it should be studied under what conditions this conclusion holds and whether this conclusion applies to international interconnected offshore networks as well.

5

CONCLUSIONS

In this research, probabilistic reliability analysis was applied to study two developments of the power system, namely EHV underground AC cables and offshore networks. The performed studies not only provide insight into the reliability impacts of these developments, but also about probabilistic power system reliability analysis in general.

EHV UNDERGROUND CABLES

Compared to overhead lines, underground cables have a significantly larger unavailability. This is mainly caused by the about 100 times longer average repair time of underground cable connections. Here, the repair time is the total time between the occurrence of the failure till the connection is brought into service again. The failure frequency of underground cables is somewhat smaller than the failure frequency of overhead lines. However, the combination of the cable circuit components (cable sections, joints, terminations) and the fact that in the Randstad380 configuration two individual cables are applied per circuit phase, lead to a failure frequency of underground cable circuits which is about 3 times larger than the failure frequency of overhead line circuits.

The studies described in chapter 3 (section 3.4) showed that the reliability of an underground cable connection can be improved in several ways. First, the failure frequencies and repair times can be reduced by e.g. advanced testing/ monitoring, improved fault localization or an optimized repair scheme. A second possibility is to use partial-cabling, where underground cables are only applied at selected locations within a connection. However, too short line sections between cable sections should be avoided then. The third option is to use an alternative configuration of the cable connection. From the studied options, the most economical solution might be the configuration with additional disconnectors, which can isolate the damaged cable within the Randstad380 configuration (half-a-circuit) after a cable failure. It must be studied whether a 75% capacity state is acceptable in the operation of the power system.

The studies described in chapter 3 (section 3.5) showed that the network reliability strongly depends on the location of the cables within the network topology. The probability of an islanded substation and the probability of an overloaded network were used

as reliability indicators in this study. The probability of an islanded substation is a characteristic of the network topology, and in this sense it is better to avoid the connection of crucial substations by underground cables only. The probability of an overloaded network depends on the network topology and the load flow within the network. A cable connection in a heavily-loaded connection has a much higher impact than a cable connection in a less loaded connection. There is a large difference between installing underground cables in only one connection route and installing cables in multiple connection routes supplied by a large generation center. It is found that one long cable connection in one connection route can still be better than two short cable connections in different connection routes. It is therefore better to avoid underground cables in multiple connection routes supplied by a large generation center or supplying a large load center.

A study on the occurrence of failures in large transmission networks described in chapter 3 (section 3.6) showed that for higher failure frequencies, longer repair times or longer cable connections, multiple failures in the network will occur more often. For longer cable connections and longer repair times, independent (double) failures of two circuits will happen more frequently than dependent failures of double circuits. This can have consequences for the design and operation of transmission networks as these independent failures including a cable circuit now require more attention. For an increasing number of cable circuits in the network, the probability of having three and four failures will increase relatively the most as more combinations of three and four cable circuit failures become possible.

In an analysis on further cabling of transmission networks in chapter 3 (section 3.7), the impact of underground cables was studied and presented in various reliability indicators for a more comprehensive assessment. This study confirmed that the risk strongly depends on the loading of the cable connection, such that underground cables should be avoided in heavily-loaded, crucial connections. It was found that for some connections, the impact of underground cables is mainly caused by the difference in impedance between underground cable and overhead line circuits. In these cases, series impedance compensation (like applied in Randstad380 Zuid) can mitigate the impact.

Table 5.1 summarizes the risk mitigation measures. The measures to mitigate the risk can roughly be divided into two groups: network design criteria and cable connection design criteria. Generally, the effect of the network design measures is much stronger than the effects of the cable connection design criteria. This was reflected in the study by smaller reliability indicators like the amount of load curtailment, the amount of redispatch and the probability of the alert state.

OFFSHORE NETWORKS

Considering offshore networks, the available failure statistics as described in chapter 4 (section 4.2) showed that transformers and submarine cables have the largest unavailability, which is mainly caused by long repair times. For wind farms located farther from the shore, it can be beneficial to collect the offshore wind energy in offshore substations (hubs-at-sea). The availability of the offshore network can be increased in this way. A comparison of AC and DC configurations in chapter 4 (section 4.4) showed that generally, the unavailability of a DC network is larger than the unavailability of an AC network, because of the additional converter components (e.g. filters, transformers, converters).

Table 5.1: Effectiveness of various risk mitigation measures.

Design measure	Effect	Design
Avoid underground cables in heavily-loaded, crucial connections	•••	network
Avoid cables in multiple connection routes supplied by a large generation center	•••	network
Prevent islanding of substations by connecting substations not only by cables	•••	network
Apply series impedance compensation, if applicable	•••	network
Use configuration with disconnectors, if acceptable in system operation	•••	cable
Reduce the failure frequencies of underground cable components	••	cable
Reduce the repair time of underground cable components	••	cable
Only one cable per circuit phase, compared to Randstad380	••	cable
Reduce the underground cable length within a (partially-cabled) connection	••	cable
Install less cable sections in a partially-cabled connection	•	cable

Although the expected amount of lost wind energy can be reduced by using hubs-at-sea, the improvement is limited. This is because the wind farms are within the same area and often, all wind farms produce maximum capacity at the same time. A further improvement can be obtained when more redundancy is created in the offshore network, but this is probably not an economical solution. For DC configurations, it can be beneficial to use a bipole configuration which is able to continue operation at half capacity after a network failure.

In a study on the Dutch offshore situation described in chapter 4 (section 4.5), a Net Present Value (NPV)-based approach was developed to find the preferred configuration of an offshore network. In the NPV, the additional costs of investment and operation were compared with the extra income of less lost wind energy. Various redundancy alternatives of a near-shore wind network were considered. This study showed that it can be economical to have some redundancy within the offshore network. More redundancy will not be economical. The study confirmed that to create more redundancy, often the whole offshore network must be upgraded, as it is very likely that all wind farms produce maximum capacity at the same time.

When the total offshore wind capacity increases, it becomes more likely to lose a large amount of wind production at a time. A study described in chapter 4 (section 4.6) on various causes of power imbalance showed that large wind forecast errors are significantly more frequent than generator failures and failures of the offshore network. In a system of about the size of the Dutch power system, wind forecast errors are probably the most severe cause of power imbalance. The onshore system must be strong enough to deal with this. It seems that if there is enough spinning reserve to deal with forecast errors and generator failures, there is also enough spinning reserve to cope with failures of the offshore network.

Regarding the question whether offshore networks should be $n-1$ redundant like the onshore transmission network, studies show that this probably is not an economical solution, as seen from the wind farm owners point-of-view. Some small level of redundancy can be economical though, when the additional investment and operation costs are smaller than the extra income because of less lost wind energy. As the offshore capacity increases, it becomes more likely to lose a large capacity at the same time. For power systems with enough conventional spinning reserve and for limited amounts of

offshore wind, this will not be a problem. But in future renewable power systems, alternatives like energy storage and demand side response could serve as redundancy for the offshore network.

PROBABILISTIC RELIABILITY ANALYSIS

The studies on the reliability impact of underground cables and offshore networks as described in this research show the importance of probabilistic reliability analysis. In both cases, deterministic approaches do not show any discriminating results. The probabilistic approaches described in this thesis can be applied to analyze the reliability impact of these developments.

When comparing probabilistic analysis with deterministic criteria, it is found that probabilistic approaches can provide more insight into the reliability of power systems. For example, deterministic criteria show whether a network is $n-1$ redundant or not, while with probabilistic analysis, the precise probability of an overloaded network can be calculated. It can then be decided whether the risk is acceptable or not. On the other hand, if there are deterministic issues in the network, these will dominate the probabilistic results as well. Probabilistic analysis therefore can be seen as a complement to rather than a replacement of deterministic criteria.

When studying the reliability of power systems, usually the results are presented in indicators related to the security of supply. Example indicators are the probability and frequency of load curtailment, the amount and costs of load curtailment, and customer indices like CAIDI, SAIFI and SAIDI. Still, the representation of the results of probabilistic reliability analysis remains a challenge. As loss of load is not the only risk for a TSO, the set of probabilistic indicators can be extended by indices which are less directly related to security of supply. Examples are the probability and amount of generation redispatch, the probability of an overloaded network and the probability of the alert $(n-0)$ state. Together with the security-of-supply related indices these provide more insight into the reliability of the transmission network.

6

Recommendations and Future Work

The studies performed during this research led to several recommendations and suggestions for future work. Like the conclusions, these can be divided into recommendations and future work for EHV underground cables, offshore networks and probabilistic reliability analysis in general.

EHV Underground Cables

In the conclusions, several risk mitigation measures were defined. As the reliability impact of underground cables strongly depends on the characteristics of a particular cable project, such as the network topology and cable configuration, it is recommended to analyze future cable projects per specific situation. The reliability impact can then be assessed taking load flow scenarios and possible future changes of the cable loading into account. Case-specific risk mitigation measures like series impedance compensation and the use of only one cable per circuit phase can then be considered as well.

A cable configuration with additional circuit breaker was suggested as risk mitigation measure. It was mentioned that this solution depends on whether a 75% cable connection capacity is acceptable in system operation. In future work, this alternative configuration should be studied in more detail. In addition to the reduced capacity during a cable failure, the impedance of the connection changes and lead to a changed load flow in the transmission network. Because this is case-specific, the possibility of this solution must be analyzed per cable project.

Offshore Networks

In this research, a Net Present Value (NPV)-based approach was used to find the preferred configuration of offshore networks. To obtain more accurate and more realistic results, it is recommended to include a varying market energy price into the calculations. Also, the dependency between market energy price and wind generation in renewable power systems can then be included in detail. It is of interest as well to apply this approach to larger offshore networks connecting multiple countries.

The causes of power imbalance in the system was analyzed in this thesis. For the studied system, it was concluded that onshore spinning reserve can serve as redundancy for the offshore network. For future power systems, with more offshore wind capacity and less onshore spinning reserve, it must be studied in more detail till what level this conclusion holds. Also, the possibilities to arrange redundancy for the offshore network by energy storage or demand side responds should be studied in more detail. This will provide more insight into the question when and where $n-1$ redundancy must be applied for offshore networks.

More in general, the possibilities to deviate from the $n-1$ redundancy criterion must be investigated in more detail. New developments like variable renewable energy source lead to a variable use of the electrical infrastructure. In the future, it might become less economical to apply $n-1$ redundancy in the whole onshore and offshore network. Furthermore, the application of new technologies like power electronics offer more possibilities to control power flows in the network. It is therefore of interest to analyze the risks of deviating from $n-1$ redundancy, but also the technological requirements for operating the transmission network under $n-0$ redundancy.

PROBABILISTIC RELIABILITY ANALYSIS

The main input of probabilistic reliability analysis are failure statistics. An accurate network reliability requires input parameters like accurate failure frequencies and well-defined repair times. Especially for new technologies like EHV underground cables and offshore networks, the availability of failure statistics is limited. For future calculations, it is important to collect more failure statistics. In this way, different technologies can be compared and the occurrence of dependent failures can be studied.

For probabilistic reliability analysis, the presentation of the results still remains a challenge. Although probabilistic analysis can provide more insight, deterministic criteria remain clear, easy to understand, and effective. Future work should be devoted to present the results of probabilistic reliability analysis in a clear, actionable and understandable way. After all, it is the interpretation of the results of probabilistic reliability analysis that leads to more insight, and not the results themselves.

A

CASE STUDY NETWORK

THE DUTCH EHV TRANSMISSION NETWORK

In this thesis, the Dutch EHV (380/220kV) transmission network is used as a case study for reliability analysis. Some studies are performed on the complete EHV network, while other studies concentrate on parts of the transmission network: the Randstad region and Maasvlakte (MVL) region. For the reliability calculations, a load/generation scenario for 2020 as provided by TenneT is used. The Dutch EHV transmission network and the scenario2020 are described in more detail in the following sections.

In figure A.1, the Dutch EHV(380/220kV) transmission network according to TenneT's Vision2030 is shown [65]. The Dutch power system is influenced by its location near the sea. For example, the availability of cooling water and the possibilities for fuel supply made the location of large power plants near the sea attractive. This has led to the large-scale generation centers Maasvlakte (MVL380), Eemshaven (EEM380) and Borssele (BSL380). As most of the load is located in the Randstad area, the network is the most dense in this part of the country. Because the northern part of the country is less populated, a 220kV (instead of 380kV) ring was built there.

In the future, large-scale offshore wind energy will be connected at several places in the network, as indicated on the map as well. In fact, the Dutch transmission network will play an important role in transporting offshore wind energy to the main load centers in the Netherlands and in other European countries.

To increase the capacity of the Dutch transmission network, various network extensions are planned. For example, figure A.1 shows the new (partially-cabled) connections belonging to the Randstad380 project. Randstad380 Zuid is already in operation while Randstad380 Noord is under construction. Another new connection that will be partially-cabled is the Spaak project, that splits the main 380kV ring into two. Other possible new developments are: new 380kV connections between EEM-ENS and BSL-GT, new substations Tilburg (TBG) and KRK, and a new connection to Germany at Doetinchem (DTC). These latter developments are still in a study phase.

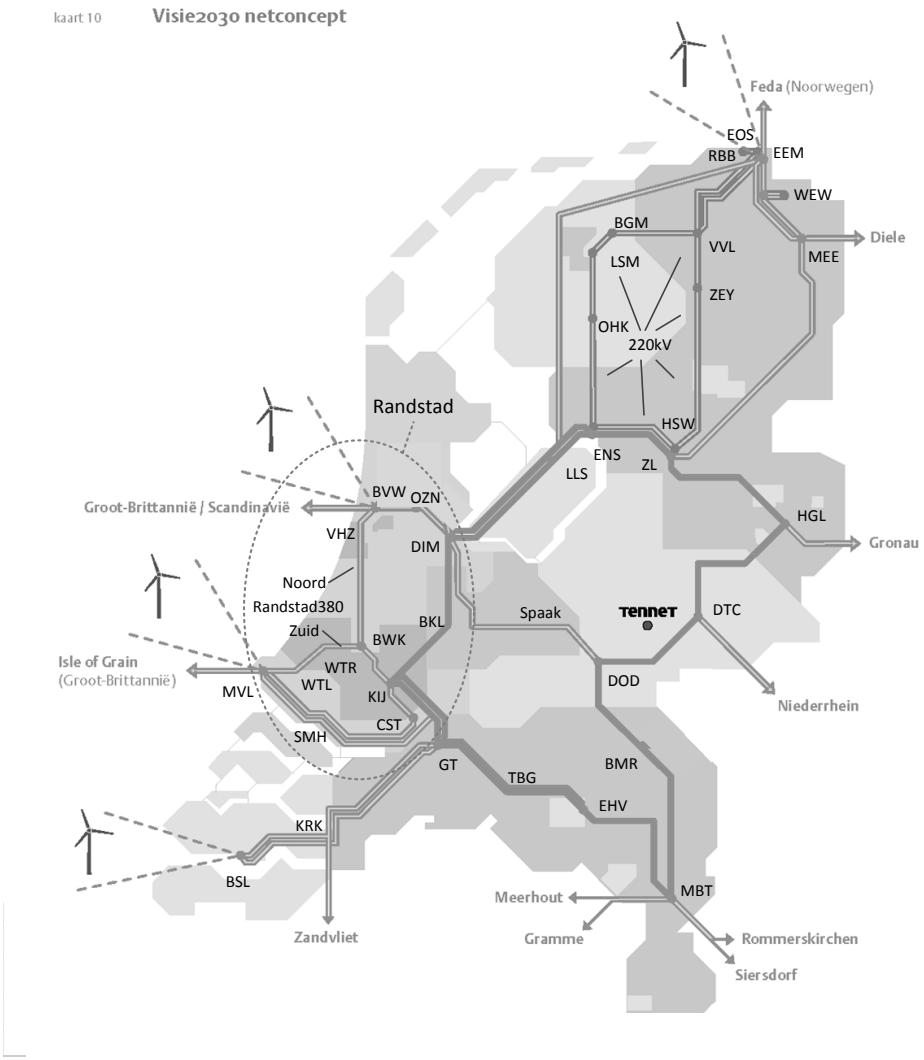

Figure A.1: The Dutch EHV(380/220kV) transmission network according to TenneT's Vision2030 [65].

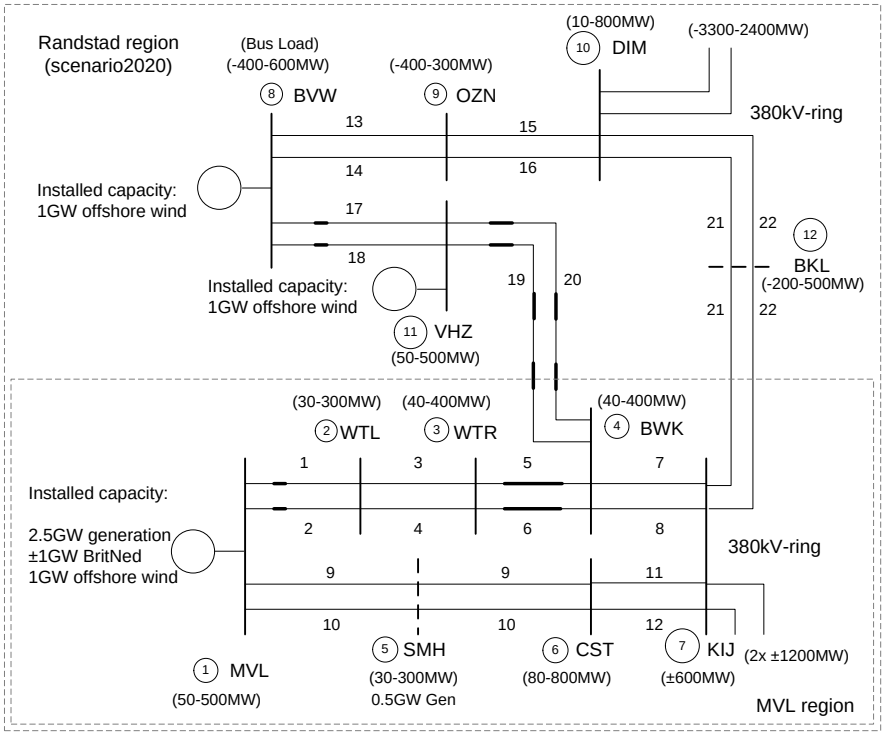

Figure A.2: Randstad380 region network. In the figure, the bus loads, line loads and installed generation per bus are shown. The locations of the underground cables of Randstad380 Noord and Zuid are indicated by bold lines.

RANDSTAD380 AND MVL380 REGION

The Randstad region, as indicated in figure A.1, includes the main load centers of the Netherlands as well as the large-scale generation center Maasvlakte (MVL). As this part of the network includes the underground cables of Randstad380 and the connection of large-scale offshore wind energy, this part of the network is particularly suitable for analysis of these two developments. Therefore, some of the reliability studies of this research concentrate on this part of the network.

Figure A.2 shows the transmission network in the Randstad region. The figure shows the connection between MVL and BVW substations and the main 380kV ring. At MVL, a large amount of conventional generation is located. Also the 1 GW BritNed cable is connected to this substation. In the future, substations MVL, BVW and VHZ are possible connection points for offshore wind energy. Substations SMH and BKL are tapping stations and indicated by dashed lines.

The figure also shows the EHV underground cables of the Randstad380 project [9]. As indicated with bold lines, there is a long cable connection (11 km) between substations

Table A.1: Installed capacity at some buses in scenario2020.

Substation	Conventional	Wind
Beverwijk (BVW)	0 GW	1 GW
Borssele (BSL)	2 GW	1 GW
Eemshaven (EEM)	1 GW	0 GW
Eemshaven Oudeschip (EOS)	3 GW	1 GW
Maasvlakte (MVL)	3 GW	1 GW
Vijfhuizen (VHZ)	0 GW	1 GW

WTR and BWK (Randstad380 Zuid). A smaller cable section (2 km) is located between MVL and WTL to cross a river. The underground cable sections of Randstad380 Noord are located between substations VHZ and BWK (2+3+3 km). A short cable section (1 km) is located between BVW and VHZ to cross another river. In this research, this situation is called the 'base case'.

Some studies in this research concentrate on an even smaller part of the transmission network, the Maasvlakte (MVL) region as indicated in figure A.2. This part still includes underground cables as well as offshore wind energy and is therefore a suitable small network for developing new methods and obtain insight.

SCENARIO2020

For the reliability studies, TenneT provided a load/generation scenario for 2020. This scenario includes the load and generation for every substation and for every hour. Actually, TenneT developed several load/generation scenarios, based on their four scenarios as described in Vision2030 [65]. The installed generation capacity at the most important substations is shown in table A.1.

The installed capacities and the ranges of the substation loadings within the Randstad area are also shown in figure A.2. These loadings can be negative as there are generation units in the underlying 150kV network too. Furthermore, the line loadings to the main 380kV ring are indicated in the figure as well.

In some of the studies in this research, scenario2020 will be changed. For example, the effects of more offshore wind are studied by increasing the installed wind capacity at some substations. It is then assumed that this wind energy is consumed or compensated at other substations. This is clearly described for the particular studies.

B

Failure Statistics of Power System Components

Failure Frequencies

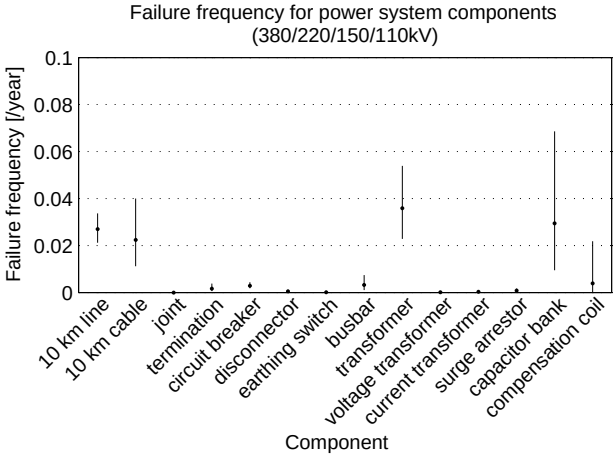

Figure B.1: Failure frequency of different power system components. The dots represent the sample means, the line indicates the χ^2-95% confidence interval.

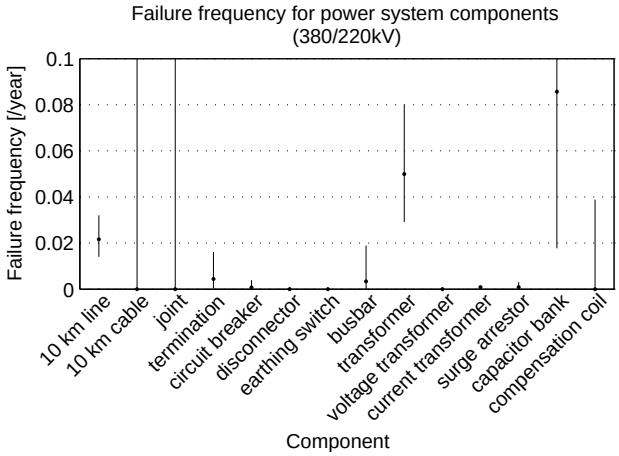

Figure B.2: Failure frequency of different power system components. The dots represent the sample means, the line indicates the χ^2-95% confidence interval.

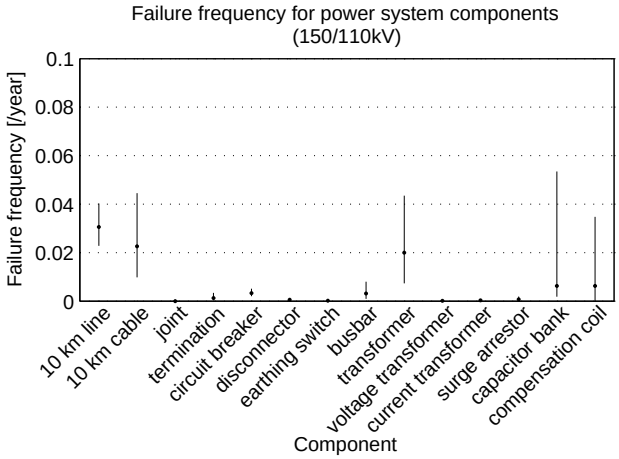

Figure B.3: Failure frequency of different power system components. The dots represent the sample means, the line indicates the χ^2-95% confidence interval.

Table B.1: Amount of involved components per failure.

Amount of components	Percentage of failures
One	92%
Two	5%
Three	2%
Four	1%
Six	0.2%
Eleven	0.2%

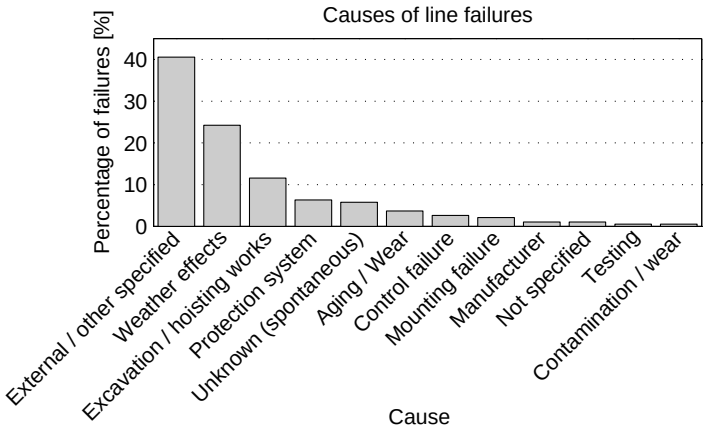

Figure B.4: Causes of overhead line failures.

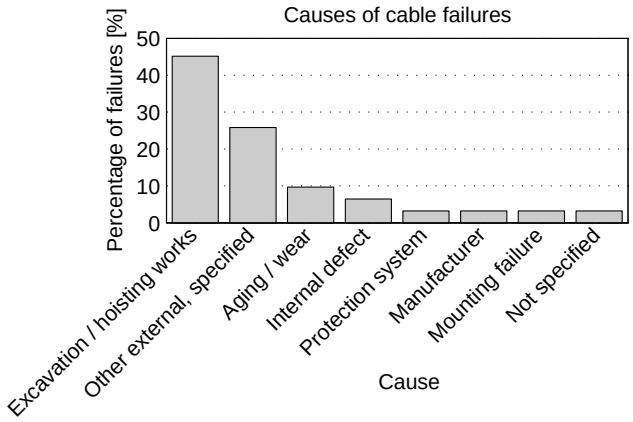

Figure B.5: Causes of cable system failures.

Table B.2: Amount of involved line circuits per failure.

Amount of components	**Percentage of failures**
One (independent)	84%
Line circuit + component	5%
Double circuit	4%
Two line circuits	2%
Three line circuits	2%
Four line circuits	1%
Five line circuits	1%
Six line circuits	1%

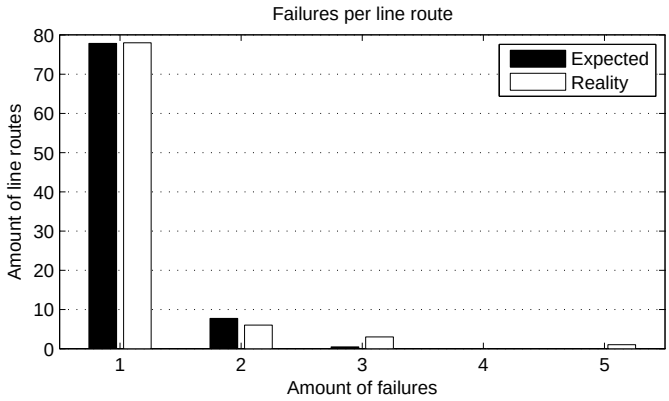

Figure B.6: Subsequent failures of the same line route.

Table B.3: Overview of the failure frequency of different system components.

Component	Failure frequency	Source (info)
Overhead line (EHV)	0.0022 (/cctkm)	NESTOR (380/220kV, 2006-2011)
Overhead line (HV)	0.0031 (/cctkm)	NESTOR (150/110kV, 2006-2011)
Cable (HV) (including joints)	0.0022 (/cctkm)	NESTOR (150/110kV, 2006-2011) (+0.002 per termination)
Joint	0.00035 (/comp.)	European TSOs study (per phase)
Termination	0.00168 (/comp.)	European TSOs study (per phase)
Cable (Randstad380) (including joints)	0.0050 (/cctkm)	European TSOs study (6 cables/circuit) (+0.020, total for all the terminations)
Circuit breaker	0.0030 (/comp.)	NESTOR (380-110kV, 2006-2011) (per circuit, set of 3 circuit breakers)
Disconnector / earthing switch	0.0002 (/comp.)	VDN (measured per phase)
Busbar	0.0030 (/comp.)	NESTOR (380-110kV, 2006-2011)
Transformer (EHV)	0.0500 (/comp.)	NESTOR (EHV, 2006-2011)
Transformer (HV)	0.0200 (/comp.)	NESTOR (HV, 2006-2011)
Instrument transformer	0.0002 (/comp.)	VDN (measured per phase)
Surge arrestor	0.0010 (/comp.)	NESTOR (380-110kV, 2006-2011)
Capacitor bank	0.0290 (/comp.)	NESTOR (380-110kV, 2006-2011)
Compensation coil	0.0040 (/comp.)	NESTOR (380-110kV, 2006-2011)
Protection failure	0.001	VDN (conditional probability)
Circuit breaker failure	0.0015	VDN (conditional probability)
Protection overreaction	0.005	VDN (conditional probability)
Spontaneous protection switching	0.010 (/comp.)	VDN (failure frequency)

REPAIR TIMES

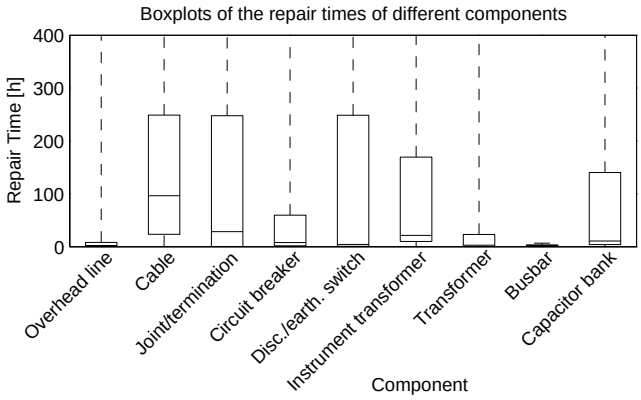

Figure B.7: Boxplots of the repair times of different system components.

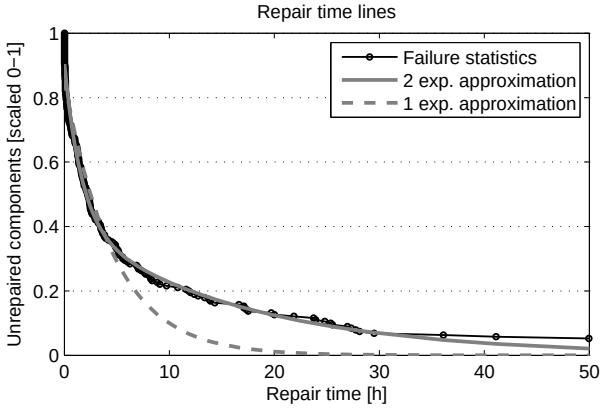

Figure B.8: Exponential approximation of the repair time of overhead lines.

The repair time can be described by a single exponential:

$$e^{-\frac{1}{T_0}} \tag{B.1}$$

Or by a combination of two exponentials:

$$c_1 \cdot e^{-\frac{1}{T_1}} + c_2 \cdot e^{-\frac{1}{T_2}} \tag{B.2}$$

Table B.4: Parameters for the exponential approximation of the repair time of different components.

Component	c_1	c_2	T_1 [h]	T_2 [h]	T_0 [h]	3rd-quartile	Average
Line	0.49	0.41	2	17	4	8	117
Cable HV	0.49	0.41	79	462	146	249	249
Joint/Termination HV	0.38	0.57	0.06	309	146	248	233
Circuit breaker	0.45	0.45	4	129	19	59	91
Disconnector / earthing switch	0.65	0.27	3	732	6	248	580
Voltage / current transformer	0.86	0.08	22	720	28	169	759
Transformer	0.45	0.45	1	41	5	23	314
Busbar					2	3	3
Capacitor bank	0.80	0.17	8	454	14	140	652
Surge arrestor					2		

C

MARKOV MODELS

MARKOV MODELS CABLE CIRCUIT FAILURES

SINGLE CIRCUIT FAILURES

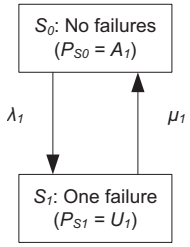

Figure C.1: Markov model of single circuit failures.

According to reliability theory [15, 16], and Markov model theory [28]:

$$P_{S_1} = U_1 = \frac{MTTR_1}{MTBF_1} = \frac{MTTR_1}{MTTF_1 + MTTR_1} = \frac{f_1 r_1}{8760} \text{ [–]} \tag{C.1}$$

$$P_{S_0} = A_1 = 1 - U_1 = 1 - \frac{f_1 r_1}{8760} \text{ [–]} \tag{C.2}$$

$$f_{S_0 \to S_1} = P_{S_0} \lambda_1 = A_1 \lambda_1 = \frac{MTTF_1}{MTBF_1} \cdot \frac{1}{MTTF_1} = \frac{1}{MTBF_1} = f_1 \text{ [–]} \tag{C.3}$$

INDEPENDENT DOUBLE CIRCUIT FAILURES

For Markov model C.3a:

$$P_{S_0} = A_1^2 = \left(\frac{MTTF_1}{MTBF_1}\right)^2 = \left(\frac{MTBF_1 - MTTR_1}{MTBF_1}\right)^2 = \left(1 - \frac{f_1 r_1}{8760}\right)^2 \text{ [–]} \tag{C.4}$$

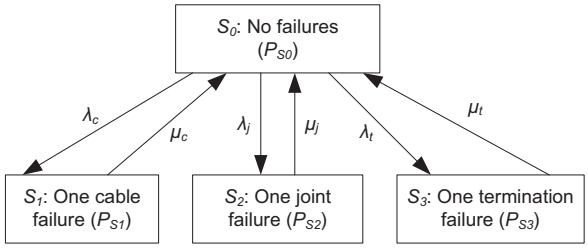

Figure C.2: Markov model of single circuit cable system failures. This model can be reduced to the two-state Markov model if the same repair time is assumed for all the cable system components. The failure rates can then be added.

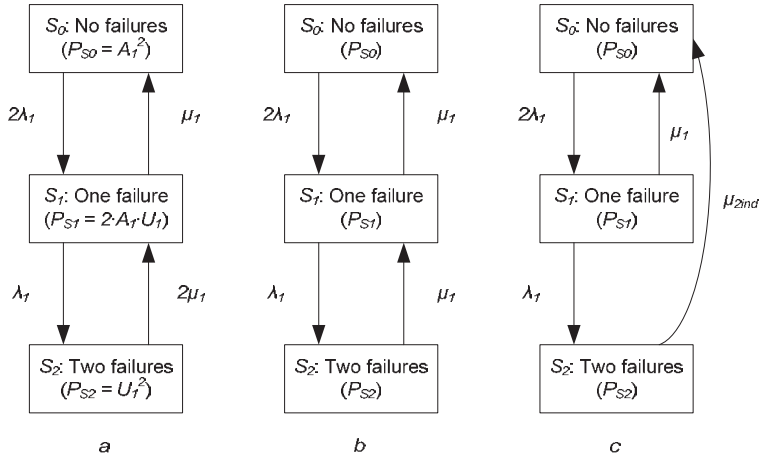

Figure C.3: Markov models for independent double circuit failures. a=independent individual repairs, b=one repair team, c=separate repair processes for independent/dependent failures. None of these represent reality perfectly well. Because of simplicity, model a is preferred.

$$P_{S_1} = \binom{2}{1} A_1 U_1 = 2 \frac{MTTF_1}{MTBF_1} \cdot \frac{MTTR_1}{MTBF_1} = 2\left(1 - \frac{f_1 r_1}{8760}\right) \frac{f_1 r_1}{8760} \; [-] \tag{C.5}$$

$$P_{S_2} = U_1^2 = \left(\frac{MTTR_1}{MTBF_1}\right)^2 = \left(\frac{f_1 r_1}{8760}\right)^2 \; [-] \tag{C.6}$$

$$f_{S_0 \to S_1} = P_{S_0} \cdot 2\lambda_1 = \left(\frac{MTTF_1}{MTBF_1}\right)^2 \cdot 2 \frac{1}{MTTF_1} = 2 \frac{1}{MTBF_1} \cdot \frac{MTTF_1}{MTBF_1} = 2 f_1 A_1 \; [-] \tag{C.7}$$

$$f_{S_1 \to S_2} = P_{S_1} \cdot \lambda_1 = \binom{2}{1} \cdot A_1 U_1 \lambda_1 = 2U_1 \cdot \frac{MTTF_1}{MTBF_1} \cdot \frac{1}{MTTF_1} =$$
$$= 2 \cdot \frac{MTTR_1}{MTBF_1} \cdot \frac{1}{MTBF_1} = 2 \cdot \frac{f_1 r_1}{8760} \cdot f_1 = \frac{2}{8760} \cdot f_1^2 r_1 = f_{2ind} \; [-] \tag{C.8}$$

Table C.1: Comparison of different Markov models for independent double circuit failures.

	Option C.3a		Option C.3b		Option C.3c	
	Line	Cable	Line	Cable	Line	Cable
$P^*_{100\%}[h/y]$	8760	8656	8760	8656	8760	8656
$P^*_{50\%}[h/y]$	0.39	103.5	0.39	103.5	0.39	102.9
$P^*_{0\%}[h/y]$	4.3e-6	0.31	8.6e-6	0.62	1.3e-5	0.92
$T_{50\%}[y]$	20.7	7.1	20.7	7.1	20.7	7.1
$T_{0\%}[y]$	9.3e5	1.2e3	9.3e5	1.2e3	9.3e5	1.2e3

The table shows the annualized probabilities of the capacity states ($P^*_{100\%}$ = both circuits available, $P^*_{50\%}$ = one circuit available and $P^*_{0\%}$ = both circuits failed, in h/y) and mean time between the states ($T_{50\%}$ and $T_{0\%}$, in [y]) using different Markov model options for an 11km double circuit cable system with the Randstad380 configuration. For option C.3c, it is assumed that the combined repair of both circuit failures takes 1.5 times the repair time of a single circuit. For the cable system, TSOs high estimate of the failure frequencies is used, a (single circuit) repair time of 730h is assumed.

DEPENDENT DOUBLE CIRCUIT FAILURES

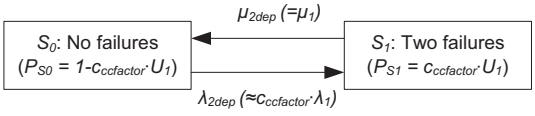

Figure C.4: Markov model for dependent double circuit failures.

Using a dependent failure factor $c_{ccfactor}$ and assuming the same repair time for both independent and dependent failures:

$$f_{2dep} = c_{ccfactor} f_1 \; [/y] \tag{C.9}$$

$$U_{2dep} = c_{ccfactor} U_1 \; [-] \tag{C.10}$$

$$A_{2dep} = 1 - U_{2dep} = 1 - c_{ccfactor} U_1 \; [-] \tag{C.11}$$

$$f_{2dep} = f_{S_0 \to S_1} = f_{S_1 \to S_0} = P_{S_1} \cdot \mu_{2dep} = U_{2dep} \cdot \mu_{2dep} \tag{C.12}$$

$$\mu_{2dep} = \frac{f_{2dep}}{U_{2dep}} = \frac{c_{ccfactor} f_1}{c_{ccfactor} U_1} = \frac{f_1}{U_1} = \frac{MTBF_1}{MTBF_1 MTTR_1} = \mu_1 \tag{C.13}$$

$$f_{2dep} = f_{S_0 \to S_1} = P_{S_0} \cdot \lambda_{2dep} = A_{2dep} \cdot \lambda_{2dep} \; [/y] \tag{C.14}$$

$$\lambda_{2dep} = \frac{f_{2dep}}{A_{2dep}} = \frac{c_{ccfactor} f_1}{1 - c_{ccfactor} U_1} = \frac{\frac{c_{ccfactor}}{MTBF_1}}{\frac{MTBF_1}{MTBF_1} - c_{ccfactor} \frac{MTTR_1}{MTBF_1}} = \\ = \frac{c_{ccfactor}}{MTBF_1 - c_{ccfactor} MTTR_1} \approx c_{ccfactor} f_1 \; [/y] \tag{C.15}$$

For $c_{ccfactor} \cdot MTTR_1 \ll MTBF_1$.

COMBINED MARKOV MODEL

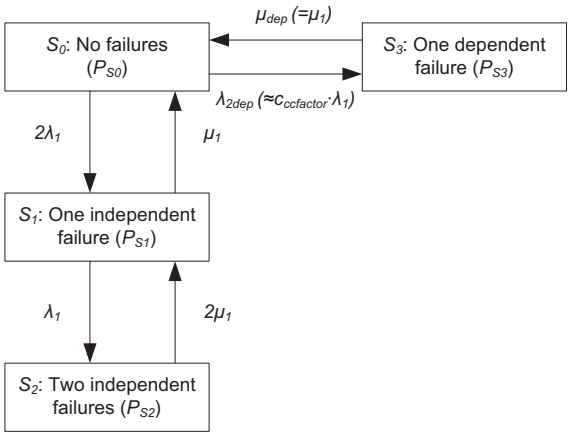

Figure C.5: Combined Markov model for failures of double circuits.

ALTERNATIVE CABLE SYSTEM CONFIGURATIONS

It is assumed that:

$$\lambda_{l1} \approx f_l \tag{C.16}$$

$$\lambda_{c1/2} \approx f_{c1/2} \tag{C.17}$$

$$\mu_l = \frac{8760}{r_l} \tag{C.18}$$

$$\mu_c = \frac{8760}{r_c} \tag{C.19}$$

$$\mu_{sw} > \mu_c > \lambda_c \tag{C.20}$$

$$\mu_{sw} \gg \lambda_c \tag{C.21}$$

SINGLE CIRCUIT CONFIGURATION 1O

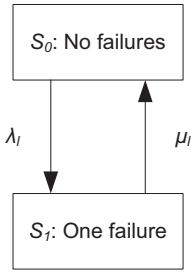

Figure C.6: Markov model of configuration 1o.

Solving the Markov model of figure C.6 gives:

$$P_{100\%} = P_{S_0} = 1 - \frac{\lambda_{l1}}{\mu_l + \lambda_{l1}} = A_{l1}\ [-] \tag{C.22}$$

$$P_{0\%} = P_{S_1} = \frac{\lambda_{l1}}{\mu_l + \lambda_{l1}} = \frac{\frac{1}{MTTF_{l1}}}{\frac{1}{MTTR_l} + \frac{1}{MTTF_{l1}}} = \frac{MTTR_l}{MTBF_{l1}} = f_l \cdot \frac{r_l}{8760} = U_l\ [-] \tag{C.23}$$

$$T_{0\%} = T_{S_0 \to S_1} = \frac{1}{P_{S_0} \cdot \lambda_{l1}} = \frac{1}{\left(1 - \frac{\lambda_{l1}}{\mu_l + \lambda_{l1}}\right) \cdot \lambda_{l1}} = \frac{\mu_l + \lambda_{l1}}{\lambda_{l1} \cdot \mu_l} =$$
$$= \frac{\frac{1}{MTTR_l} + \frac{1}{MTTR_l}}{\frac{1}{MTTR_l \cdot MTTF_{l1}}} = MTTF_{l1} + MTTR_l = MTBF_{l1} = \frac{1}{f_l}\ [y] \tag{C.24}$$

$$r_{0 \to 100\%} = \frac{8760}{\mu_l} = r_l\ [h] \tag{C.25}$$

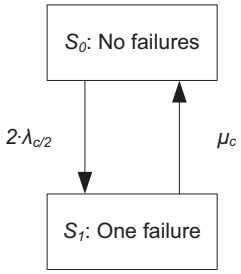

Figure C.7: Markov model of configuration 1a.

SINGLE CIRCUIT CONFIGURATION 1A

Solving the Markov model of figure C.7 gives:

$$P_{0\%} = P_{S_1} = \frac{2\lambda_{c1/2}}{\mu_c + 2\lambda_{c1/2}} = \frac{\frac{2}{MTTF_{c1/2}}}{\frac{1}{MTTR_c} + \frac{2}{MTTF_{c1/2}}} = \frac{2 \cdot MTTR_c}{MTBF_{c1/2} + MTTR_c} \approx$$

$$\approx \frac{2 \cdot MTTR_c}{MTBF_{c1/2}} = 2f_{c1/2} \cdot \frac{r_c}{8760} = 2U_{c1/2} = U_c\ [-] \quad \text{(C.26)}$$

$$T_{0\%} = T_{S_0 \to S_1} = \frac{1}{P_{S_0} \cdot 2\lambda_{c1/2}} \approx \frac{1}{2f_{c1/2}} = \frac{1}{f_c}\ [y] \quad \text{(C.27)}$$

$$r_{0 \to 100\%} = \frac{8760}{\mu_c} = r_c\ [h] \quad \text{(C.28)}$$

SINGLE CIRCUIT CONFIGURATION 1B

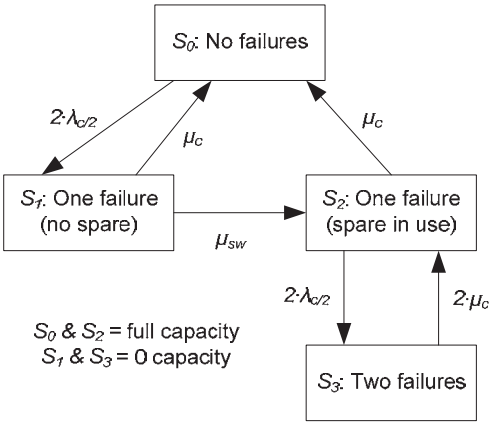

Figure C.8: Markov model of configuration 1b.

Solving the Markov model of figure C.8 gives:

$$P_{0\%} = P_{S_1} + P_{S_3}\ [-] \quad \text{(C.29)}$$

$$T_{0\%} = \frac{1}{f_{S_0 \to S_1} + f_{S_2 \to S_3}} = \frac{1}{P_{S_0} \cdot 2\lambda_{c1/2} + P_{S_2} \cdot 2\lambda_{c1/2}} \; [y] \tag{C.30}$$

$$r_{0 \to 100\%} = 8760 \cdot \frac{P_{S_1} \cdot \frac{1}{\mu_{sw} + \mu_c} + P_{S_3} \cdot \frac{1}{2\mu_c}}{P_{S_1} + P_{S_3}} \; [h] \tag{C.31}$$

SINGLE CIRCUIT CONFIGURATION 1C

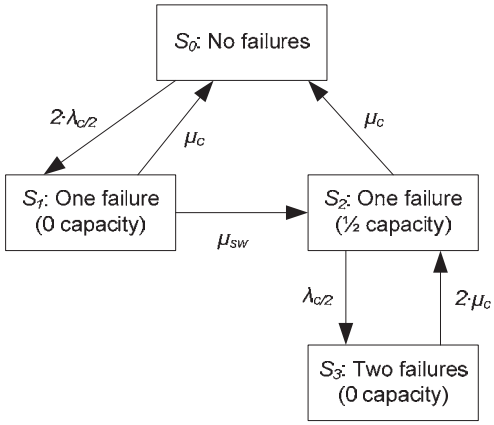

Figure C.9: Markov model of configuration 1c.

Solving the Markov model of figure C.9 gives:

$$P_{50\%} = P_{S_2} \; [-] \tag{C.32}$$

$$P_{0\%} = P_{S_1} + P_{S_3} \; [-] \tag{C.33}$$

$$T_{50\%} = T_{S_1 \to S_2} = \frac{1}{P_{S_1} \cdot \mu_{sw}} \; [y] \tag{C.34}$$

$$T_{0\%} = \frac{1}{f_{S_0 \to S_1} + f_{S_2 \to S_3}} = \frac{1}{P_{S_0} \cdot 2\lambda_{c1/2} + P_{S_2} \cdot \lambda_{c1/2}} \; [y] \tag{C.35}$$

$$r_{0 \to 100\%} = r_{S_1 \to S_0} = 8760 \cdot \frac{1}{\mu_c} = r_c \; [h] \tag{C.36}$$

$$r_{50 \to 100\%} = r_{S_2 \to S_0} = 8760 \cdot \frac{1}{\mu_c} = r_c \; [h] \tag{C.37}$$

$$r_{0 \to 50\%} = \frac{P_{S_1} \cdot r_{S_1 \to S_2} + P_{S_3} \cdot r_{S_3 \to S_2}}{P_{S_1} + P_{S_3}} = 8760 \cdot \frac{P_{S_1} \cdot \frac{1}{\mu_{sw}} + P_{S_3} \cdot \frac{1}{2\mu_c}}{P_{S_1} + P_{S_3}} \; [h] \tag{C.38}$$

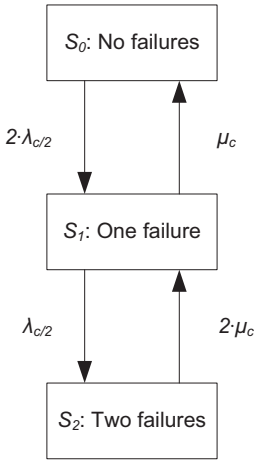

Figure C.10: Markov model of configuration 1d.

SINGLE CIRCUIT CONFIGURATION 1D

Solving the Markov model of figure C.10 gives:

$$P_{50\%} = P_{S_1}\ [-] \tag{C.39}$$

$$P_{0\%} = P_{S_2}\ [-] \tag{C.40}$$

$$T_{50\%} = T_{S_0 \to S_1} = \frac{1}{P_{S_0} \cdot 2\lambda_{c1/2}}\ [y] \tag{C.41}$$

$$T_{0\%} = T_{S_1 \to S_2} = \frac{1}{P_{S_1} \cdot 2\lambda_{c1/2}}\ [y] \tag{C.42}$$

$$r_{50\to 100\%} = r_{S_1 \to S_0} = 8760 \cdot \frac{1}{\mu_c} = r_c\ [h] \tag{C.43}$$

$$r_{0\to 50\%} = r_{S_2 \to S_1} = 8760 \cdot \frac{1}{2\mu_c} = \frac{1}{2} r_c\ [h] \tag{C.44}$$

DOUBLE CIRCUIT CONFIGURATION 2O

Solving the Markov model of figure C.11 gives:

$$P_{50\%} = P_{S_1} = 2 \cdot U_l \cdot A_{l1} = 2 \cdot \left(f_l \cdot \frac{r_l}{8760}\right) \cdot \left(1 - f_l \cdot \frac{r_l}{8760}\right)\ [-] \tag{C.45}$$

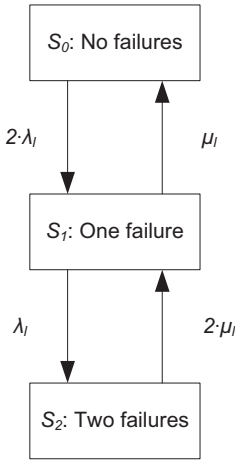

Figure C.11: Markov model of configuration 2o.

$$P_{0\%} = P_{S_2} = U_l^2 = \left(f_l \cdot \frac{r_l}{8760}\right)^2 \ [-] \tag{C.46}$$

$$T_{50\%} = T_{S_0 \to S_1} = \frac{1}{P_{S_0} \cdot 2\lambda_{l1}} \ [y] \tag{C.47}$$

$$T_{0\%} = T_{S_1 \to S_2} = \frac{1}{P_{S_1} \cdot \lambda_{l1}} \ [y] \tag{C.48}$$

$$r_{50 \to 100\%} = r_{S_1 \to S_0} = 8760 \cdot \frac{1}{\mu_l} = r_l \ [h] \tag{C.49}$$

$$r_{0 \to 50\%} = r_{S_2 \to S_1} = 8760 \cdot \frac{1}{2\mu_l} = \frac{1}{2} r_l \ [h] \tag{C.50}$$

DOUBLE CIRCUIT CONFIGURATION 2A

Solving the Markov model of figure C.12 gives:

$$P_{50\%} = P_{S_1} \ [-] \tag{C.51}$$

$$P_{0\%} = P_{S_2} \ [-] \tag{C.52}$$

$$T_{50\%} = T_{S_0 \to S_1} = \frac{1}{P_{S_0} \cdot 4\lambda_{c1/2}} \ [y] \tag{C.53}$$

$$T_{0\%} = T_{S_1 \to S_2} = \frac{1}{P_{S_1} \cdot 2\lambda_{c1/2}} \ [y] \tag{C.54}$$

$$r_{50 \to 100\%} = r_{S_1 \to S_0} = 8760 \cdot \frac{1}{\mu_c} = r_c \ [h] \tag{C.55}$$

$$r_{0 \to 50\%} = r_{S_2 \to S_1} = 8760 \cdot \frac{1}{2\mu_c} = \frac{1}{2} r_c \ [h] \tag{C.56}$$

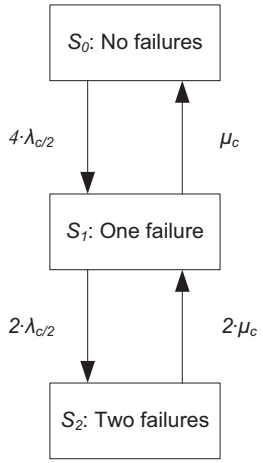

Figure C.12: Markov model of configuration 2a.

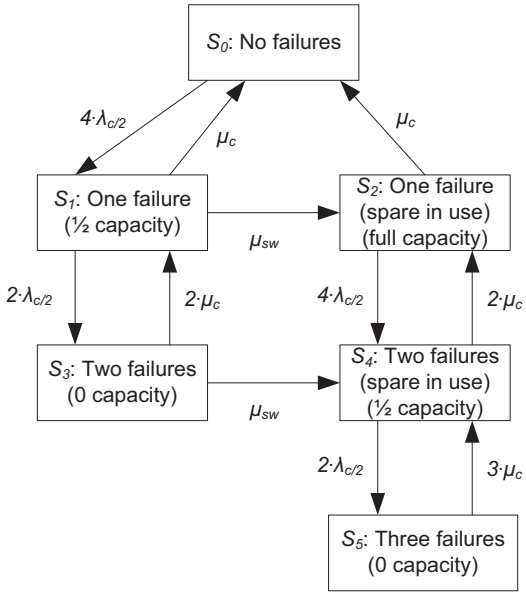

Figure C.13: Markov model of configuration 2b.

DOUBLE CIRCUIT CONFIGURATION 2B

Solving the Markov model of figure C.13 gives:

$$P_{50\%} = P_{S_1} + P_{S_4}\ [-] \tag{C.57}$$

$$P_{0\%} = P_{S_4} + P_{S_6}\ [-] \tag{C.58}$$

$$T_{50\%} = \frac{1}{f_{S_0 \to S_1} + f_{S_2 \to S_4}} = \frac{1}{(P_{S_0} + P_{S_2}) \cdot 4\lambda_{c1/2}}\ [y] \tag{C.59}$$

$$T_{0\%} = \frac{1}{f_{S_1 \to S_3} + f_{S_4 \to S_5}} = \frac{1}{(P_{S_1} + P_{S_4}) \cdot 2\lambda_{c1/2}}\ [y] \tag{C.60}$$

$$r_{50 \to 100\%} = 8760 \cdot \frac{P_{S_1} \cdot \frac{1}{\mu_c + \mu_{sw}} + P_{S_4} \cdot \frac{1}{2\mu_c}}{P_{S_1} + P_{S_4}}\ [h] \tag{C.61}$$

$$r_{0 \to 50\%} = 8760 \cdot \frac{P_{S_3} \cdot \frac{1}{2\mu_c + \mu_{sw}} + P_{S_5} \cdot \frac{1}{3\mu_c}}{P_{S_3} + P_{S_5}}\ [h] \tag{C.62}$$

DOUBLE CIRCUIT CONFIGURATION 2C

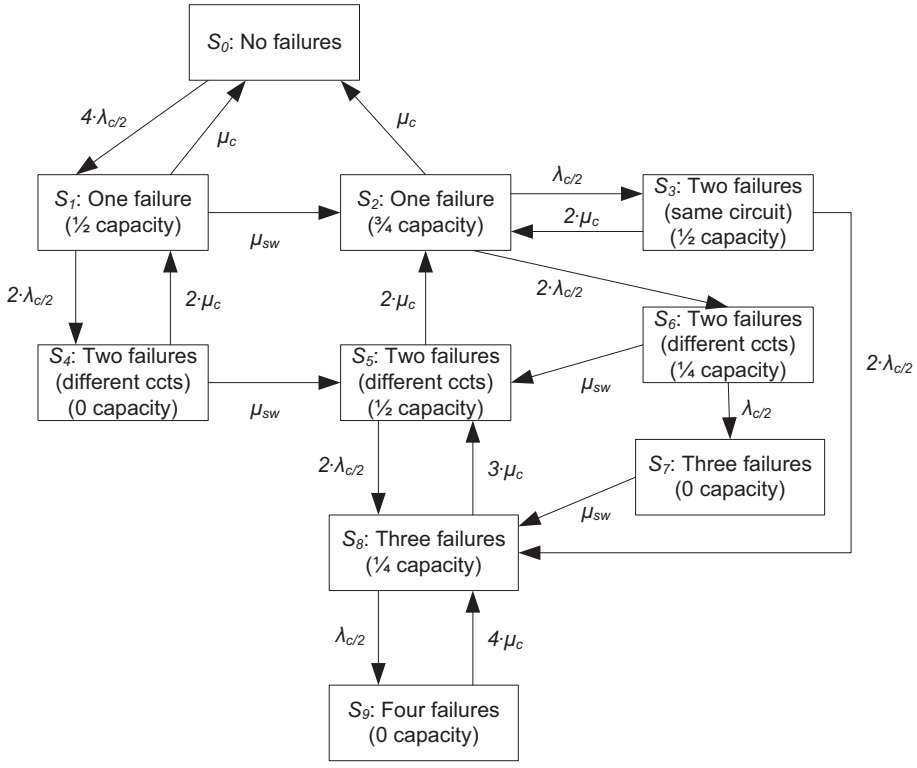

Figure C.14: Markov model of configuration 2c.

Solving the Markov model of figure C.14 gives:

$$P_{75\%} = P_{S_2}\ [-] \tag{C.63}$$
$$P_{50\%} = P_{S_1} + P_{S_3} + P_{S_5}\ [-] \tag{C.64}$$
$$P_{25\%} = P_{S_6} + P_{S_8}\ [-] \tag{C.65}$$
$$P_{0\%} = P_{S_4} + P_{S_7} + P_{S_9}\ [-] \tag{C.66}$$
$$T_{75\%} = T_{S_2 \to S_0} = \frac{1}{P_{S_2} \cdot \mu_c}\ [y] \tag{C.67}$$
$$T_{50\%} = \frac{1}{f_{S_0 \to S_1} + f_{S_2 \to S_3}} = \frac{1}{P_{S_0} \cdot 4\lambda_{c1/2} + P_{S_2} \cdot \lambda_{c1/2}}\ [y] \tag{C.68}$$
$$T_{25\%} = \frac{1}{f_{S_2 \to S_6} + f_{S_3 \to S_8}} = \frac{1}{(P_{S_2} + P_{S_3}) \cdot 2\lambda_{c1/2}}\ [y] \tag{C.69}$$

$$T_{0\%} = \frac{1}{f_{S_1 \to S_4} + f_{S_6 \to S_7} + f_{S_8 \to S_9}} = \frac{1}{P_{S_1} \cdot 2\lambda_{c1/2} + (P_{S_6} + P_{S_8}) \cdot \lambda_{c1/2}}\ [y] \tag{C.70}$$

$$r_{75 \to 100\%} = r_{S_2 \to S_0} = \frac{1}{\mu_c} = r_c\ [h] \tag{C.71}$$

$$r_{half \to 3/4} = \frac{P_{S_1} \cdot r_{S_1 \to S_2} + P_{S_3} \cdot r_{S_3 \to S_2} + P_{S_5} \cdot r_{S_5 \to S_2}}{P_{S_1} + P_{S_3} + P_{S_5}} = \\ = 8760 \cdot \frac{P_{S_1} \cdot \frac{1}{\mu_{sw}} + (P_{S_3} + P_{S_5}) \cdot \frac{1}{2\mu_c}}{P_{S_1} + P_{S_3} + P_{S_5}}\ [h] \tag{C.72}$$

$$r_{25 \to 50\%} = \frac{P_{S_6} \cdot r_{S_6 \to S_5} + P_{S_8} \cdot r_{S_8 \to S_5}}{P_{S_6} + P_{S_8}} = 8760 \cdot \frac{P_{S_6} \cdot \frac{1}{\mu_{sw}} + P_{S_8} \cdot \frac{1}{3\mu_c}}{P_{S_6} + P_{S_8}}\ [h] \tag{C.73}$$

$$r_{0 \to 25\%} = \frac{P_{S_7} \cdot r_{S_7 \to S_8} + P_{S_9} \cdot r_{S_9 \to S_8}}{P_{S_7} + P_{S_9}} = 8760 \cdot \frac{P_{S_7} \cdot \frac{1}{\mu_{sw}} + P_{S_9} \cdot \frac{1}{4\mu_c}}{P_{S_7} + P_{S_9}}\ [h] \tag{C.74}$$

DOUBLE CIRCUIT CONFIGURATION 2D

Solving the Markov model of figure C.15 gives:

$$P_{75\%} = P_{S_1}\ [-] \tag{C.75}$$
$$P_{50\%} = P_{S_2}\ [-] \tag{C.76}$$
$$P_{25\%} = P_{S_3}\ [-] \tag{C.77}$$
$$P_{0\%} = P_{S_4}\ [-] \tag{C.78}$$

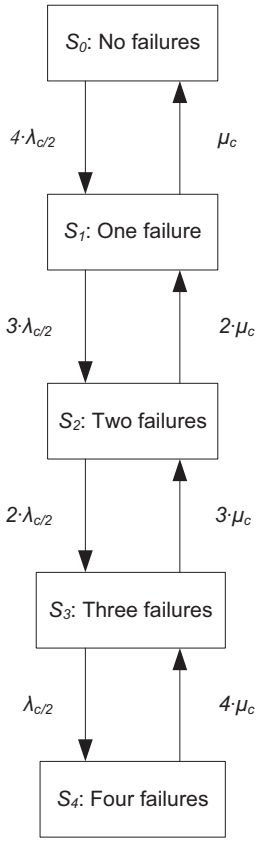

Figure C.15: Markov model of configuration 2d.

$$T_{75\%} = T_{S_0 \to S_1} = \frac{1}{P_{S_0} \cdot 4\lambda_{c1/2}} \; [y] \tag{C.79}$$

$$T_{50\%} = T_{S_1 \to S_2} = \frac{1}{P_{S_1} \cdot 3\lambda_{c1/2}} \; [y] \tag{C.80}$$

$$T_{25\%} = T_{S_2 \to S_3} = \frac{1}{P_{S_2} \cdot 2\lambda_{c1/2}} \; [y] \tag{C.81}$$

$$T_{0\%} = T_{S_3 \to S_4} = \frac{1}{P_{S_3} \cdot \lambda_{c1/2}} \; [y] \tag{C.82}$$

$$r_{75 \to 100\%} = r_{S_1 \to S_0} = 8760 \cdot \frac{1}{\mu_c} = r_c \; [h] \tag{C.83}$$

$$r_{50 \to 75\%} = r_{S_2 \to S_1} = 8760 \cdot \frac{1}{2\mu_c} = \frac{1}{2} r_c \; [h] \tag{C.84}$$

$$r_{25 \to 50\%} = r_{S_3 \to S_2} = 8760 \cdot \frac{1}{3\mu_c} = \frac{1}{3} r_c \; [h] \tag{C.85}$$

$$r_{0 \to 25\%} = r_{S_4 \to S_3} = 8760 \cdot \frac{1}{4\mu_c} = \frac{1}{4} r_c \; [h] \tag{C.86}$$

D

MATHEMATICAL SYSTEM STATE MODEL

This model is based on several assumptions:

- For the components, failure frequencies and repair times are used. Both the failure process and the repair process follow the single exponential distribution.
- The system is assumed to consist of double circuits only.
- The purpose of this study is to analyze the probability and Mean Time Between Failures of various order contingencies. The consequences for the load flow in the system are not considered. Therefore, the actual topology of the system does not have any influence on the results of the calculations.
- Both independent failures and dependent double circuit failures are considered. The dependent failure factor $c_{ccfactor}$ is used. Other kinds of dependent failures, like cascading failures or higher-order dependent failures, are not considered.

For the calculations, a (partial) Markov model will be developed that describes the failure states of the transmission system. Two properties of Markov models will be used to determine the probabilities and the transition frequencies of the system states.

The probability of a particular system state is the product of the (independent and dependent) unavailabilities of the components. For example, if component j and k have failed independently, the probability of this system state can be calculated as:

$$P_{S_{j,k,ind}} = \left(A_1 A_2 ... A_{j-1} U_j A_{j+1} ... A_{k-1} U_k A_{k+1} ... A_N\right) \cdot P_{S_{0dep}} =$$
$$= U_k \cdot U_j \cdot \prod_{i=1,2...\neq(k,j)}^{N} (A_i) \cdot P_{S_{0dep}} \; [-] \tag{D.1}$$

Where:

$P_{S_{j,k,ind}}$ = probability of state: j and k failed independently [-]
A_i = availability of component i [-]
U_i = unavailability of component i [-]
N = number of components in the system [-]
$P_{S_{0dep}}$ = probability of having no dependent failures [-]

The second property of Markov models is that the transition frequency of the system states can be calculated from the system state probabilities and the failure frequencies of the components. For example, if from the previous state component l also fails independently, the transition frequency can be calculated as:

$$f_{S_{j,k,ind} \rightarrow S_{j,k,l,ind}} = P_{S_{j,k,ind}} \cdot \lambda_l \approx P_{S_{j,k,ind}} \cdot f_l$$
$$\approx U_k \cdot U_j \cdot \prod_{i=1,2...\neq(k,j)}^{N} (A_i) \cdot P_{0dep} \cdot f_l \; [/y] \tag{D.2}$$

Where:
$f_{S_{j,k,ind} \rightarrow S_{j,k,l,ind}}$ = transition frequency from state $S_{j,k,ind}$ to state $S_{j,k,l,ind}$ [/y]
λ_l = failure rate of component l [/y]
f_l = failure frequency of component l [/y]
Using $\lambda_l \approx f_l$.

Using these properties, a partial Markov model can be created as shown in figure D.1. The upper state is the normal operation state in which there are no component failures.

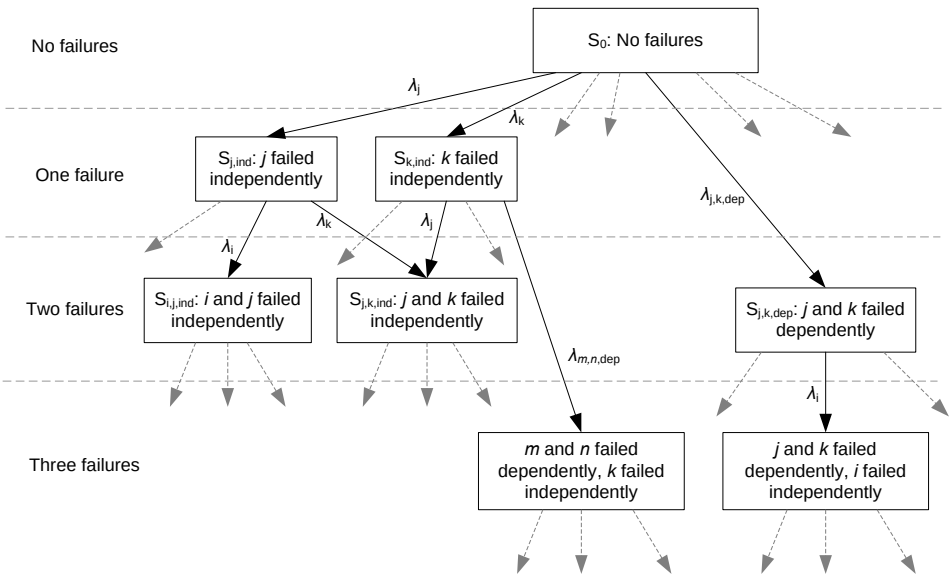

Figure D.1: A part of the Markov model used to calculate the amount of component failures.

From this normal operation state, components can fail independently (like components *j* and *k* in the figure), which leads to one failure in the network. Combinations of independent failures (like *i,j* and *j,k* in the figure) lead to two failures within the network.

Dependent component failures are also possible. This is shown on the right in the figure (for components *j* and *k*). A dependent failure directly leads to two failures within the network. As only dependent double circuit failures are considered, in the figure it is assumed that components *j* and *k* are a double circuit.

As can be seen, combinations of independent and dependent failures can occur as well. This will lead to three component failures within the network. Moreover, combinations of two dependent failures are also possible, leading to four component failures within the network.

As indicated in the figure, the amount of failure states increases dramatically for the higher-order failure states. Therefore, only the upper levels of the Markov model are considered in the further studies.

The state model is also illustrated in figure D.2. On the left, an overview of the considered contingency levels (up to 4 failures) is shown. On the right, the classification into independent and dependent failure states is shown.

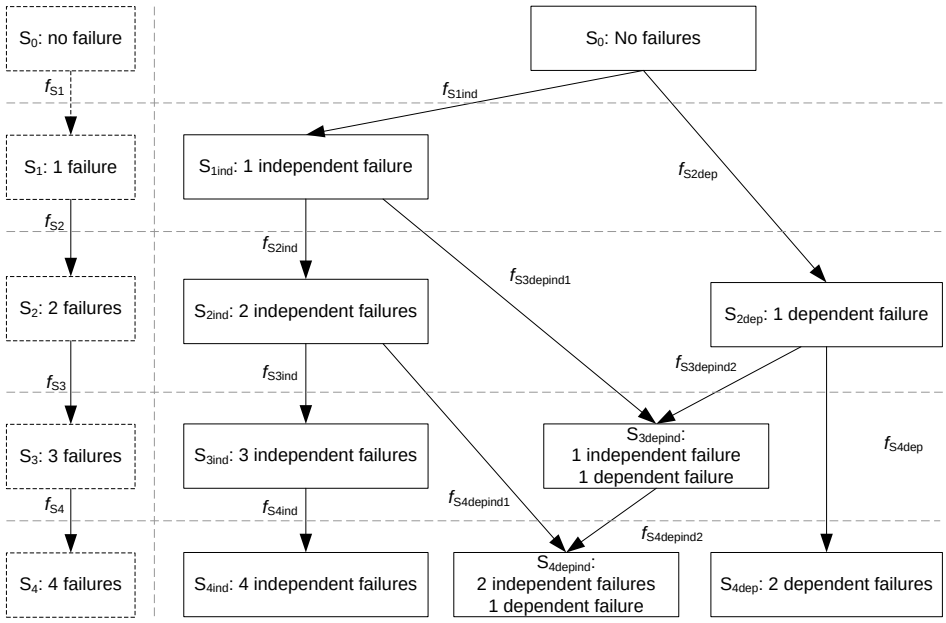

Figure D.2: State model used to calculate the amount of failures. The state model shown on the right is a simplified version of the Markov model used to calculate the state probabilities and transition frequencies of independent and dependent component failures. The model on the left is a further simplification, indicating only the states with 1,2, etc. component failures and the corresponding transition frequencies.

According to the mathematical model, some states are excluded. For example, the independent failures of component j and the dependent failure of components j and k are omitted. In reality, this system state is not possible because after a component failure, the component is disconnected from the system and can not fail anymore. In the mathematical model, the probability of this state is ascribed to the probability of the dependent failure of components j and k.

In the following calculations:

P_{S_0} = probability of no failures in the network [-]
P_{S_n} = probability of state n (n failures in the network) [-]
$P_{S_{nind}}$ = probability of n independent failures [-]
$P_{S_{ndep}}$ = probability of n dependent failures [-]
$P_{S_{3depind}}$ = probability of 1 dependent and 1 independent failure (3 failures) [-]
$P_{S_{4depind}}$ = probability of 1 dependent and 2 independent failures (4 failures) [-]
N = components in the system [-]
f_{S_n} = transition frequency of state n [/y]

If the reliability of every component in the system is described by:

$A_i = 1 - U_i$ = availability of component i [-]
$U_i = f_i \cdot \frac{r_i}{8760}$ = unavailability of component i [-]
f_i = failure frequency of component i [/y]
r_i = repair time of component i [h]
c_{cc} = dependent failure factor [-]

Then, the probabilities of the system states can be described by:

$$P_{S_0} = P_{S_{0ind}} \cdot P_{S_{0dep}} \ [-] \tag{D.3}$$

$$P_{S_1} = P_{S_{1ind}} \ [-] \tag{D.4}$$

$$P_{S_2} = P_{S_{2ind}} + P_{S_{2dep}} \ [-] \tag{D.5}$$

$$P_{S_3} = P_{S_{3ind}} + P_{S_{3depind}} \ [-] \tag{D.6}$$

$$P_{S_4} = P_{S_{4ind}} + P_{S_{4depind}} + P_{S_{4dep}} \ [-] \tag{D.7}$$

$$P_{S_{0ind}} = \prod_{i=1}^{N} (A_i) \ [-] \tag{D.8}$$

$$P_{S_{1ind}} = \sum_{j=1}^{N} \left(U_j \prod_{i=1,2...\neq j}^{N} (A_i) \right) P_{S_{0dep}} \ [-] \tag{D.9}$$

$$P_{S_{2ind}} = \sum_{k=2}^{N} \left(\sum_{j=1}^{k-1} \left(U_k U_j \prod_{i=1,2...\neq (k,j)}^{N} (A_i) \right) \right) P_{S_{0dep}} \ [-] \tag{D.10}$$

$$P_{S_{3ind}} = \sum_{l=3}^{N} \left(\sum_{k=2}^{l-1} \left(\sum_{j=1}^{k-1} \left(U_l U_k U_j \prod_{i=1,2...\neq (l,k,j)}^{N} (A_i) \right) \right) \right) P_{S_{0dep}} \ [-] \tag{D.11}$$

$$P_{S_{4ind}} = \sum_{m=4}^{N} \left(\sum_{l=3}^{m-1} \left(\sum_{k=2}^{l-1} \left(\sum_{j=1}^{k-1} \left(U_m U_l U_k U_j \prod_{i=1,2\ldots\neq(m,l,k,j)}^{N} (A_i) \right) \right) \right) \right) P_{S_{0dep}} \ [-] \tag{D.12}$$

$$P_{S_{0dep}} = \prod_{i=1,3\ldots}^{N-1} (1 - c_{cc} U_i) \ [-] \tag{D.13}$$

$$P_{S_{2dep}} = \sum_{j=1,3\ldots}^{N-1} \left(c_{cc} U_j \prod_{i=1,3\ldots\neq j}^{N-1} (1 - c_{cc} U_i) \right) \cdot P_{S_{0ind}} \ [-] \tag{D.14}$$

$$P_{S_{4dep}} = \sum_{k=1,3\ldots}^{N-1} \left(\sum_{j=1,3\ldots}^{k-2} \left(c_{cc} U_k c_{cc} U_j \prod_{i=1,3\ldots\neq(k,j)}^{N-1} (1 - c_{cc} U_i) \right) \right) P_{S_{0ind}} \ [-] \tag{D.15}$$

$$P_{S_{3depind}} = \sum_{l=1,3\ldots}^{N-1} \left(\sum_{k=1\neq(l,l+1)}^{N} \left(c_{cc} U_l U_k \prod_{j=1,3,\ldots}^{N-1} (1 - c_{cc} U_j) \prod_{i=1}^{N} (A_i) \right) \right) \ [-] \tag{D.16}$$

$$P_{S_{4depind}} = \sum_{m=1,3\ldots}^{N-1} \left(\sum_{l=2\neq(m,m+1)}^{N} \left(\sum_{k=1\neq(m,m+1)}^{l-1} (c_{cc} U_m U_l U_k \cdot \right. \right. \\ \left. \left. \cdot \prod_{j=1,3,\ldots}^{N-1} (1 - c_{cc} U_j) \prod_{i=1}^{N} (A_i)) \right) \right) \tag{D.17}$$

The state transition frequencies then can be calculated as:

$$f_{S_1} = P_{S_0} \sum_{i=1}^{N} (f_i) \ [/y] \tag{D.18}$$

$$f_{S_2} = f_{S_{2ind}} + f_{S_{2dep}} \ [/y] \tag{D.19}$$

$$f_{S_3} = f_{S_{3ind}} + f_{S_{3depind1}} + f_{S_{3depind2}} \ [/y] \tag{D.20}$$

$$f_{S_4} = f_{S_{4ind}} + f_{S_{4depind1}} + f_{S_{4depind2}} + f_{S_{4dep}} \ [/y] \tag{D.21}$$

$$f_{S_{2ind}} = \sum_{j=1}^{N} \left(U_j \prod_{i=1,2\ldots\neq j}^{N} (A_i) P_{S_{0dep}} \sum_{k=1\neq j}^{N} (f_k) \right) \ [/y] \tag{D.22}$$

$$f_{S_{3ind}} = \sum_{k=2}^{N} \left(\sum_{j=1}^{k-1} \left(U_k U_j \prod_{i=1,2\ldots\neq(k,j)}^{N} (A_i) P_{S_{0dep}} \sum_{l=1\neq(j,k)}^{N} (f_l) \right) \right) \ [/y] \tag{D.23}$$

$$f_{S_{4ind}} = \sum_{l=3}^{N} \left(\sum_{k=2}^{l-1} \left(\sum_{j=1}^{k-1} \left(U_l U_k U_j \prod_{i=1,2\ldots\neq(l,k,j)}^{N} (A_i) P_{S_{0dep}} \sum_{m=1\neq(j,k,l)}^{N} (f_m) \right) \right) \right) \ [/y] \tag{D.24}$$

$$f_{S_{2dep}} = P_{S_0} \sum_{i=1,3\ldots}^{N-1} (c_{cc} f_i) \ [/y] \tag{D.25}$$

$$f_{S_{4dep}} = \sum_{j=1,3\ldots}^{N-1} \left(c_{cc} U_j \prod_{i=1,3\ldots\neq j}^{N-1} (1 - c_{cc} U_i) P_{S_{0ind}} \sum_{k=1,3\ldots\neq j}^{N-1} (c_{cc} f_k) \right) \ [/y] \tag{D.26}$$

$$f_{S_{3depind1}} = \sum_{j=1}^{N} \left(U_j \prod_{i=1,2...\neq j}^{N} (A_i)\, P_{S_{0dep}} \sum_{k=1,3...\neq(j,j-1)}^{N-1} (c_{cc} f_k) \right) [/y] \tag{D.27}$$

$$f_{S_{3depind2}} = \sum_{j=1,3...}^{N-1} \left(c_{cc} U_j \prod_{i=1,3...\neq j}^{N-1} (1 - c_{cc} U_i)\, P_{S_{0ind}} \sum_{k=1,2...\neq(j,j+1)}^{N} (f_k) \right) [/y] \tag{D.28}$$

$$f_{S_{4depind1}} = \sum_{k=2}^{N} \left(\sum_{j=1}^{k-1} \left(U_k U_j \prod_{i=1,2...\neq(k,j)}^{N} (A_i)\, P_{S_{0dep}} \sum_{l=1,3...\neq(j,j-1,k,k-1)}^{N-1} (c_{cc} f_l) \right) \right) [/y] \tag{D.29}$$

$$f_{S_{4depind2}} = \sum_{l=1,3...}^{N-1} \left(\sum_{k=1\neq(l,l+1)}^{N} \left(c_{cc} U_l U_k \prod_{j=1,3,...}^{N-1} \left(1 - c_{cc} U_j\right) \prod_{i=1}^{N} (A_i) \sum_{m=1,2...\neq(k,l,l+1)}^{N} (f_m) \right) \right) \tag{D.30}$$

And the Mean Time Between Failures becomes:

$$MTBF_{S_n} = \frac{1}{f_{S_n}} [y] \tag{D.31}$$

Although the model described above is used for the calculations in this report, an approximation of this model can be made as well. If an average component failure frequency of f_{av} and an average unavailability of U_{av} are assumed, the state probabilities can be approximated by:

$$P_{S_{0ind}} = (1 - U_{av})^N [-] \tag{D.32}$$

$$P_{S_{1ind}} = N U_{av} (1 - U_{av})^{N-1} \cdot P_{S_{0dep}} [-] \tag{D.33}$$

$$P_{S_{2ind}} = \binom{N}{2} U_{av}^2 (1 - U_{av})^{N-2} \cdot P_{S_{0dep}} [-] \tag{D.34}$$

$$P_{S_{3ind}} = \binom{N}{3} U_{av}^3 (1 - U_{av})^{N-3} \cdot P_{S_{0dep}} [-] \tag{D.35}$$

$$P_{S_{4ind}} = \binom{N}{4} U_{av}^4 (1 - U_{av})^{N-4} \cdot P_{S_{0dep}} [-] \tag{D.36}$$

$$P_{S_{0dep}} = (1 - c_{cc} U_{av})^{N/2} [-] \tag{D.37}$$

$$P_{S_{2dep}} = (N/2) c_{cc} U_{av} (1 - c_{cc} U_{av})^{N/2-1} \cdot P_{S_{0ind}} [-] \tag{D.38}$$

$$P_{S_{4dep}} = \binom{N/2}{2} (c_{cc} U_{av})^2 (1 - c_{cc} U_{av})^{N/2-2} \cdot P_{S_{0ind}} [-] \tag{D.39}$$

$$P_{S_{3depind}} = (N-2)(N/2-1) U_{av} (1 - U_{av})^{N-1} \cdot (c_{cc} U_{av}) (1 - c_{cc} U_{av})^{N/2-1} [-] \tag{D.40}$$

$$P_{S_{4depind}} = \binom{N-2}{2} (N/2-2) U_{av}^2 (1 - U_{av})^{N-2} \cdot (c_{cc} U_{av}) (1 - c_{cc} U_{av})^{N/2-1} [-] \tag{D.41}$$

With this approximation, the increase in probabilities of independent contingencies for more unreliable components (or larger systems) can now be clarified by the large amount of combinations of these states.

The state transition frequencies now become:

$$f_{S_1} = P_{S_0} N f_{av} \ [/y] \tag{D.42}$$
$$f_{S_{2ind}} = P_{S_{1ind}} (N-1) f_{av} \ [/y] \tag{D.43}$$
$$f_{S_{3ind}} = P_{S_{2ind}} (N-2) f_{av} \ [/y] \tag{D.44}$$
$$f_{S_{4ind}} = P_{S_{3ind}} (N-3) f_{av} \ [/y] \tag{D.45}$$
$$f_{S_{2dep}} = P_{S_0} (N/2) c_{cc} f_{av} \ [/y] \tag{D.46}$$
$$f_{S_{4dep}} = P_{S_{2dep}} (N/2-1) c_{cc} f_{av} \ [/y] \tag{D.47}$$
$$f_{S_{3depind1}} = P_{S_{1ind}} (N/2-1) c_{cc} f_{av} \ [/y] \tag{D.48}$$
$$f_{S_{3depind2}} = P_{S_{2dep}} (N-2) f_{av} \ [/y] \tag{D.49}$$
$$f_{S_{4depind1}} = P_{S_{2ind}} (N/2-2) c_{cc} f_{av} \ [/y] \tag{D.50}$$
$$f_{S_{4depind2}} = P_{S_{3depind}} (N-3) f_{av} \ [/y] \tag{D.51}$$

BIBLIOGRAPHY

BIBLIOGRAPHY

[1] K. B. Klaassen, J. C. L. van Peppen, and A. Bossche, *Bedrijfszekerheid, theorie en techniek*. Delft: Delftse Uitgevers Maatschappij, 1988.

[2] European Commission on Climate Action, "2020 Climate and Energy Package." Available online at: http://ec.europa.eu/ (last accessed: 2014), 2009.

[3] European Commission on Climate Action, "Vision and Strategy for European Electricity Networks for the Future." Available online at: http://ec.europa.eu/ (last accessed: 2014), 2006.

[4] M. A. M. M. van der Meijden, "A sustainable and reliable electricity system; Inevitable and challenging. (Inauguration speech)." Delft University of Technology, Netherlands, 2012.

[5] Ecofys, "2045 outlook and implications for offshore wind in the North Seas - ," tech. rep., Ecofys (by order of TenneT and Energinet), 2017.

[6] EWEA, European Wind Energy Association, "Wind Energy Scenarios for 2030." Available online at: https://www.ewea.org/.../EWEA-Wind-energy-scenarios-2030.pdf (last accessed: 2017), 2015.

[7] D. Hass, G. Pels Leusden, J. Schwarz, and H. Zimmermann, "Das (n-1)-Kriterium in der Planung von Übertragungsnetzen," *Elektrizitätswirtschaft*, vol. 80 no.25, 1981.

[8] J. de Decker, A. Woyte, B. Schödwell, J. Völker, and C. Srikandam, "Directory of Offshore Grid Initiatives, Studies & Organisations," tech. rep., OffshoreGrid, 2009.

[9] TenneT TSO, Ministries of EZ and I&M, "Randstad380 project website." Available online at: http://www.randstad380kv.nl/, 2015.

[10] L. Wu, "Impact on EHV/HV Underground Power Cables on Resonant Grid Behavior, PhD thesis," tech. rep., Technical University Eindhoven, Eindhoven, the Netherlands, 2014.

[11] G. Hoogendorp, "Steady State and Transient Behavior of Underground Cables in 380 kV Transmission Grids, PhD thesis," tech. rep., Delft University of Technology, Delft, the Netherlands, 2016.

[12] S. Meijer, J. P. W. de Jong, J. J. Smit, B. W. Tuinema, H. Lugschitz, G. Svejda, M. Klein, W. Fischer, C. Henningsen, and A. Gualano, "Availability and Risk Assessment of 380kV Cable Systems in Transmission Grids," in *44th Cigré Session*, (Paris, France), 2012.

[13] Autoriteit Consument en Markt, "Netcode Elektriciteit," tech. rep., Autoriteit Consument en Markt, The Netherlands, 2014.

[14] Mathworks, "MATLAB Product Description." www.mathworks.com/products/matlab (last accessed: July 2017), 2011.

[15] R. Billinton and R. N. Allan, *Reliability Evaluation of Power Systems*. New York: Plenum Press, 2nd ed., 1996.

[16] W. Li, *Risk Assessment of Power Systems - Models, Methods, and Applications*. Canada: Wiley Interscience - IEEE Press, 2005.

[17] W. Li, *Probabilistic Transmission System Planning*. Canada: Wiley Interscience - IEEE Press, 2011.

[18] B. W. Tuinema, "Reliability of Sustainable Power Systems - Course Reader," tech. rep., Department of Electrical Engineering, Electrical Sustainable Energy, Delft University of Technology, Delft, The Netherlands, 2016.

[19] M. Cepin, *Assessment of Power System Reliability – Methods and Applications*. London: Springer, 2011.

[20] TenneT TSO B.V., "TenneT Beleidsdocument Risk Matrix," tech. rep., TenneT TSO, Arnhem, the Netherlands, 2010.

[21] S. R. Khuntia, B. W. Tuinema, J. L. Rueda Torres, and M. A. M. M. van der Meijden, "Time Horizons in the Planning and Operation of Transmission Networks: An Overview," *IET Generation, Transmission & Distribution*, vol. 10(4), pp. 841–848, 2016.

[22] B. W. Tuinema, M. Gibescu, and W. L. Kling, "Availability Evaluation of Offshore Wind Energy Networks within the Dutch Power System," in *IEEE Joint IAS/PELS/PES Benelux Chapter, Young Researchers Symposium: Smart Sustainable Power Delivery, 2010. YRS '10*, (Leuven, Belgium), 2010.

[23] R. E. Getreuer, B. W. Tuinema, J. L. Rueda Torres, and M. A. M. M. van der Meijden, "Multi-Parameter Approach for the Selection of preferred offshore Power Grids for Wind Energy," in *IEEE International Energy Conference, EnergyCon2016,*, (Leuven, Belgium), 2016.

[24] R. Billinton and M. Fotuhi-Riruzabad, "A basic framework for generation system operating health analysis," *IEEE Transactions on Power Systems*, vol. 9, no. 3, pp. 1610–1617, 1994.

[25] M. T. Schilling, A. M. Rei, M. B. do Coutto Filho, and J. C. Stacchini de Souza, "On the Implicit Probabilistic Risk embedded in the Deterministic n-α Type Criteria," in *7th International Conference on Probabilistic Methods Applied to Power Systems (PMAPS2002)*, (Napels, Italy), 2002.

[26] W. L. Kling, "Planning en Bedrijfsvoering van Electriciteitsvoorziening systemen, lecture notes," tech. rep., Department of Electrical Engineering, Mathematics and Computer Science, Electrical Power Systems, Delft University of Technology, Delft, 2006.

[27] R. Billinton and R. N. Allan, *Reliability Evaluation of Engineering Systems*. New York: Plenum Press, 2nd ed., 1992.

[28] R. D. Yates and D. J. Goodman, *Probability and Stochastic Processes*. United States: John Wiley & Sons, Inc, 2005.

[29] F. Wang, B. W. Tuinema, M. Gibescu, and M. A. M. M. van der Meijden, "Reliability Evaluation of Substations Subject to Protection System Failures, MSc Thesis," tech. rep., Department of Electrical Engineering, Delft University of Technology, Delft, the Netherlands, 2012.

[30] F. Wang, B. W. Tuinema, M. Gibescu, and M. A. M. M. van der Meijden, "Reliability Evaluation of Substations Subject to Protection System Failures," in *Powertech2013,*, (Grenoble, France), 2013.

[31] N. Kandalepa, B. W. Tuinema, J. L. Rueda Torres, and M. A. M. M. van der Meijden, "Reliability Modeling of Transmission Networks: An explanatory Study on further EHV Underground Cabling in the Netherlands, MSc Thesis," tech. rep., Department of Electrical Engineering, Delft University of Technology, Delft, the Netherlands, 2015.

[32] N. Madras, *Lectures on Monte Carlo Methods*. Province, Rhode Island: Americal Mathematical Society, 1 ed., 2002.

[33] G. Hartshorn, B. Lanz, and B. Broussard, "Assuring cable reliability," *IEEE Industry Applications Magazine*, vol. 15, pp. 66–74, 2009.

[34] F. Petzold, H. Schlapp, E. Gulski, P. Seitz, and B. Quak, "Advanced solution for on-site diagnosis of distribution power cables," *IEEE Transactions on Dielectrics and Electrical Insulation*, vol. 15, pp. 1584–1589, 2008.

[35] M. A. Dakka, A. Bulinski, and Bamji, "On-site diagnostics of medium-voltage underground cross-linked polyehtylene cables," *IEEE Electrical Insulation Magazine*, vol. 27, pp. 34–44, 2011.

[36] C. K. Lee, K. S. Kwak, T. S. Yoon, and J. B. Park, "Cable fault localization using instantaneous frequency estimation in gaussian-enveloped linear chirp reflectometry," *IEEE Transactions on Instrumentation and Measurement*, vol. 62, pp. 129–139, 2013.

[37] C. F. Jensen, O. M. K. K. Nanayakkara, A. D. Rajapakse, U. S. Gudmundsdottir, and C. L. Bak, "Online fault location on ac cables in underground transmission systems using sheath currents," *Elsevier Electric Power Systems Research*, vol. 115, pp. 74–79, 2014.

[38] S. Kulkarni, S. Santoso, and T. A. Short, "Incipient fault location algorithm for underground cables," *IEEE Transactions on Smart Grids*, vol. 5, pp. 1165–1174, 2014.

[39] M. Stotzel, M. Zdrallek, and W. H. Wellssow, "Reliability calculation of mv-distribution networks with regard to ageing in xlpe-insulated cables," *IEEE Proc. Generation, Transmission and Distribution*, vol. 148, pp. 597–602, 2001.

[40] G. Mazzanti, "The combination of electro-thermal stress, load cycling and thermal transients and its effects on the life of high voltage ac cables," *IEEE Transactions on Dielectrics and Electrical Insulation*, vol. 16, pp. 1168–1179, 2001.

[41] R. Liu and S. Boggs, "Cable life and the cost of risk," *IEEE Electrical Insulation Magazine*, vol. 25, pp. 13–19, 2009.

[42] D. Benato, R. Napolitano, "State-space model for availability assessment of ehv ohl-ugc mixed power transmission link," *Elsevier Electric Power systems Research*, vol. 99, pp. 45–52, 2013.

[43] D. Benato, R. Napolitano, "Overall cost comparison between cable and overhead lines including the costs for repair after random failures," *IEEE Transactions on Power Delivery*, vol. 27, pp. 1213–1222, 2012.

[44] Cigré Working Group B1.10, "Update of Service Experience of HV Underground and Submarine Cable Systems, TB379," tech. rep., Cigré, April 2009.

[45] S. Meijer, J. Smit, X. Chen, W. Fischer, and L. Colla, "Return of Experience of 380 kV XLPE Landcable Failures," in *Jicable - 8th International Conference on Insulated Power Cables*, (Versailles, France), 2011.

[46] S. Meijer, J. Smit, X. Chen, and E. Gulski, "Monitoring Facilities for Failure Rate Reduction of 380 kV Power Cables," in *Jicable - 8th International Conference on Insulated Power Cables*, (Versailles, France), 2011.

[47] B. W. Tuinema, M. Gibescu, M. A. M. M. van der Meijden, and L. van der Sluis, "Reliability Evaluation of Underground Cable Systems used in Transmission Networks," in *12th International Conference on Probabilistic Methods Applied to Power Systems, 2012. PMAPS '12,*, (Istanbul, Turkey), 2012.

[48] TenneT TSO, "NESTOR (Nederlandse Storingsregistratie) Database 2006-2010," 2011.

[49] FNN Forum Netztechnik / Netzbetrieb im VDE, "Ermittlung von Eingangsdaten zur Zuverlässigkeitsberechnung aus der FNN-Störungsstatistik." Available online at: http://www.fgh.rwth-aachen.de/verein/publikat/veroeff/FGH IAEW Eingangsdaten Zuverlaessigkeitsberechnung 2013.pdf, Last accessed: 2013.

[50] D. Benato, R. Napolitano, "Reliability assessment of ehv gas-insulated transmission lines: Effect of redundancies," *IEEE Transactions on Power Delivery*, vol. 23, pp. 2174–2181, 2008.

[51] L. Cheng, H. Feng, Y. Chang, and C. Singh, "Reliability analysis of hts cable systems," *IEEE Transactions on Power Delivery*, vol. PP, p. 1, 2014.

[52] N. Kandalepa, B. W. Tuinema, J. L. Rueda Torres, and M. A. M. M. van der Meijden, "Reliability Modeling of Transmission Networks: An explanatory Study on further EHV Underground Cabling in the Netherlands," in *IEEE International Energy Conference, EnergyCon2016,*, (Leuven, Belgium), 2016.

[53] L. Xu and S. Islam, "Reliability issues of offshore wind farm topology," in *10th International Conference on Probabilistic Methods Applied to Power Systems, PMAPS08*, 2008.

[54] M. Zhao, Z. Chen, and F. Blaabjerg, "Optimisation of electrical system for offshore wind farms via genetic algorithm," *IET Renewable Power Generation*, vol. 3, pp. 205–216, 2009.

[55] H. Lingling and F. Yang, "Reliability evaluation of the offshore wind farm," in *Power and Energy Engineering Conference (APPEEC10)*, 2010.

[56] S. Lumbreras and A. Ramos, "Optimal design of the electrical layout of an offshore wind farm applying decomposition strategies," *IEEE Transactions on Power Systems*, vol. 28, pp. 1434–1441, 2013.

[57] O. Dahmani, S. Bourguet, M. Machmoum, P. Guerin, and P. Rhein, "Reliability analysis of the collection system of an offshore wind farm," in *9th Internation Conference on Ecological Vehicles and Renewable Energies (EVER14)*, 2014.

[58] I. Athamna, M. Zdrallek, E. Wiebe, and F. Koch, "Sensitivity analysis of offshore wind farm topology based on reliability calculation," in *International Conference on Probabilistic Methods Applied to Power Systems, PMAPS14*, 2014.

[59] P. Bresesti, W. L. Kling, R. L. Hendriks, and R. Vailati, "Hvdc connection of offshore wind farms to the transmission system.," *IEEE Transactions on Energy Conversion*, vol. 22, pp. 37–43, 2007.

[60] M. Banzo and A. Ramos, "Stochastic optimization model for electric power system planning of offshore wind farms," *IEEE Transactions on Power Systems*, vol. 26, pp. 1338–1348, 2011.

[61] A. M. L. Leita da Silva, W. S. Sales, L. A. da Fonseca Manso, and R. Billinton, "Long-term probabilistic evaluation of operating reserve requirements with renewable sources," *IEEE Transactions on Power Systems*, vol. 25, pp. 106–116, 2010.

[62] K. Rohrig and B. Lange, "Improvement of the power system reliability by prediction of wind power generation," in *IEEE Power Engineering Society General Meeting (PES-GM07)*, 2007.

[63] Z. Yi and A. A. Chowdhury, "Reliability Assessment of Wind Integration in Operating and Planning of Generation Systems," in *IEEE Power & Energy Society General Meeting PES09*, 2009.

[64] TenneT TSO B.V., "Offshore Energie - TenneT brengt energie van zee naar land," tech. rep., TenneT TSO B.V., Arnhem, the Netherlands, 2010.

[65] TenneT TSO B.V., "Visie2030," tech. rep., TenneT TSO B.V., Arnhem, the Netherlands,, 2008.

[66] K. Rudion, "Offshore Power System Planning - Selected Aspects, Habilitation Thesis at the Otto-von-Guericke University," tech. rep., University Magdeburg, Germany, 2012.

[67] K. Rudion and A. Orths, "Reliability Investigations for a DC Offshore Power System," in *Power and Energy Society General Meeting (PES), 2013. PES-GM '13*, (Vancouver, Canada), 2013.

[68] Rijksdienst voor Ondernemend Nederlands, RVO, "Wind SDE+ 2014." Available online at: http://www.rvo.nl/subsidies-regelingen/wind-sde-2014, 2014.

[69] Schoenmakers, D., "Optimization of the coupled grid connection of offshore wind farms, MSc thesis," tech. rep., Technical University of Eindhoven, Netherlands, 2008.

[70] ABB, "XLPE Submarine Cable Systems Attachment to XLPE Land Cable Systems - User's Guide." Available online at: http://www.abb.com/, 2014.

[71] ABB, "ABB HVDC mass impregnated cables." Available online at: http://www.abb.com/, 2014.

[72] ABB, "ABB HVDC Light Cables - Submarine and Land Power Cables." Available online at: http://www.abb.com/, 2014.

[73] B. W. Tuinema, J. L. Rueda Torres, and M. A. M. M. van der Meijden, "Network Redundancy versus Generation Reserve in Combined Onshore-Offshore Transmission Networks," in *PowerTech2015,*, (Eindhoven, the Netherlands), 2015.

[74] North American Electric Reliability Corporation (NERC), "Generation Availability Report (GAR)." http://www.nerc.com, 2011.

[75] M. Gibescu, A. J. Brand, and W. L. Kling, "Estimation of Variability and Predictability of Large-scale Wind Energy in The Netherlands," *Wind Energy - Wiley Interscience*, vol. 12, pp. 241–260, 2009.

GLOSSARY

LIST OF SYMBOLS AND NOTATION

Reliability theory:

$F(t)$	= failure distribution (or unreliability function) [-]
$R(t)$	= reliability function [-]
$f(t)$	= failure density distribution [/y]
$h(t)$	= hazard rate [/y]
$MTBF$	= Mean Time Between Failures (=T) [y]
$MTTF$	= Mean Time To Failure (=d) [y]
$MTTR$	= Mean Time To Repair (=r) [y]
T	= Mean Time Between Failures (=$MTBF$) [y]
d	= Mean Time To Failure (=$MTTF$) [y]
r	= repair time (i.e. Mean Time To Repair, =$MTTR$) [y] (often in [h])
λ	= failure rate (= $1/MTTF$) [/y]
μ	= repair rate (= $1/MTTR$) [/y]
f	= failure frequency (= $1/MTBF$) [/y]
A	= availability (= $MTTF/MTBF$) [-]
U	= unavailability (= $MTTR/MTBF$) [-]

Subscripts:

$\ldots_{av}$	= ... average
$\ldots_{i}$	= ... of component i
$\ldots_{1}$	= .. of single circuit failures
$\ldots_{2}$	= ... of double circuit failures
$\ldots_{2dep}$	= ... of dependent double circuit failures
$\ldots_{2ind}$	= ... of independent double circuit failures
$\ldots_{line}$	= ... of an overhead line (three phases) [per cctkm]
$\ldots_{l1}$	= ... of a single overhead line circuit
$\ldots_{l2dep}$	= ... of dependent double circuit failures in overhead lines
$\ldots_{l2ind}$	= ... of independent double circuit failures in overhead lines
$\ldots_{cable}$	= ... of an underground cable (one cable per phase) [per cctkm]
$\ldots_{joint}$	= ... of a single joint [per component]
$\ldots_{term}$	= ... of a single termination [per component]
$\ldots_{c1}$	= ... of a single cable circuit
$\ldots_{c1/2}$	= ... of half a cable system circuit (i.e. one cable per phase , including joints and terminations)
$\ldots_{c2dep}$	= ... of dependent double circuit failures in cable systems
$\ldots_{c2ind}$	= ... of independent double circuit failures in cable systems
$\ldots_{pc1}$	= ... of a single circuit partially-cabled connection

$\ldots_{pc2dep}$ = ... of dependent double circuit failures in a partially-cabled connection
$\ldots_{pc2ind}$ = ... of independent double circuit failures in a partially-cabled connection

Other variables:

c_{cc} = dependent failure factor [-]
f_{csys} = failure frequency of all the cable system components
l_{cable} = total cable (circuit) length [km]
l_{line} = total overhead line length [km]
l_{cpart} = cable part length [km]
l_{total} = total connection length [km]
n_{ic} = number of individual cables per circuit phase [-]
N_{csec} = number of embedded cable sections [-]
μ_{sw} = switching rate of the disconnectors or the spare cable [/y]

Markov models and system states:

S_0 = state 0 (no failures)
S_n = state n
T = transition matrix
$\mathbf{p}$ = state probability vector [-]
I = identity matrix
P_{S_n} = probability of state n [-]
$P_{x\%}$ = probability of having x% transmission capacity [-]
$T_{x\%}$ = mean time between the x% capacity states [y]
S_{nind} = n independent failures within the network
S_{ndep} = n dependent failures within the network
$S_{3depind}$ = 1 dependent and 1 independent failure within the network
$S_{4depind}$ = 1 dependent and 2 independent failures within the network
$f_{S_m \to S_n}$ = transition frequency from state m to state n [/y]
$r_{S_m \to S_n}$ = average repair time from state m to state n [h]
$r_{x \to y\%}$ = average repair time from x% to y% capacity [h]

Functions:

$\lceil X \rceil$ = ceil function (rounding X to the nearest integer towards infinity)
X^* = annualized value (of a probability, unavailability or availability) [h/y]
$\cap$ = intersection operator
$\cup$ = union operator
$P[A|B]$ = probability of event A, given that event B occurs [-]

LIST OF ABBREVIATIONS

AC	Alternating current
DC load flow	Linearized load flow
DG	Distributed Generation
DSO	Distribution System Operator
EHV	Extra-High Voltage (380/220kV in NL)
HV	High Voltage (150/110kV in NL)

HVAC	High-Voltage Alternating Current
HVDC	High-Voltage Direct Current
$n-0$ situation	Operation with all n grid elements in service
$n-1$ situation	Operation with $n-1$ grid elements in service
$n-\alpha$ situation	Operation with $n-\alpha$ elements in service
$n-0$ redundant	Able to operate with (minimally) all n grid elements in service
$n-1$ redundant	Able to operate with (minimally) $n-1$ grid elements in service
$n-\alpha$ redundant	Able to operate with (minimally) $n-\alpha$ elements in service
OHL	Overhead Line
PST	Phase-Shifting Transformer
RES	Renewable Energy Sources
TSO	Transmission System Operator
UGC	Underground Cable

ACKNOWLEDGMENT

When I was a child, I always used to visit my grandfather during the school holidays. Together we did various electrical experiments like creating sparks with a capacitor, repairing broken devices and testing fuses with our specially-designed short-circuit plug. It was then when I developed my first interest in electrical engineering and I decided that I would like to become an electrical engineer myself later. My grandfather Louis Vroom is therefore the first one to thank here, for introducing me into the field of electrical engineering and teaching me the first basics.

After my school time, I started my bachelor study electrical engineering at Delft University. I was able to develop my knowledge of electrical engineering with the help of dedicated teachers. I continued my bachelor study with a master study in the field of electrical power engineering. There, I was able to develop my knowledge even further and became interested in probabilistic approaches and reliability analysis of power systems. During my graduation project, I could experiment with this probabilistic reliability analysis on an interesting case study of the integration of large-scale offshore wind energy in the Netherlands, under supervision of prof. Wil Kling and dr. Madeleine Gibescu. I am very thankful for their support during my master research, the interesting discussions and their help with successfully completing my master study.

Reaching the end of my graduation project, I thought it would be nice to continue my studies in a Ph.D. research. Wil Kling introduced me to prof. Mart van der Meijden ('someone from TenneT is interested in your work and will join your master presentation'), and in cooperation with TenneT TSO my plan of doing a Ph.D. was made possible. First, I was supervised by prof. Lou van der Sluis and dr. Madeleine Gibescu, later by prof. Mart van der Meijden and dr. José Rueda Torres. In March 2015, the sad news came that Wil passed away. It is very sad that he past away so early, and I would have been proud to show him the results of my work. During my Ph.D. I have had some good times and some hard times (probably the famous 'mid-PhD dip'). With the help of my supervisors, I was able to find trust and enthusiasm in my work again and eventually completed my research. I would therefore like to thank Lou, Madeleine, Mart and José for their guidance and enthusiasm, but also for their critical technical remarks and help to place my research in a larger context. Without your support I would not have been able to successfully complete my research.

My Ph.D. research was performed in cooperation with TenneT TSO. This cooperation gave me the opportunity to look into the kitchen of a large TSO, which helped me a lot to keep my research realistic and useful. I would like to thank my main supervisors from TenneT: Sander Meijer, Robert Kuik and Rob Ross, but also all the other colleagues from TenneT who helped me to understand the TSO practice or helped me with supervising master students. I would also like to thank the master students I supervised: Fatih, Fengli, Niki, Reinout and Zahrina. Supervising students leads to many interesting discussions and stimulates to think carefully about the methods that we apply. In

this sense, I can say that I probably learned as much as them during their supervision. I would like to thank my office mates as well: first Ana and Barry, later Mario, Swasti, Kaikai and Elyas, for having serious and less serious discussions and creating a friendly working environment. I also would like to thank all my other colleagues of the IEPG group, and the secretaries (Ellen, Sharmila, Ilona, Claudia) for their support.

In my personal life I receive much support from my close relatives and friends. First and most important, I would like to thank my parents Jan Willem and Nelleke. They always will support me and will always keep trust in me, whatever happens. I also would like to thank my sister Nienke, from which I receive much support as well, during good and hard times. I would like to thank my brother-in-law Maurice for being a good brother-in-law and my nephew Sem for being a cute nephew. I thank Cees for his helpful coaching and advice. I also would like to thank my musical friends Paul, Frank and Linda, with whom I share the same (good) taste of music and (even better) sense of humor.

So again, I would like to thank everyone for their valuable support, in both my professional and personal life. Without you, I would not be the person I am and would not be able to do the things I like to do.

Bart Tuinema
Delft, November 2017.

BIOGRAPHY AND PUBLICATIONS

BIOGRAPHY

Bart W. Tuinema was born in The Hague, The Netherlands, on February 5, 1984. He received his B.Sc. and M.Sc. degrees from Delft University of Technology, Delft, The Netherlands, in 2007 and 2009 respectively. In his M.Sc. research he studied the reliability of offshore networks for wind energy and the impact on the reliability of onshore power systems. In 2010, he joined the Intelligent Electrical Power Grids (IEPG) group of the Electrical Sustainable Energy (ESE) department of Delft University of Technology as a Ph.D. researcher. In his Ph.D. research, he studied the reliability of power systems with respect to new developments like EHV underground cables and networks for large-scale offshore wind energy. He is currently working in the same group as a postdoc researcher, and is involved in teaching activities and the MIGRATE project (Massive InteGRATion of power Electronic devices).

BOOK CONTRIBUTIONS

2. J.L. Rueda Torres, F. Gonzalez-Longatt, "Data Mining and Probabilistic Power System Security - Dynamic Vulnerability Assessment and Intelligent Control", *Wiley*, 2017.

1. B.W. Tuinema, J.L. Rueda Torres, M.A.M.M. van der Meijden, "Reliability of Sustainable Power Systems - Course Reader", *Delft University of Technology*, August, 2016.

JOURNAL PUBLICATIONS

2. S.R. Khuntia, B.W. Tuinema, J.L. Rueda, M.A.M.M. van der Meijden, "Time Horizons in the Planning and Operation of Transmission Networks: An Overview", *IET Generation, Transmission, Distribution*, Vol.10/4, October, 2016.

1. B.W. Tuinema, J.L. Rueda, L. van der Sluis, M.A.M.M. van der Meijden, "Reliability of Transmission Links consisting of Overhead Lines and Underground Cables", *IEEE Trans. Power Delivery*, Vol.31/3, September, 2016.

CONFERENCE PUBLICATIONS

9. N. Kandalepa, B.W. Tuinema, J.L. Rueda, M.A.M.M. van der Meijden, "Reliability Modelling of Transmission Networks: An Explanatory Study on further Underground Cabling in the Netherlands", in *Proc. Energycon2016*, Leuven, Belgium, April, 2016.

8. R.E. Getreuer, B.W. Tuinema, J.L. Rueda, M.A.M.M. van der Meijden, "Multi-Parameter Approach for the Selection of preferred offshore Power Grids for Wind Energy", in *Proc. Energycon2016*, Leuven, Belgium, April, 2016.

7. B.W. Tuinema, J.L. Rueda, M.A.M.M. van der Meijden, "Network Redundancy versus Generation Reserve in Combined Onshore-Offshore Transmission Networks", in *Proc. PowerTech2015*, Eindhoven, the Netherlands, June, 2015.

6. F. Wang, B.W. Tuinema, M. Gibescu, M.A.M.M. van der Meijden, "Reliability Evaluation of Substations Subject to Protection System Failures", in *Proc. Powertech2013*, Grenoble, France, June, 2013.

5. S. Meijer, J.P.W. de Jong, J.J. Smit, B.W. Tuinema, H. Lugschitz, G. Svejda, M. Klein, W. Fischer, C.G. Henningsen, A. Gualano, "Availability and Risk Assessment of 380 kV Cable Systems in Transmission Grids", in *Proc. 44th Cigré Session*, Paris, France, August, 2012.

4. B.W. Tuinema, M. Gibescu, M.A.M.M. van der Meijden, L. van der Sluis, "Reliability Evaluation of Underground Cable Systems used in Transmission Networks", in *Proc. 12th International Conf. on Probabilistic Methods Applied to Power Systems (PMAPS2012)*, Istanbul, Turkey, June, 2012.

3. B.W. Tuinema, M. Gibescu, L. van der Sluis, M.A.M.M. van der Meijden, "Probabilistic Reliability Analysis of Future Power Systems – Survey and Example", in *Proc. Innovative Smart Grid Technologies Conference (ISGT2011)*, Manchester, United Kingdom, December, 2011.

2. B.W. Tuinema, M. Gibescu, M.A.M.M. van der Meijden, L. van der Sluis, W.L. Kling, "Trends in Probabilistic Power System Reliability Analysis – A Survey", in *Proc. International Universities' Power Engineering Conference (UPEC2011)*, Soest, Germany, September, 2011.

1. B.W. Tuinema, M. Gibescu, W.L. Kling, "Availability Evaluation of Offshore Wind Energy Networks within the Dutch Power System", in *Proc. IEEE Joint IAS/PELS/PES Benelux Chapter, Young Researchers Symposium: Smart Sustainable Power Delivery (YRS2010)*, Leuven, Belgium, March, 2010.

For the future, several developments of the power system are expected. Offshore, a large-scale expansion of wind generation will be implemented. This wind energy will be collected and transmitted to the shore by an offshore grid. Onshore, the transmission network needs to be reinforced to transmit the power to the main load centres. Traditional overhead lines are facing increasing opposition from local society, such that underground extra-high voltage cables are a promising alternative. As these new developments will influence the reliability of the power system, it is of importance to thoroughly study their impact. In this thesis, the reliability of EHV underground cables and offshore networks for wind energy is analysed, from the reliability of the individual components to the impact on the reliability of the power system as a whole. Mitigation measures to improve the reliability of power systems with EHV cables and offshore networks are suggested and their effects are assessed. The methods applied in this research show how the reliability of other future developments of power systems can be analysed as well.

ISBN 978-94-6299-778-3